

Distribution Agreement

In presenting this thesis or dissertation as a partial fulfillment of the requirements for an advanced degree from Emory University, I hereby grant to Emory University and its agents the non-exclusive license to archive, make accessible, and display my thesis or dissertation in whole or in part in all forms of media, now or hereafter known, including display on the world wide web. I understand that I may select some access restrictions as part of the online submission of this thesis or dissertation. I retain all ownership rights to the copyright of the thesis or dissertation. I also retain the right to use in future works (such as articles or books) all or part of this thesis or dissertation.

Signature:

Mark Baillie

Date

Towards the Development of Non-Toxic Therapeutics in the Fight Against Cancer

By

Mark Baillie
Ph.D.
Chemistry

Dr. Dennis C. Liotta
Advisor

Dr. Lanny Liebeskind
Committee Member

Dr. David Lynn
Committee Member

Accepted:

Lisa A. Tedesco, Ph.D.
Dean of the James T. Laney School of Graduate Studies

Date

Towards the Development of Non-Toxic Therapeutics in the Fight Against Cancer

By

Mark Baillie
B.S., Bucknell University, 2003

Advisor: Dr. Dennis C. Liotta, Ph.D.

An abstract of
a dissertation submitted to the Faculty of the
James T. Laney School of Graduate Studies of Emory University
in partial fulfillment of the requirements for the degree of
Doctor of Philosophy
in Chemistry
2011

Abstracts

Towards the Development of Non-Toxic Therapeutics in the Fight Against Cancer

By Mark Baillie

Chapter 1: Synthesis and Application of Novel Tail-Modified Enigmol Analogs. Sphingolipids are a set of signaling molecules that are intricately involved in cancer progression. **Enigmol** (2*S*-amino-octadecane-3*S*,5*S*-diol) is a sphingoid base derivative that reregulates apoptosis in cancer cells by interacting with the sphingolipid signaling pathways. Herein we report the synthesis of a set of **Enigmol** analogs featuring fluorination and rigidification of the tail. Geometric alterations and rigidification between C-11 and C-12 decreased efficacy of these compounds to induce cell death in prostate cancer cell lines (PC-3 and LNCaP) when compared to **Enigmol**, while compounds with fluorination at multiple points in the tail retained anticancer activity *in vitro*. Pharmacokinetic properties and a biological distribution profile of the C-18 trifluoromethyl analog **2** (R = CF₃) dosed orally in rats at 10 mg/kg showed nearly three fold increase in plasma levels and tissue concentrations as compared with **Enigmol**. Most notable was the substantial increase in bioavailability, which was found to be 76% for **2** as compared to 11% for **Enigmol**. Trifluoromethyl-containing compound **2** is a promising lead molecule that we plan to further pursue as an anti-cancer compound for the clinical treatment of prostate cancer.

Chapter 2: Following in the Steps of Otto Warburg. Design and Synthesis of Potential Pyruvate Kinase Inhibitors.

Chapter 3: Design and Synthesis of Novel CXCR4 Modulators for Treatment of Macular Degeneration.

Towards the Development of Non-Toxic Therapeutics in the Fight Against Cancer

By

Mark Baillie
B.S., Bucknell University, 2003

Advisor: Dr. Dennis C. Liotta, Ph.D.

A dissertation submitted to the Faculty of the
James T. Laney School of Graduate Studies of Emory University
in partial fulfillment of the requirements for the degree of
Doctor of Philosophy
in Chemistry
2011

Acknowledgements

I would like to first thank Dr. Liotta for allowing me to join his lab as an inexperienced chemist. His guidance and hands off approach has allowed be to become a confident and independent researcher. For funding, I need to thank the National Cancer Institute (NCI) for a National Cooperative Drug Discovery Groups (NCDDG) grant (U19-CA87525) and the Emory Institute for Drug Discovery (EIDD) for funding and consultation. I also would like to thank many members of the EIDD including Dr. Manu Saindane for his assistance with scale up of the alkyne zipper reaction and valuable insight, Dr. Terry Moore for his thought provoking conversations, Dr. Jay Holt for his critical evaluations regarding this project, Drs. Sarah Pruett, Rick Arrendale, Randy Howard, Prabhakar Reddy, with the assistance of Deborah Culver and Taylor Evers for the immense efforts on the PK study for reported herein, and Dr. Michael Natchus for being a powerful guiding force. Serdar Kurtkaya and Dr. Pieter Burger have provided immense computational insight for me along this path. Eric Miller has been a very positive addition to this project, always asking questions that make us step back and think about the project in a more critical light. Dr. Greg Bluemling, and Katie Chepiga have dedicated significant efforts towards insuring accuracy of the manuscripts on this project. Dr. Ustun Sunay for guiding me in my early days as a naive synthetic chemist, as well as for comic relief. Thanks to Dr. Mike Hager for being an amazing inspiration and invaluable resource. For the mentorship and guidance I have received from Drs. Lanny Liebeskind, Dave Lynn, Pat Marsteller, and Khalid Salaita, I am eternally grateful. Additionally, the movers and shakers that have helped me get things done around here have been invaluable; specifically Cindy Gaillard, Marcus Rodriguez, Patti Barnett, Steve Krebs, and Shaoxiong Wu. Finally, without the support of my family and amazing girlfriend Dr. Tiffany Weinkopff I would have not made it through this process.

1 Table of Contents

Chapter 1: Synthesis and Application of Novel Tail-Modified Enigmol Analogs.....	1
1.1 Introduction	1
1.1.1 Background and Significance	1
1.1.2 Developing a Cancer Therapeutic.....	5
1.1.3 ¹⁹ F MRI Application	11
1.2 Synthesis of Target Compounds	12
1.2.1 Liebeskind-Srogl Route and Side Reaction Investigation	12
1.2.2 Synthesis <i>Via</i> Aldol Reaction	20
1.3 Biological Evaluation.....	28
1.3.1 <i>In vitro</i> Evaluation of Enigmol Analogs Against Prostate Cancer	28
1.3.2 Pharmacokinetic Evaluation	29
1.3.3 ¹⁹ F MRI Study Results	32
1.4 Discussion	35
1.5 Conclusions	37
1.6 Methods and Experimental Protocol.....	38
1.6.1 Experimental Procedure for the Synthesis of Tail-modified Enigmols:.....	38
1.6.2 Biological Protocols.....	75
Chapter 2: Following in the steps of Otto Warburg. Design and Synthesis of Potential Pyruvate Kinase Inhibitors.....	1
2.1 Introduction	82
2.1.1 Background and Significance	82
2.1.2 Design of Novel PK Inhibitors	85
2.2 Results	87
2.2.1 Synthesis of Novel PKI's.....	87
2.2.2 Chemical Routes Attempted to Obtain the Difluorophosphate PKI's	90
2.3 Biological Evaluation.....	92
2.3.1 <i>In vitro</i> Cell-based Assays	92
2.3.2 <i>In vitro</i> Cell-free Assay.....	94
2.4 Discussion	95
2.5 Conclusion.....	96
2.6 Methods and Experimental Protocol.....	96
2.6.1 Experimental Protocol for Synthesis	96

2.6.2	Biological Evaluation of anti-cancer agents	107
Chapter 3: Design and Synthesis of Novel CXCR4 Modulators for Treatment of Macular Degeneration		
		82
3.1	Introduction	109
3.1.1	Background and Significance	109
3.1.2	Developing a CXCR4 Modulator	114
3.2	Results	117
3.2.1	Synthesis of Novel WZ-41 Analogs	117
3.3	Biological Evaluation	119
3.3.1	<i>In vitro</i> Cell-based TN-14003 Binding Assay Results	119
3.3.2	<i>In vitro</i> Vasculature Formation Assay Results	122
3.4	Conclusions	123
3.5	Methods and Experimental Protocol	124
3.5.1	Experimental Procedure for the Synthesis of Novel WZ-41 Analogs	124
3.5.2	Experimental Protocol for TN-14003 Binding Assay	138

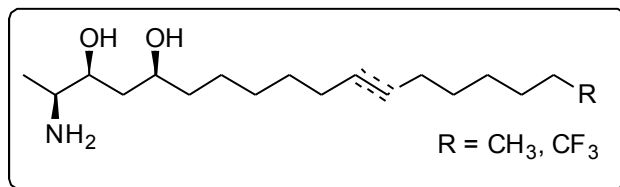
Figure 1: Common structural examples of the sphingolipid family. Sphingoid bases sphinganine and sphingosine showed above the sphingolipids ceramide and further functionalized derivative sphingomyelin	2
Figure 2: Highly simplified <i>de novo</i> sphingolipid synthetic pathway. In the ceramide/S1P rheostat, ceramide and sphingosine inhibit cell growth while S1P increases cell growth.....	3
Figure 3: Pictorial representation of the ceramide/S1P rheostat ⁹ for a healthy cell (A) and a cancerous cell (B).	4
Figure 4: Conception of an anti-cancer agent, Enigmol, which drew from sphingosine and fumonisins B ₁	6
Figure 5: Mouse xenograft study comparing the efficacy of Enigmol to hormone ablation in androgen-dependant tumors (A) or docetaxel in androgen-independent tumors (B). ²³	8
Figure 6: Proposed sites for modification on the tail of Enigmol.....	9
Figure 7: Proposed synthetic targets probing the affect of fluorination and geometric restrictions in the tail of Enigmol.	11
Figure 8: Rationalization for the loss of stereochemistry based on the formation of the aromatic intermediate 65. To capitalize on the equilibrium, we proposed the chiral directing group attached to the nitrogen (67).	18
Figure 9: Pharmacokinetic data comparing mean plasma concentrations of Enigmol to CF ₃ -enigmol (2) over 24 hours.....	30
Figure 10: Mean rat tissue, plasma, and RBC concentrations at 24 hours post administration of Enigmol versus trifluoromethyl-enigmol 2 (10 mg/kg P.O. dose). Analysis performed by the DMPK lab, EIDD.....	32
Figure 11: ¹ H (left) and ¹⁹ F (right) MRI images of rat brain, dosed with 2.....	34
Figure 12: Structures of molecules that take advantage of the dependence of a cancer cell on glycolysis.	84

Scheme 13: Conversion of phosphoenolpyruvate (PEP) to pyruvate, catalyzed by Pyruvate Kinase. This reaction results in the net gain of one unit of ATP by the consumption of ADP.	84
Figure 14: Comparison of phosphoenolpyruvate (PEP) with our proposed phosphonate PKI's. The red bond highlights the removal of the cleavable P-O bond, replaced by a P-C bond. Blue atoms show site of halogenations, which hold potential to tune PK isoform specificity.	85
Figure 15: Specific examples of proposed pro-drug PKI's.	86
Figure 16: PEP analog pro-drugs 4–8 previously reported in literature, ⁶⁵ synthesized for comparison in this study. 3-BrPA and its ester derivative are commercially available.	86
Figure 17: Pyruvate Kinase inhibition assay performed with the 2 tri-acid compounds 33 and 34.	95
Figure 18: Cross section of the human eye.	109
Figure 19: A schematic representation of the cornea, showing the possible pathways for molecules to diffuse through to the anterior chamber. ⁸¹	111
Figure 20: Predictive relationship between solute distribution coefficient Φ and permeability of the individual layers (A) and the whole cornea (B). Molecular radius is represented by line type. ⁸¹ These trends for over 150 compounds were calculated based on models determined and tested in a composite porous medium. ⁸¹	112
Figure 21: Structure of the bicyclam compound AMD3100, an inhibitor of CXCR4.	114
Figure 22: Lead CXCR4 antagonists developed in our laboratory by Weiqiang Zhan.	115
Figure 23: A) CXCL12 displacing peptide TN14003 used in the competitive binding assay. B) Bioassay used to measure interaction of novel compounds with CXCR4 on MB-231 breast cancer cells. Novel compound (green) competes with high affinity biotinylated-peptide TNF14003 (blue/purple). After washing away the unbound substrate, streptavidin-rhodamine conjugate complexes with biotinylated peptide. Inhibition of peptide binding by drug dampens fluorescent signal output.	121

Table 1: Optimization of reaction conditions for cyclization utilizing Liebeskind-Srogl conditions. Followed by LCMS. Yield reported was isolated yield. (-) means isolation not attempted.	17
Table 2: Survey of oxidative conditions for removal of <i>N</i> -benzyl protecting group from 35a. All reaction progress was followed by LCMS. No inert atmosphere or exclusion of water was utilized in these small scale reactions (20 – 80 mg).	25
Table 3: Optimized conditions for oxidative removal of <i>N</i> -benzyl protecting group with Dess Martin periodinane.	25
Table 4: Efficacy of Enigmol analogs against prostate cancer cells for 24 h, and cytotoxicity was assessed by WST-1 assay. cLogP calculated with QuikProp on Maestro.	28
Table 5: Mean pharmacokinetic parameters for Enigmol and CF ₃ -enigmol (2). Performed by the DMPK lab, EIDD.	30
Table 6: Mean rat tissue concentrations of Enigmol and trifluoromethyl-enigmol 2 shown in Figure 10.	32
Table 7: Summary of cancer cell growth inhibition assays results. IC ₅₀ 's were calculated for various synthetic PKI's in breast (MDA-MB231) and prostate (PC-3) cancer cells in culture. ..	93
Table 8: Computational and biological testing values for WZ-41 and analogues. cLogP values were calculated with QuikPro in Maestro.	121
Table 9: Tubule formation assay results from S.R.I.	123

Chapter 1: Synthesis and Application of Novel Tail-Modified Enigmol Analogs

ABSTRACT: Sphingolipids are a set of signaling molecules that are intricately involved in cancer progression. **Enigmol** (2*S*-amino-octadecane-3*S*,5*S*-diol) is a sphingoid



base derivative that reregulates apoptosis in cancer cells by interacting with the sphingolipid signaling pathways. Herein we report the synthesis of a set of **Enigmol** analogs featuring fluorination and rigidification of the tail. Geometric alterations and rigidification between C-11 and C-12 decreased efficacy of these compounds to induce cell death in prostate cancer cell lines (PC-3 and LNCaP) when compared to **Enigmol**, while compounds with fluorination at multiple points in the tail retained anticancer activity *in vitro*. Pharmacokinetic properties and a biological distribution profile of the C-18 trifluoromethyl analog **2** (R = CF₃) dosed orally in rats at 10 mg/kg showed nearly three fold increase in plasma levels and tissue concentrations as compared with **Enigmol**. Most notable was the substantial increase in bioavailability, which was found to be 76% for **2** as compared to 11% for **Enigmol**. Trifluoromethyl-containing compound **2** is a promising lead molecule that we plan to further pursue as an anti-cancer compound for the clinical treatment of prostate cancer.

1.1 Introduction

1.1.1 Background and Significance

Prostate cancer is the most common male cancer rivaling breast cancer for number of cases diagnosed in 2011. The American Cancer Society estimates that greater than 240,000 new cases will be diagnosed this year, with over 30,000 deaths.¹ Nearly 80% of prostate cancer causes begin with a strong dependence on hormones, termed androgen-dependant, which are treated by hormone ablation with drugs or orchiectomy.² Hormone ablation therapy side effects include osteoporosis, muscle wasting, anemia, weight gain, fatigue, breast tenderness, and erectile dysfunction. Once the disease progresses beyond a reliance on hormones, a form termed androgen-independent, the tumor is generally more aggressive requiring chemotherapeutic agents such as docetaxel to slow cancer progression. Chemotherapy can decrease the aggressiveness of the tumor, but requires intravenous administration and suffers from decreased immune system, hair and nail loss, fluid retention, peripheral neuropathy, along with nausea, diarrhea, and fatigue. In the face of these less than ideal side effects, there is a demand for less toxic and more effective prostate cancer therapy options.

Sphingolipids are a class of compounds found throughout biological systems. Structurally, a subset of the sphingolipids called sphingoid bases, exemplified by **sphingosine** and **sphinganine** (Figure 1), are typified by a polar head group containing two alcohols and a single basic amine, connected to a long lipid tail. When the free amine in the head group is acylated, as in **ceramide**, the molecule is termed a sphingolipid. The length of the acyl chain can vary, but most commonly falls in the range of 16 to 22 carbons. The structural diversity of these molecules is immense, and has been reviewed in the literature.³ Briefly, this diversity includes alterations in the number and placement of the alcohols within the head group, the number and

location of double bonds, and also the length of the alkyl tail and the acyl chain. Inter-conversion between the various sphingolipids, where **ceramide** is thought to be the pivotal molecule, is a highly fluid process regulated by a multitude of enzymes. **Ceramide** can be functionalized at the primary hydroxyl group with sugars, phosphates, and other moieties to add significant diversity to the structure and role of these molecules.

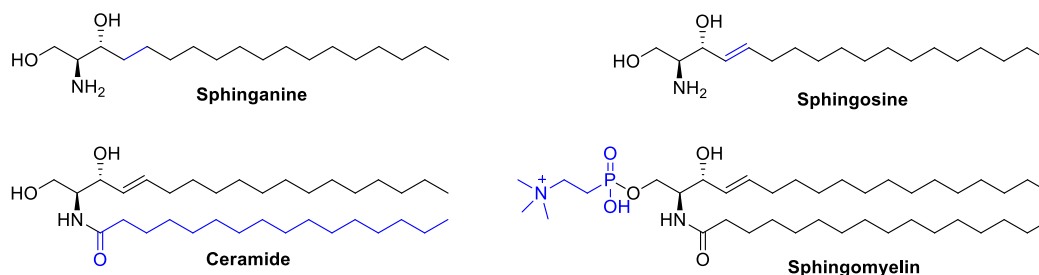


Figure 1: Common structural examples of the sphingolipid family. Sphingoid bases **sphinganine** and **sphingosine** showed above the sphingolipids **ceramide** and further functionalized derivative **sphingomyelin**.

Sphingolipids were initially reported in the late nineteenth century by Thadichum and co-workers as components of the cell membrane lipid bilayer.⁴ They were appropriately named after the Sphinx as their structure and function would elude researchers for years to come. These molecules were found to play a structural role in lipid rafts within the cellular membrane, and are involved in cell-cell communication and recognition on the cell surface.⁵ An extremely simplified version of the *de novo* biosynthetic pathway is shown in Figure 2, highlighting the inter-conversion between the molecules in this family. There are a number of enzymes that introduce unsaturation, acylation, and phosphorylation to yield the molecules shown. The relative ratio of each of these molecules is tightly regulated in healthy cells.

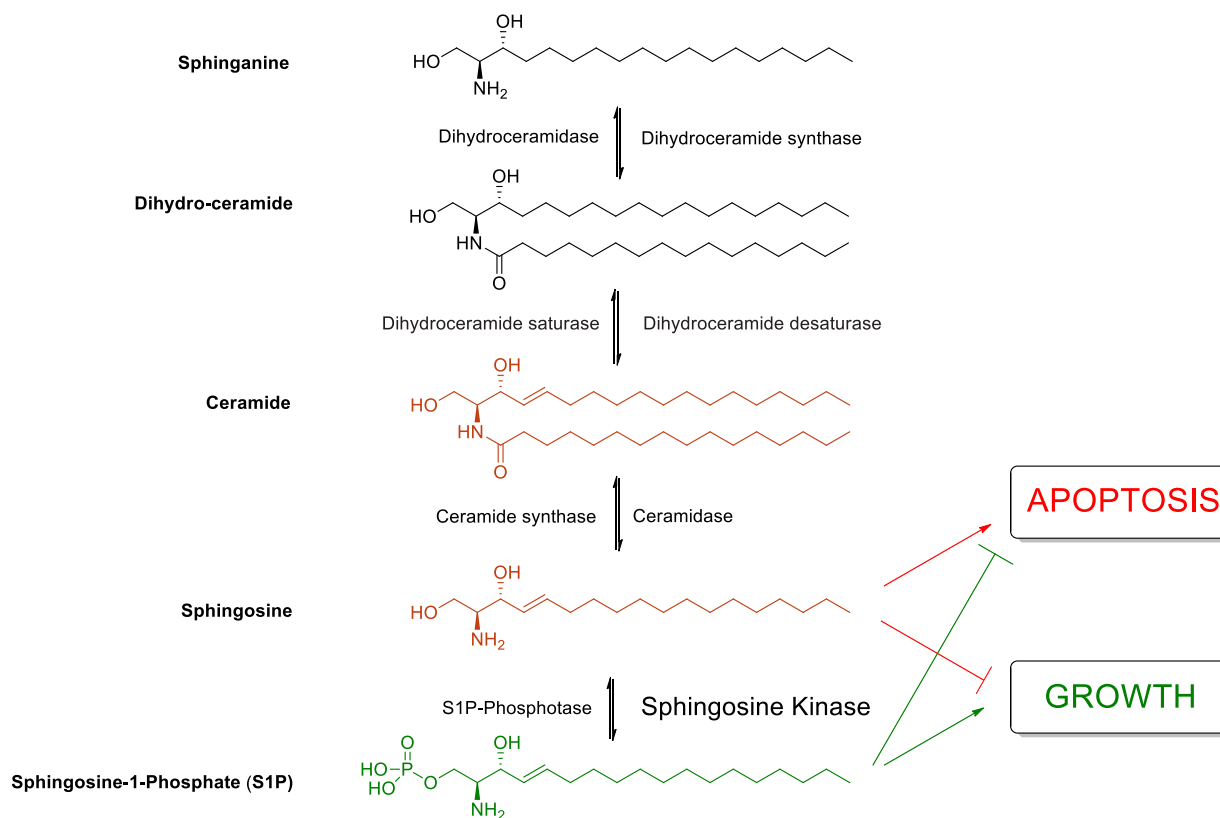


Figure 2: Highly simplified *de novo* sphingolipid synthetic pathway. In the **ceramide/S1P** rheostat, **ceramide** and **sphingosine** inhibit cell growth while **S1P** increases cell growth.

During the past two decades, sphingolipids have gained tremendous attention for their role in signaling pathways within the cell.⁶ In particular, Sarah Spiegel and co-workers at Virginia Commonwealth University have very carefully dissected the role of sphingolipids in relation to regulating programmed cell death, or apoptosis.⁷ They helped define the intricate balance between molecules that promote cell death (**ceramide** and **sphingosine**) and those that promote cell growth (**sphingosine-1-phosphate, S1P**). In healthy cells, the relative levels of these compounds are properly matched to allow for cell propagation, and when necessary, cell termination. Sphingosine kinase, responsible for phosphorylating **sphingosine** to generate **S1P**, seems to be a key player in regulating the relative concentrations of sphingolipids in regards to cell viability, as illustrated in Figure 3A. In cancer cells, this balance is not well maintained. Instead, there is a disproportionately high expression of sphingosine kinase,⁸ which tips the

balance by increasing the concentration of **S1P**. As depicted in Figure 3B, this imbalance slows apoptosis and allows for unregulated cell growth. This phenomenon was termed by Sarah Spiegel as the “**ceramide/S1P rheostat**”.⁹

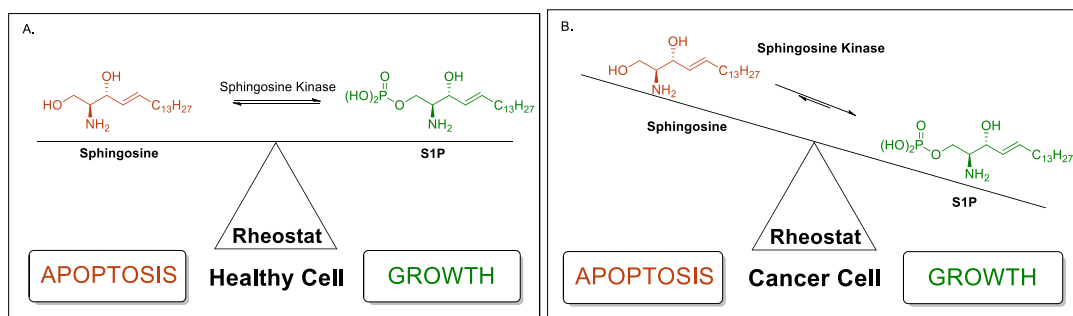


Figure 3: Pictorial representation of the **ceramide/S1P rheostat**⁹ for a healthy cell (A) and a cancerous cell (B).

Although sphingosine kinase was initially hypothesized to be an oncogene, evidence for this has not yet been found.¹⁰ However, the relationship of cancer cells and this enzyme has been described as an addiction by Nigel et al., by which cancer cells rely heavily on the increased production of **S1P** to promote cell viability.¹¹ Sphingosine kinase exists as two distinct isoforms, SK1 and SK2. SK1 is predominantly cytosolic while SK2 is bound to the endoplasmic reticulum and nucleus.¹¹ Simultaneous embryonic knockout of both enzymes has been determined to be lethal, while a single knockout of one (either SK1 or SK2) is not.¹² Based on this information, there seems to be some degree of overlap in function of the two isoforms. However, the selective knockdown (using siRNA) of SK1 in cancer cells leads to apoptosis, while cells persist without SK2.¹³ In clinical settings, increased expression of SK1 is directly correlated with higher drug resistant profile of the tumor and decreased patient prognosis.¹⁴ Recent literature has shown a swell of interest towards targeting sphingosine kinase for cancer therapy. SK1 has been a primary target for a number of groups that hope to suppress the **ceramide/S1P rheostat** in an attempt to reregulate cell growth. Very recently, Kennedy and co-workers developed an SK1 subtype selective inhibitor with an IC_{50} of 75 nM against SK1 *in vitro*.¹⁴ Although this

compound was very potent against SK1 with >100-fold selectivity over SK2, it failed to induce cell death in the U-937 leukemia cancer cell line. Despite this, the sphingolipid signaling pathway has been shown to be a viable therapeutic target. Several groups have developed immunosuppressant **S1P**-receptor inhibitors for treatment of diseases such as multiple sclerosis and rheumatoid arthritis. These include FDA approved Gilenya from Novartis,¹⁵ LX2931 and LX2932 from Lexicon,¹⁶ and ACT-128800 from Acelson Pharmaceuticals.^{17,18}

Inhibition of sphingosine kinase has also been targeted for suppression of uncontrolled cancer cell growth. **Fumonisin B₁** is a naturally occurring toxin produced by the fungus species *Fusarium* that infects maize utilized for feedstock and human consumption (Figure 4). The toxicity of this molecule has been attributed to inhibition of ceramide synthase and ceramidase, which leads to an increase in the concentration of the cytotoxic signaling molecules **sphinganine** and **sphingosine**.¹⁹ Merrill and co-workers have proposed a mechanism of action that highlights the **sphinganine**-mimicking tricarballic acid functionality interacting with ceramide synthase.²⁰ However, the toxicity of this molecule is not specific for cancer cells, making it a poor therapeutic agent. Instead, **fumonisin B₁** is utilized as a molecular tool for studying the inhibition of these enzymes.

1.1.2 Developing a Cancer Therapeutic

In the early 1990's, Liotta's laboratory designed a sphingoid base analog for inhibition of cancer cell growth. As depicted in Figure 4, this novel scaffold was designed to incorporate the properties of the mildly anti-proliferative **sphingosine** with the highly toxic nature of **fumonisin B₁**. The safety profile of **sphingosine** is far greater than that of **fumonisin B₁**, yet **sphingosine** contains a primary hydroxyl group at C-1 which allows for phosphorylation, converting the anti-growth molecule to its pro-growth variant **S1P**. Removal of the C-1 alcohol on **sphingosine**

could potentially eliminate the polarized effects of this signaling molecule, but the polarity of the molecule would be significantly changed. By borrowing from the head group of **fumonisin B₁**, which lacks this primary hydroxyl group yet contains a 1,3-diol and one free amine, Liotta hypothesized that the anti-proliferative effects of **sphingosine** may be maintained while avoiding phosphorylation at C-1 by sphingosine kinase to generate a pro-proliferative byproduct such as **S1P**. Additionally, the C-5 hydroxyl group of **fumonisin B₁** maintained the polar functionality of **sphingosine** in the head group. In concert, the alternate head group of **fumonisin B₁**, which lacks a C-1 hydroxyl group together with the mild, functional-group free tail of **sphingosine** resulted in a new compound named **Enigmol** ((2*S*,3*S*,5*S*)-2-aminooctadecane-3,5-diol), shown in Figure 4.²¹

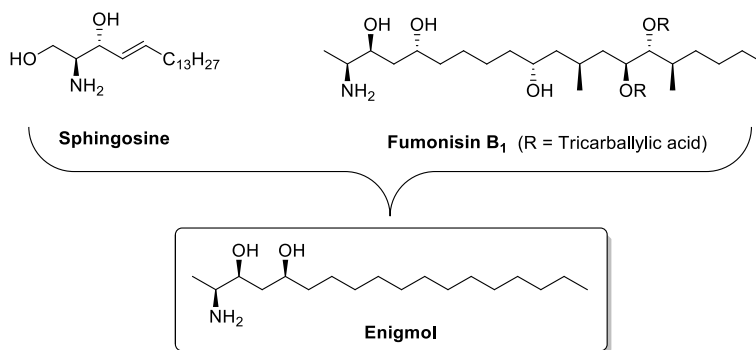


Figure 4: Conception of an anti-cancer agent, **Enigmol**, which drew from **sphingosine** and **fumonisin B₁**.

Investigation of the anti-proliferative effects was performed in collaboration with Merrill's laboratory. Initial evaluation of **Enigmol** against the National Cancer Institute's 57 cancer cell lines (NCI-60) showed EC₅₀'s of 0.4-14 μM.²² In these studies, we found that **Enigmol** was more effective than **sphinganine** or **sphingosine** against colon cancer cells, which are known to be sensitive to sphingolipids.²² In collaboration with Petros's laboratory at the Winship Cancer Institute, we investigated the efficacy of **Enigmol** against prostate cancer. In these mouse xenograft models, we found that **Enigmol** was efficacious against androgen-independent and androgen-sensitive (PC-3 and LNCaP respectively) tumors. Additionally, a

daily oral dose of 10 mg/kg of **Enigmol** resulted in equally efficacious suppression of tumor growth (Figure 5) as the current gold standard of treatment for each type of cell line (castration and docetaxel, respectively).²³ In recent years, a number of other groups have shown that there is significant interest in 1-deoxy,5-hydroxy sphingosine analogs, particularly for application as cancer therapeutics.²⁴

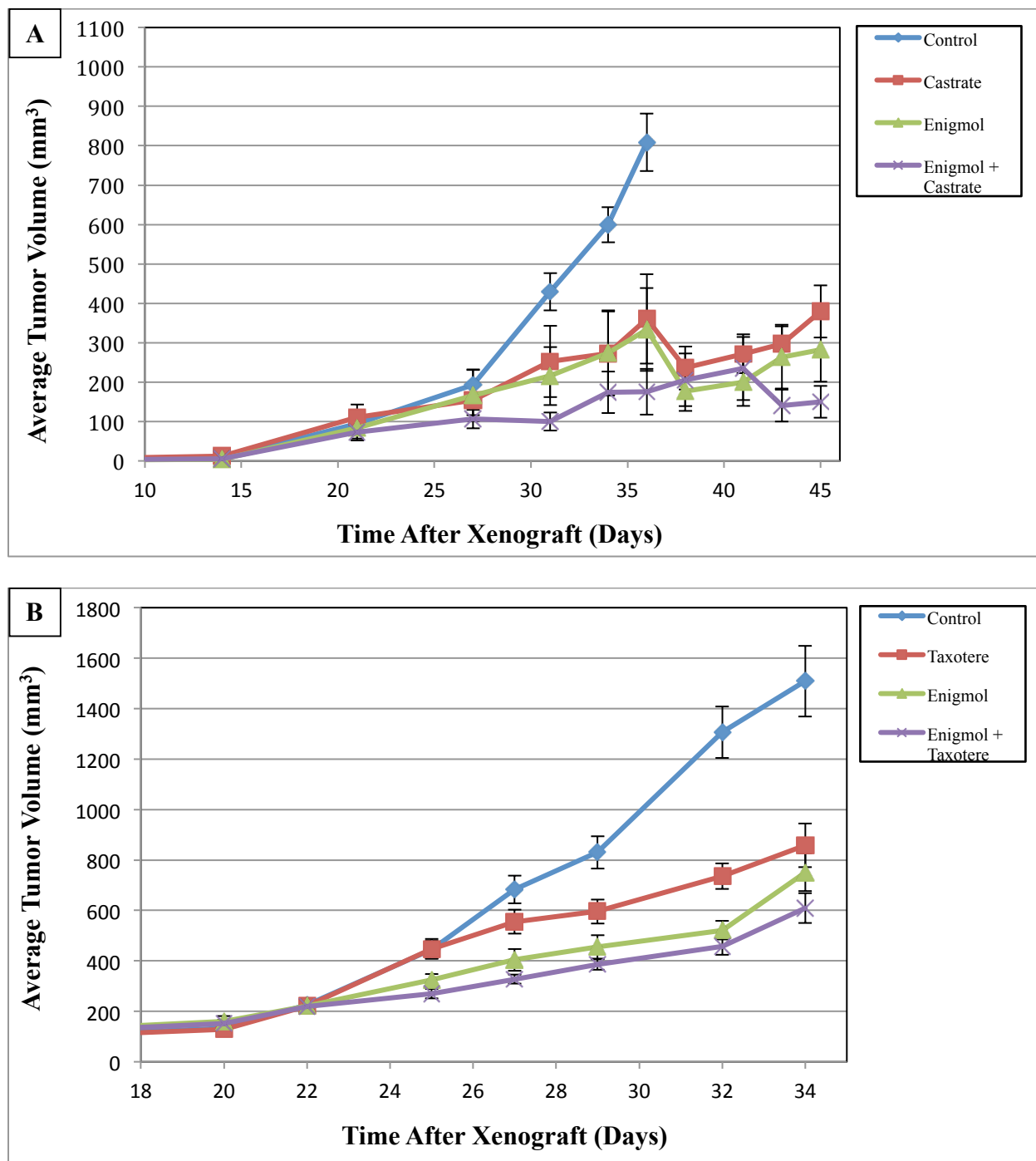


Figure 5: Mouse xenograft study comparing the efficacy of **Enigmol** to hormone ablation in androgen-dependant tumors (A) or docetaxel in androgen-independent tumors (B).²³

We hypothesized that the sphingolipid-mimicking action of **Enigmol** was largely due to the similar physical properties, namely a cationic head group with a long, flexible alkyl tail. Very

few modifications have been pursued within the long alkyl tail of **Enigmol**. To explore this region of the molecule, we set out to determine the affect of two distinct sets of changes shown in Figure 6. Firstly, we inserted fluorines in the middle and end of the tail, and secondly we introduced unsaturation in the middle of the tail between C-11 and C-12.

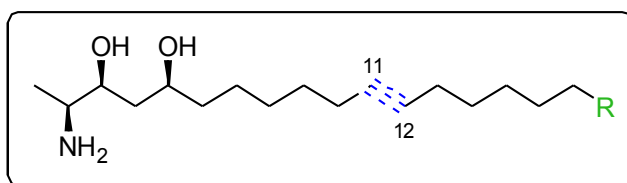


Figure 6: Proposed sites for modification on the tail of **Enigmol**.

While fluorine exhibits a similar atomic radius to hydrogen, it has a much higher electron density and electronegativity. Substitution of hydrogen for fluorine imparts the molecule with a slight increase in lipophilicity. For medicinal chemists, fluorines are typically used to replace hydrogen to decrease metabolism at a particular site. Although fatty acids are known to undergo metabolism at the omega position (last carbon on the tail), sphingolipids are not subject to this route of degradation.²⁵ When fluorinating the tail of **Enigmol**, we were interested in probing how small increases in lipophilicity in the middle and end of the tail would affect interactions with the regulatory proteins involved in lipid signaling. The increase in fluorination may strengthen hydrophobic interactions already utilized by the sphingosine like alkyl tail. These changes were hypothesized to increase partitioning into cellular membranes, delivering more of the drug from the plasma into tissues. Hence, we designed compounds **1** and **2** (Figure 7) to contain a difluoromethylene at C-11 and a trifluoromethyl group at C-18 respectively. In addition, we were interested in the fundamental property (natural isotope ¹⁹F, spin = ½) of fluorine that allows us to analyze fluorine containing molecules by NMR. This property could also allow us to detect fluorinated analogs with non-invasive magnetic resonance imaging (MRI). The ability to visualize these compounds could make it possible to determine the position and concentration of

our fluorinated analogs in the body with the use of MRI. An analogous imaging approach is ^{18}F PET, which uses radioactive labels that are quantifiable from outside the body, but has the side effect of emitting harmful positrons. In contrast to ^{18}F , ^{19}F is inert and does not emit any harmful radiation. This concept has been applied in animal models for the boron containing molecule ^{19}F -BPA-fructose for use in neutron-capture therapy, and it will be discussed in section 1.1.3.²⁶

Our second plan to introduce unsaturation in the center of the tail would allow us to determine the importance of a completely flexible tail free of geometric constraints. Such a change was hypothesized to alter membrane retention, as well as the ability of the lipid to interact with native lipids. Restricting tail flexibility has the potential to decrease the potency of **Enigmol** by deviating further from natural sphingolipid scaffold, lessening its ability to interact with native pools of sphingolipids where we hypothesize they impart their affect. Modifying the tail to include a single unit of unsaturation changes the shape of the molecule significantly. This could prevent associated **Enigmol** analogs from inhibiting enzymes involved in the sphingolipid rheostat, which, in turn, may diminish their anti-cancer activity. To asses these alterations, we designed alkyne containing **Enigmol** analog **3**, as well as the *trans*- and *cis*-**Enigmol** derivatives **5** and **7**. As will be discussed in section 1.2.2, the synthetic route utilized allowed us to access the trifluoromethyl derivatives **4**, **6**, and **8** with relative ease.

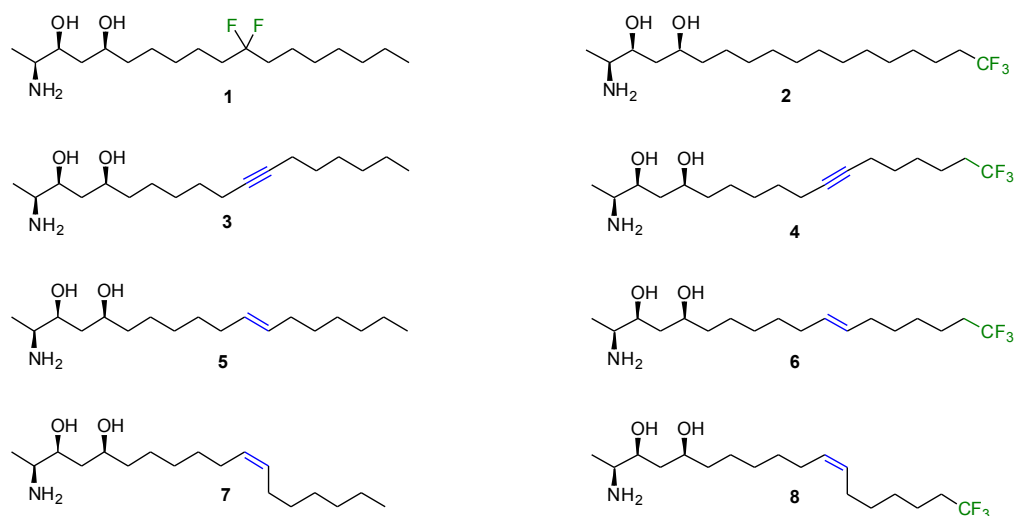


Figure 7: Proposed synthetic targets probing the affect of fluorination and geometric restrictions in the tail of **Enigmol**.

1.1.3 ^{19}F MRI Application

Magnetic Resonance Imaging (MRI) monitors the chemical environment of protons in the body, which are diamagnetic (spin = $\frac{1}{2}$), and it monitors how they respond to radio pulses in a strong magnetic field. Unlike Computer Tomography (CT) or Positron Emission Tomography (PET) imaging, MRI does not use any harmful ionizing radiation. Although most drug molecules contain protons, they cannot be visualized *in vivo* by MRI. This is because nearly every molecule in our body also contains hydrogen, making it impossible to distinguish a drug from the surrounding molecules. Fluorine is not naturally found in animals (aside from very small quantities from fluoride enriched teeth and bones in humans), reducing the background signal to nearly zero when using MRI to monitor fluorinated drugs. The use of MRI to determine the concentration *and* location of a fluorinated small molecule therefore becomes possible, and has been recently demonstrated.²⁶ ^{19}F MRI was used by Porcari and co-workers to determine the maximal concentration, in tumorous rat brain, of the boron-capture therapy agent ^{19}F -labeled boronphenylalanine-fructose complex (^{19}F -**BPA-fr**), which contains a single fluorine. The goal of this research was to determine the optimum time post injection of ^{19}F -**BPA-fr** for clinicians to

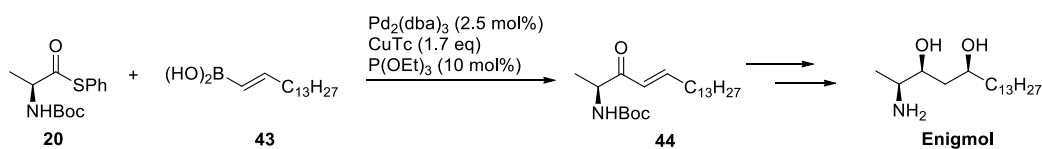
dose patients with radiation to maximize the therapeutic effect, while minimizing damage to non-tumor tissue. In order to obtain sufficient concentrations of ^{19}F -**BPA-fr** in the brain, an incredibly large dose (300 mg/kg) of the compound was injected directly into the carotid artery, resulting in a peak blood concentration of 100 mM. It was determined that their peak tissue concentration in the brain tumor was near 30 mM (2 hours post dose), which they were able to visualize by MRI.

Previous biodistribution studies by Liotta and co-workers have shown that **Enigmol** orally dosed in mice can result in drug accumulation in the brain, lung, and liver in concentrations greater than 100 μM .²⁷ This result makes fluorinated **Enigmol** analogs **1** and **2** potential candidates for ^{19}F -MRI. To maximize fluorine signal, it is desirable to have a larger number of fluorine atoms per molecule, lowering the number of molecules necessary to detect the compound. Therefore we decided to investigate the visibility of the trifluoromethyl containing **Enigmol** analog **2** in rats by an ^{19}F -tuned MRI. This will be further discussed in section 1.3.3.

1.2 Synthesis of Target Compounds

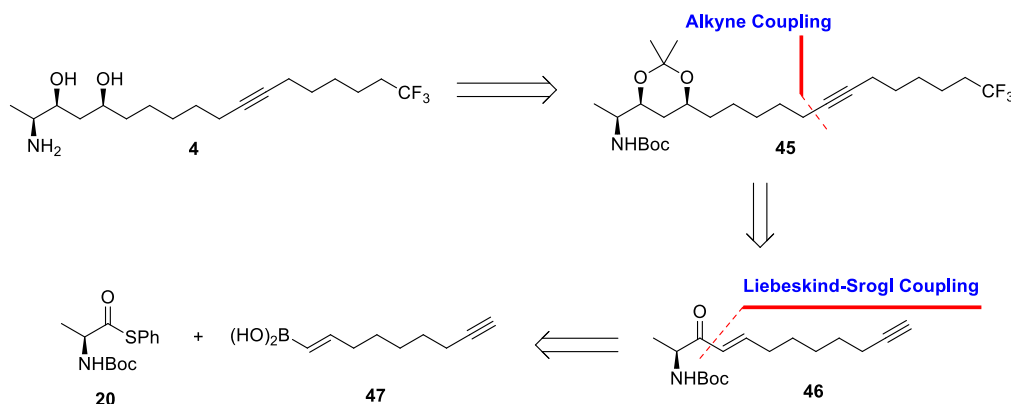
1.2.1 Liebeskind-Srogl Route and Side Reaction Investigation

Enigmol has recently been synthesized by our group utilizing the Liebeskind-Srogl coupling reaction as the key step.²³ This synthesis is summarized in Scheme 1, giving access to all four of the C-2(*S*) diastereomers in 6 steps with greater than 70% overall yield.



Scheme 1: Application of the Liebeskind-Srogl coupling to create scaffold for **Enigmol**.

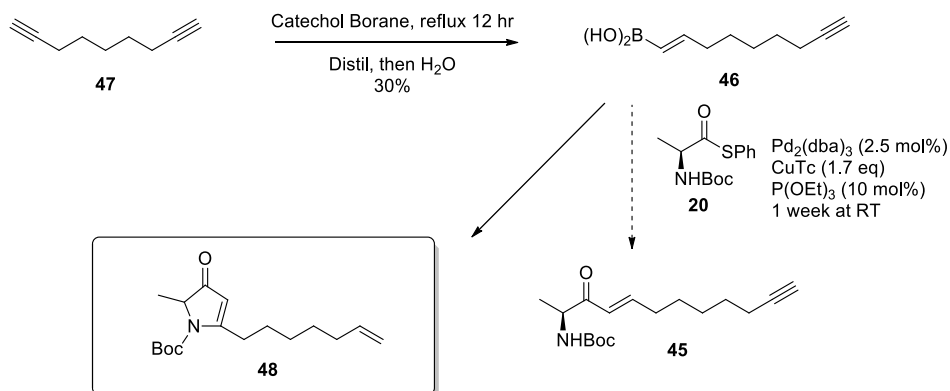
When initially devising a synthetic route to attain the tail-modified **Enigmol** analogs **3-8**, we envisioned utilizing this elegant route, which does not require a reductive deprotection as a final manipulation. In contrast to the final debenzoylation in the aldol method, this route would allow us to retain an alkene or alkyne. To apply the Liebeskind-Srogl coupling scheme to obtain product **4**, we devised a retrosynthetic route shown in Scheme 2. The first disconnection would require an acidic deprotection of **45**, which would come from an alkyne coupling to connect the tail functionality. The main carbon-carbon bond forming step would utilize the Liebeskind-Srogl coupling reaction between thiol ester **20** and vinylboronic acid **47**, which contains the desired terminal alkyne. However, this route did not yield the target molecules. Instead, we stumbled upon a very interesting side reaction that warranted further investigation. That side reaction will be the focus of this chapter.



Scheme 2: Retrosynthetic scheme envisioned to yield the tail-modified **Enigmol 4**.²³

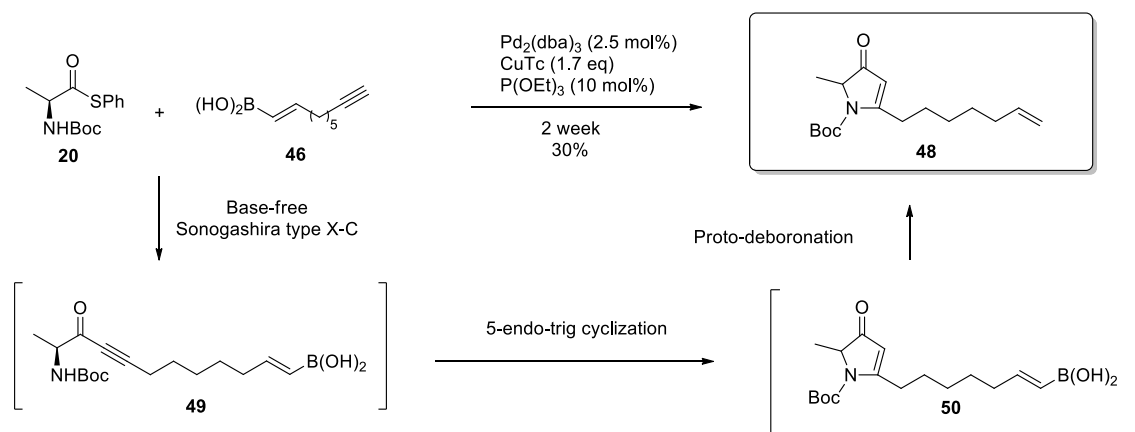
As shown in Scheme 3, conversion of diyne **47** to the mono-catechol borane intermediate, followed by hydrolysis gave the mono-vinylboronic acid **46**. Although we did not anticipate any trouble with the Liebeskind-Srogl coupling, reaction of **46** with the thiolester **20** did not yield the desired product **45**. It is important to note that this reaction was followed, not only by TLC, but also by LCMS, a technique that yields a convoluted spectrum for Boc-protected amines as the carbamate fragments very easily, leaving a host of detectable masses. Rarely is the

parent M+H ion observed. After prolonged reaction time at room temperature (>1 week), an unexpected product was isolated from the reaction mixture that showed the anticipated Boc-fragmentation pattern by LCMS. After a very thorough spectral analysis using multiple NMR techniques (^1H , ^{13}C , APT, DEPT, HMQC and HMBC), the isolated product was determined to be the cyclic product **48**, shown in Scheme 3.



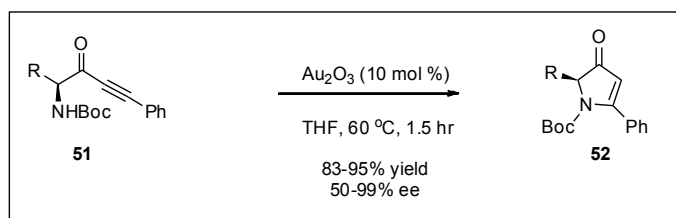
Scheme 3: Side reaction observed under standard Liebeskind-Srogl coupling conditions.

If the reaction proceeded through the intended product **45**, it would subsequently have to undergo an oxidative ring closure followed by a reduction of the terminal alkyne to produce **48**. As a more plausible hypothesis, we proposed that the terminal alkyne was involved in a Sonogashira-like coupling with the thiol ester **20** to yield ynone **49**, which then underwent a 5-endo-trig cyclization with the protected nitrogen to form the pyrrolinone **50**. Finally a protodeboronation would give **48**, as depicted in Scheme 4.



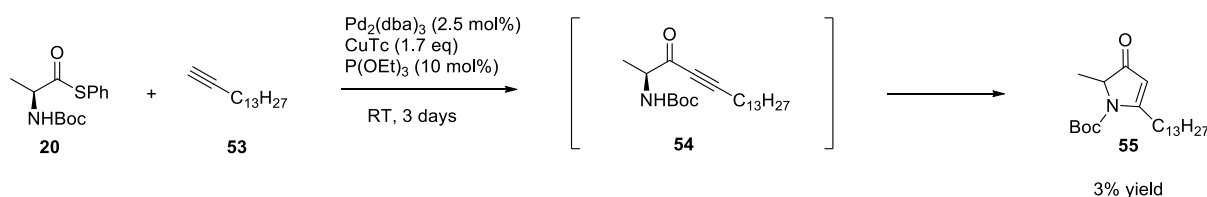
Scheme 4: Proposed mechanism for formation of the cyclized product **48**.

Literature precedence lends support to all three of these reactions individually. Cross coupling between a terminal alkyne and a thiol ester²⁸ or aromatic thiophenol²⁹ in the presence of copper and palladium has been reported. Both of these reactions occur under standard Sonogashira coupling conditions which require the addition of a base. The lack of base would be unique to our reaction. 5-endo-trig cyclization of a Boc-protected alpha-amino yne-one has also been reported using a gold-oxide catalyst.³⁰ In this example, the authors expended significant efforts to optimize the cyclization to avoid racemization of stereochemical information from the starting material **51** shown in Scheme 5. From our initial experiments, we had no evidence of stereochemical retention, but were aware that this factor would be crucial to the applicability of this multi-step reaction. Finally, proto-deboronation is known to occur as a side reaction during Suzuki couplings.³¹



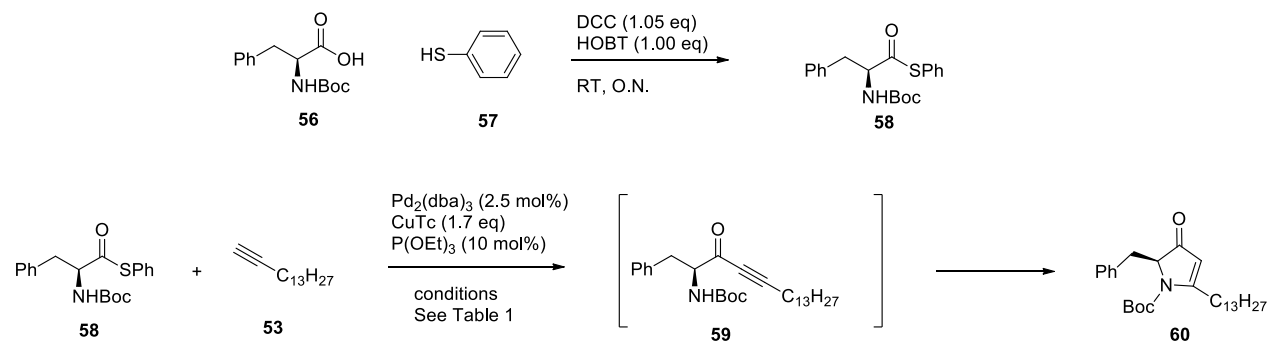
Scheme 5: Literature precedence for 5-endo-trig cyclization of an alpha-amino yne-one reported by Uriac *et al.*³²

To determine if the reaction was initiated by a Sonogashira-type cross coupling, I began with the simplified starting material **53**, which eliminated the vinyl-boronic acid and only contained a terminal alkyne (Scheme 6). To my delight, the terminal alkyne did yield the cyclized product **55**, which supported our hypothesized route depicted in Scheme 4. Despite the low yield, these results gave us initial support into the mechanism that yielded the unexpected product **48**.



Scheme 6: Test substrate pentadecyne, when subject to Liebeskind-Srogl coupling conditions, yielded the cyclized product **55**.

Aware that our potentially useful reaction was able to convert simple starting materials to a complex core structure in one step, there were two major questions that needed to be answered to determine the utility of our chemistry. First, is the starting material stereochemistry retained during the transformation? Second, can the yield be increased to >80% in order to compete with the two-step variant reported by Uriac and co-workers.³² In order to determine the extent to which stereochemistry was retained through the multi-step reaction, we synthesized both enantiomers of the UV active thiol ester **58** from phenylalanine (Scheme 7). Enantiopurity was then confirmed by chiral HPLC. Enantiopure **58** was subjected to the Liebeskind-Srogl coupling at various temperatures, and was followed by LCMS. As shown in Table 1, maximal yield of the cyclic product was obtained after 2 hours at 60 °C. Although the product from this reaction was found to be optically active, the e.e. was determined to be only 13%.

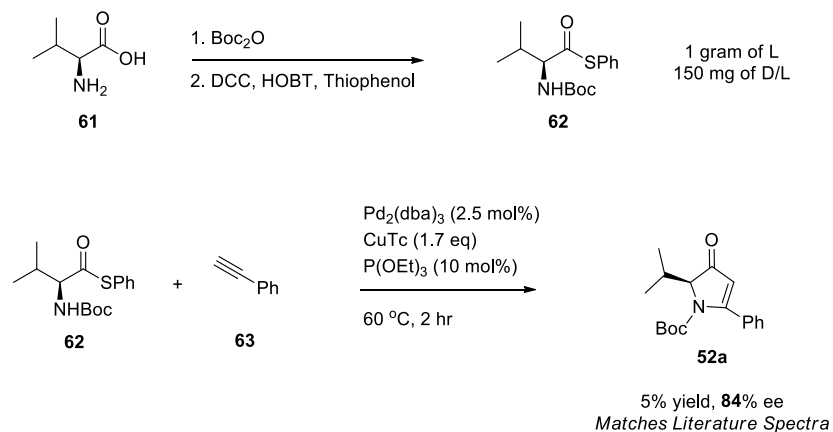


Scheme 7: Synthesis of the UV active derivative for characterization of e.e.

Table 1: Optimization of reaction conditions for cyclization utilizing Liebeskind-Srogl conditions. Followed by LCMS. Yield reported was isolated yield. (-) means isolation not attempted.

Temperature	Time*	Yield (acyclic)	Yield (cyclic)
RT	4 days	-	3%
60 °C	2 hrs	44%	27%
90 °C	2.5 hrs	-	15%
200 °C (MW)	10 min	0%	0%

Uriac and co-workers found that increasing the steric bulk of the amino acid substituent (R in Scheme 5) from the small methyl or benzyl group to a bulkier sec-butyl or isopropyl group increased their e.e. significantly. Therefore, we synthesized the *N*-Boc thiol-ester of valine (Scheme 8) and coupled this with phenylacetylene to produce the exact product reported previously.³² The isopropyl containing cyclized product was found to have an 84% e.e., a significant improvement in comparison to the 13% e.e. attained with the less bulky benzyl side chain. However, this was still not high enough to compete with previous reports of >95% e.e. In addition, our thermal optimization showed a maximal yield of 27%, which in concert with a mediocre e.e. decreased the utility of our reaction to the general synthetic field.



Scheme 8: Increasing the steric bulk of the R-group yielded an 84% e.e.

I speculated that the racemization in our reaction occurs from the tautomerization of the desired product **64** through an aromatic species **65**, which then equilibrates to either the starting material or the alternate enantiomer **66**. In a final attempt to harness this tandem reaction, I hypothesized that we could capitalize on the racemization of the stereocenter if there was some sort of chiral directing group that biased the equilibrium. Inspired by the work of John Ellman, I envisioned that introduction of a chiral sulfinyl-protecting group on the amine (**67**) may allow us access to a single diastereomeric product **68**.³³

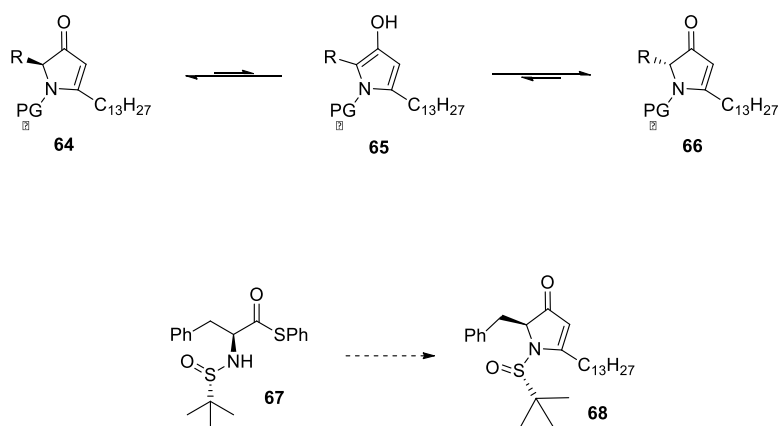
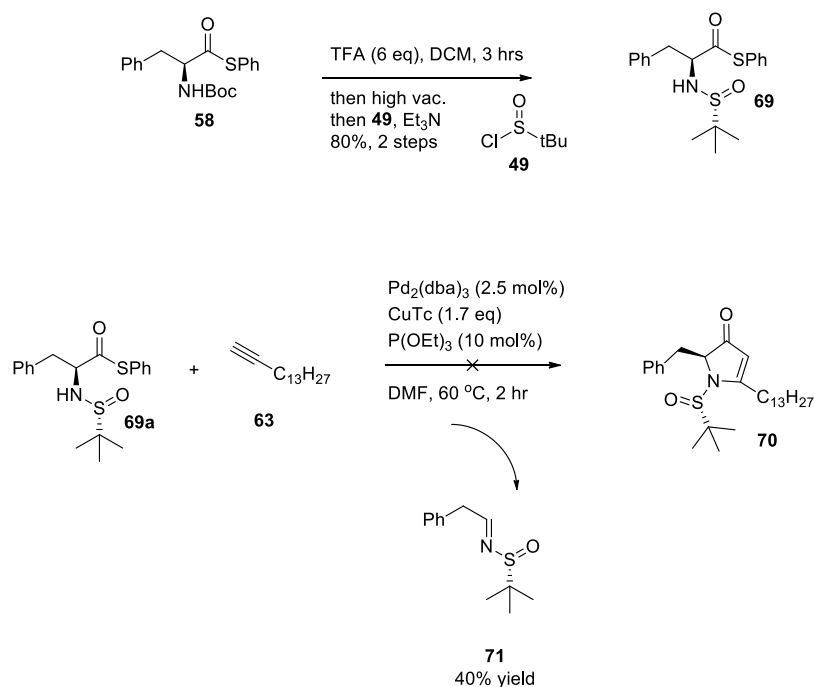


Figure 8: Rationalization for the loss of stereochemistry based on the formation of the aromatic intermediate **65**. To capitalize on the equilibrium, we proposed the chiral directing group attached to the nitrogen (**67**).

To synthesize **67**, I decided to exchange the protecting group on intermediate **58**. I first removed the Boc-group with TFA, then reacted the amine with tert-butyl-sulfinylchloride **49** to

create the mixture of sulfinyl amide diastereomers,³⁴ which were separable by chromatography. It was found that isolation of the deprotected free-amine was plagued by production of thiophenol and polymerization. Instead, I utilized the TFA salt of the amine and used an extra equivalent of base during coupling with the sulfinyl-chloride. In the subsequent reaction, each diastereomer of **69** failed to yield the desired product under the previously optimized reaction conditions mentioned above. Instead, the decarbonylated product **71** was isolated in 40% yield. Formation of this byproduct has been previously observed upon heating of the Liebeskind-Srogl reaction, and it has been reported by Liebeskind and co-workers.³⁵ After a retrospective investigation of LCMS data from the low yielding reactions mentioned above (to form **52a** and **60**), I was able to confirm significant production of the decarbonylation byproduct from the Boc-containing starting materials. Until this byproduct was characterized with the stable sulfinyl-amide protecting group (which made LCMS identification vastly simpler), we had difficulty explaining the low yields observed.



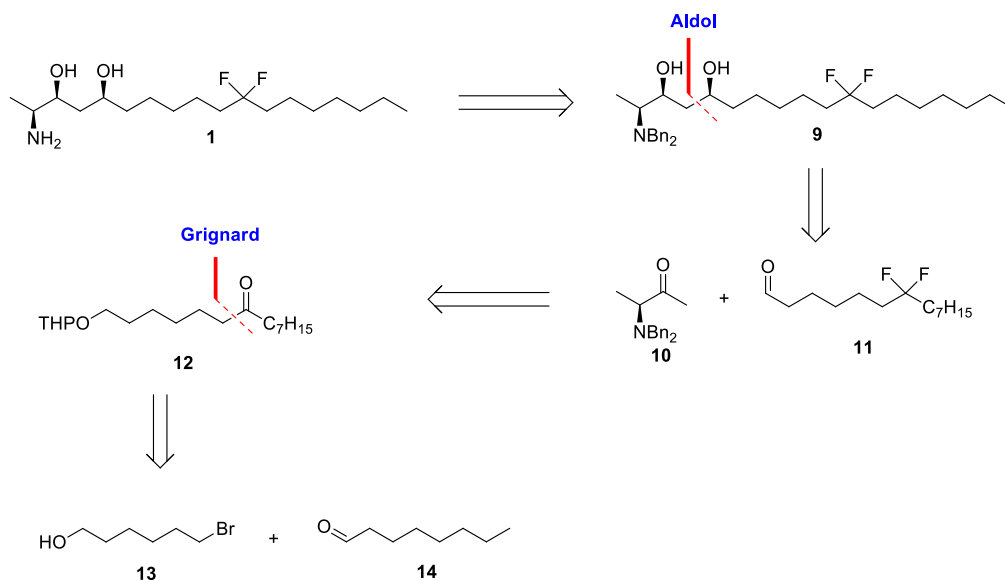
Scheme 9: Synthetic efforts towards biasing the cascade reaction with a chiral directing group.

I speculate that none of the desired cyclic product **70** was observed in this reaction due to the increased steric bulk of the *tBu*-sulfinylamide in relation to the Boc-protected variant. If revisited, perhaps a smaller protecting group such as an isopropyl sulfinylamide would allow for product formation while still acting as a directing group.

1.2.2 Synthesis *Via* Aldol Reaction

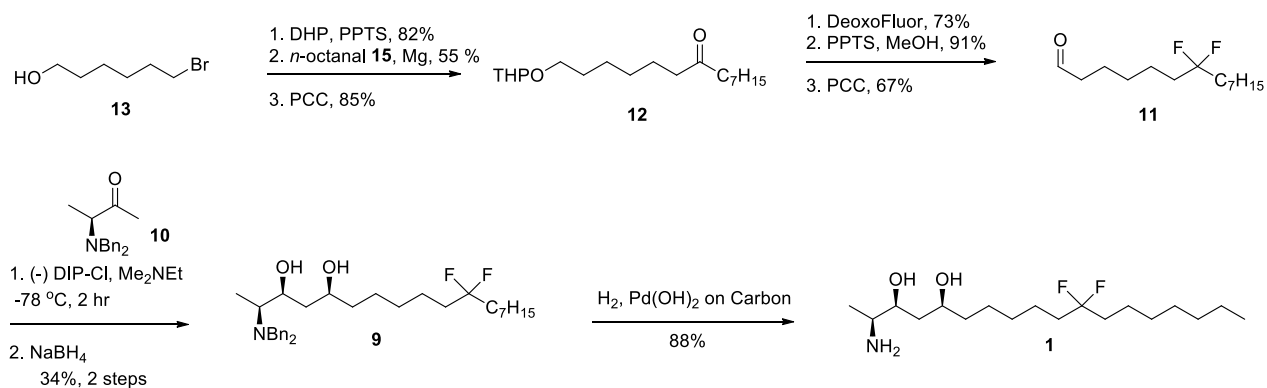
To access tail modified enigmols shown in Figure 7, I returned to the aldol route developed in our lab.³⁶ However, to preserve the alkene or alkyne moieties in the tail, we devised a deprotection sequence that did not rely on the reductive hydrogenolysis. This sub-chapter details how we successfully optimized conditions to obtain the unsaturated **Enigmol** analogs that were initially proposed.

The retrosynthesis for the C-11 difluoro-enigmol **1** is shown in Scheme 10. The product is envisioned to come from deprotection of a *N,N*-dibenzyl precursor **9**, which would come from a boron-mediated aldol reaction, developed in our lab, to create the key carbon-carbon bond.³⁶ The methyl-ketone **10** has been previously reported, while the difluoro-aldehyde **11** would come from a nucleophilic fluorination of an internal ketone **12**. A Grignard reaction was thought to connect the two commercially available starting materials **13** and **14**.



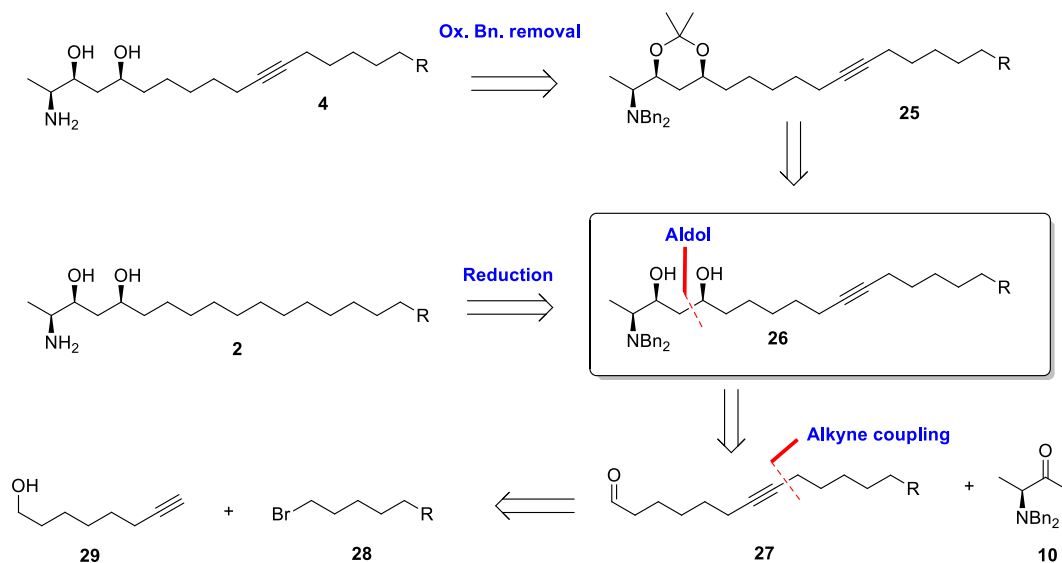
Scheme 10: Retrosynthetic scheme for the C-11 difluoro-enigmol analog **1**.

The synthesis required special preparation of a fluorine containing tetradecanal, described in Scheme 11. Starting from the bromo-alcohol **13**, the alcohol was protected with dihydropyran and catalytic acid. The bromine was then converted to the corresponding Grignard reagent with magnesium shavings, which then reacted with octanal to yield the alcohol, which was immediately oxidized to the ketone with pyridinium chlorochromate (PCC). The ketone **12** was next reacted with the nucleophilic fluorinating agent DeoxofluorTM to yield the difluoromethylene at what would become the C-11 carbon. To access the necessary aldehyde **11**, the tetrahydropyran (THP) protecting group was removed and the primary alcohol was oxidized with PCC. The aldehyde was then subject to the boron mediated aldol conditions developed in our laboratory,³⁶ which is known to racemize upon purification. Hence, the crude product was reduced as per standard protocol to yield the all *syn* product **9**. Reduction of the C-3 carbonyl in this step to the alcohol is directed by the neighboring bulky *N,N*-dibenzyl group, and gives very high diastereoselectivity (>99:1, diastereomers are separable by silica gel chromatography).³⁷ The final free amine **1** is furnished by hydrogenolysis with Pearlman's catalyst.



Scheme 11: Synthesis of C-11 difluoro-enigmol **1**.

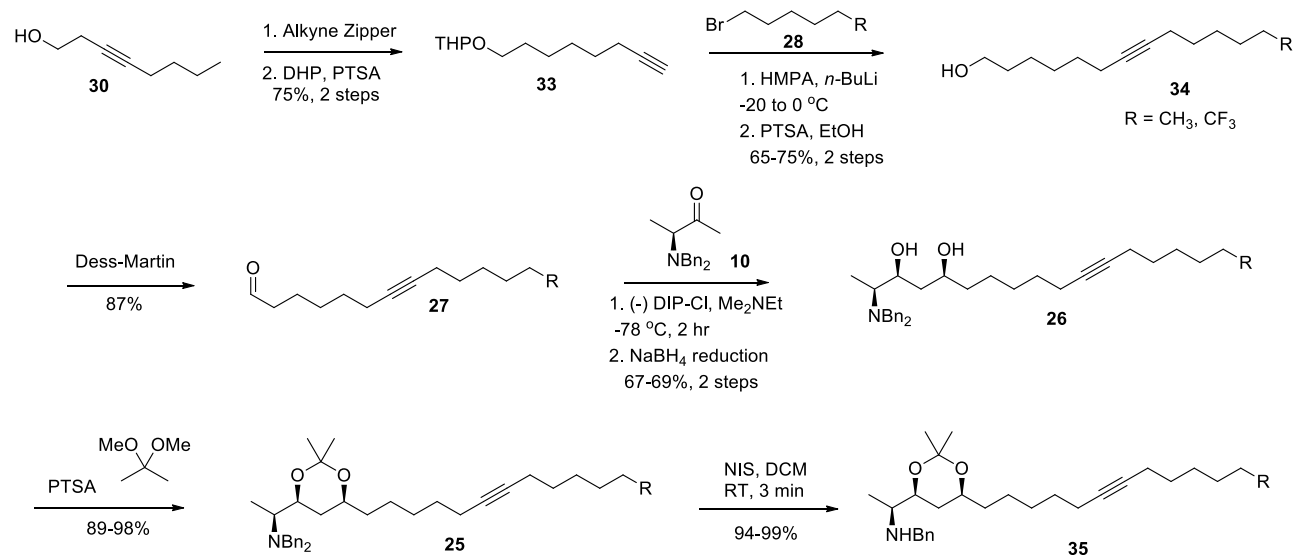
The synthesis of the tail modified enigmols **2-8** also utilized a boron-mediated aldol for the key bond forming step.³⁶ As with the aforementioned difluoro-analog **1**, novel aldehydes had to be constructed to contain what would become the tail modifications. However, the anticipated challenge in the synthesis of the geometrically constrained analogs relates to the final reductive deprotection. Under an atmosphere of hydrogen in the presence of Pearlman's catalyst, the unsaturation between C-11 and C-12 would be removed. Therefore, this section details the approach devised to remove the *N,N*-dibenzyl protecting group under oxidative conditions to preserve the unsaturation. For the retrosynthesis (Scheme 12), final alkyne containing products **3/4** were envisioned to come from the oxidative cleavage of the benzyl protecting groups on the nitrogen, which are required to set the stereochemistry in the aldol reaction in the preceding step. The aldol precursors were imagined to be the functionalized aldehydes **27**, which would be reacted with the aforementioned methyl-ketone **10**. Finally, the aldehyde was thought to stem from the alkyne coupling of a terminal alkyne and alkyl bromide such as **28** and **29**, which are either commercially available or reported in the literature.³⁸



Scheme 12: General retrosynthetic scheme for tail-modified **Enigmol** analogs containing unsaturation between C-11 and C-12 and/or fluorination at C18. R represents either CH₃ or CF₃.

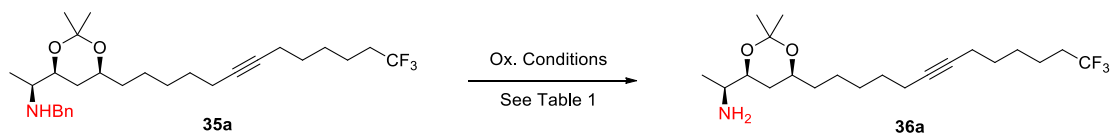
The synthesis was begun with 3-octyne-1-ol (**30**), which was subject to the alkyne zipper reaction with ethylenediamine and sodium hydride to furnish the terminal alkyne according to the procedure published by Denmark.³⁹ A subsequent protection of the alcohol gave **33** that was set up for an alkyne coupling reaction with an alkyl-bromide (1-bromohexane or 1-bromo-6-trifluoromethylhexane). From this point forward, R will represent either CF₃ or CH₃ (a and b respectively) as the procedure was identical for both until the final step, which will be discussed. When a silyl alcohol protecting group (TBS) was initially used instead of THP for **33**, the desired product was obtained but with diminishing yields during scale up. The major byproducts that detracted from product formation during scale up were determined to come from silyl-transfer of the TBS group to the alkyne, resulting in <50% yield. However, with the use of a THP acetal protecting group, the reaction proceeded smoothly.⁴⁰ Immediately after the alkyne coupling reaction, the THP group was removed (prior to purification) to greatly simplify chromatographic separation of the long chain coupled product **34** from the deprotected derivative of starting material **33**. The terminal alcohol was then oxidized with Dess-Martin periodinane made in

house⁴¹ to consistently give high yields of the aldehyde **27** with no purification necessary. The aldehyde was used immediately in the key carbon-carbon bond forming step, a boron mediated aldol reaction we have previously reported, reacting with the enolate from optically pure **10**. The resultant beta-hydroxyketone was then reduced to give compound **26**.



Scheme 13: Preparation of functionalized aldehydes for use in the aldol reaction to give advanced, semi-protected intermediates.

In order to preserve the alkyne moiety in the tail, the previously utilized reductive hydrogenolysis method for de-benzylation would not be suitable. To circumvent this, the 1,3-diol was protected as the corresponding acetonide (**25**). Cleavage of one benzyl group occurred rapidly in the presence of *N*-iodosuccinimide (NIS), although prolonged exposure (>5 minutes) produced iodination of the internal alkyne.⁴² Quantitative yields were obtained without purification using this reagent. For removal of the remaining benzylation group, a variety of conditions were screened (Table 2).



Scheme 14: Oxidative removal of the final *N*-benzyl protecting group.

Table 2: Survey of oxidative conditions for removal of *N*-benzyl protecting group from **35a**. All reaction progress was followed by LCMS. No inert atmosphere or exclusion of water was utilized in these small scale reactions (20 – 80 mg).

Conditions	Temperature	Time	Conversion by LCMS
IBX	45 °C	12 hrs	100%
Dess-Martin periodinane	RT	12 hrs	100%
CAN	RT	48 hrs	NR
DDQ	RT	30 min	Decomposition
Conc. HCl	110 °C	5 min	Decomposition
AlCl ₃ , Anisole	RT	12 hrs	Decomposition
DIAD	RT	48 hrs	40%

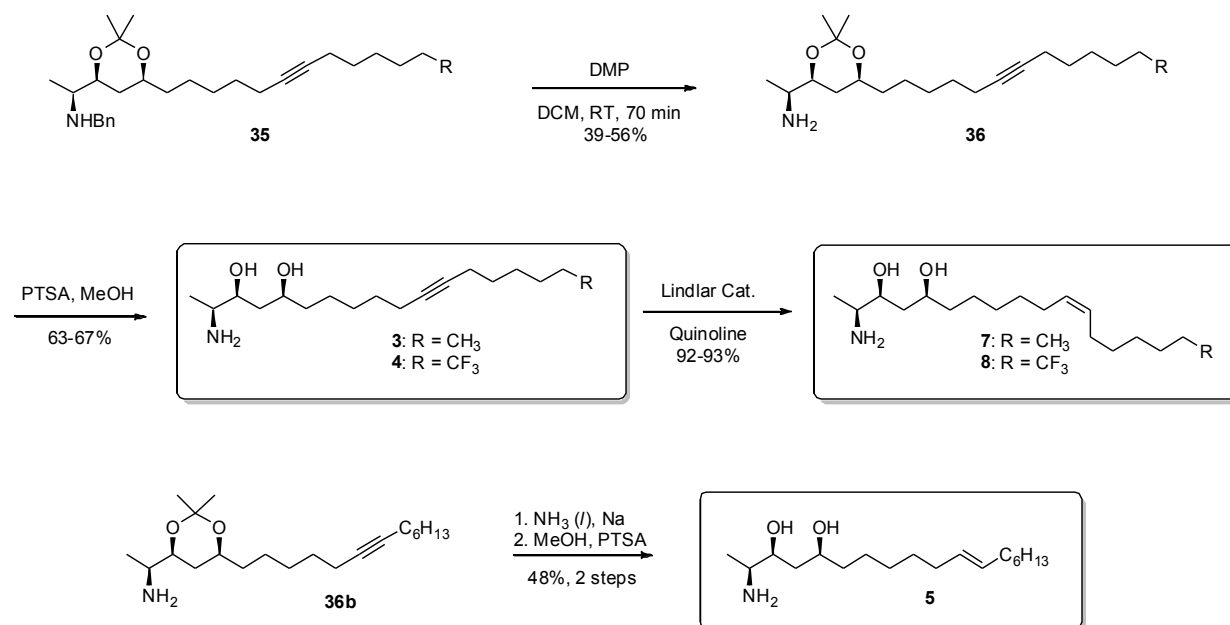
After further investigation and scale-up of both IBX and Dess-Martin periodinane, Dess-Martin was found to be far superior, as shown in Table 3. This source of hypervalent iodine provided the best results if allowed to react for 90 to 110 minutes and not more as byproducts became prevalent that were not observed in small scale reactions.

Table 3: Optimized conditions for oxidative removal of *N*-benzyl protecting group with Dess Martin periodinane.

Conditions	Equivalents	Temperature	Time	Yield
Dess-Martin periodinane	1.5	RT	70 min	39% (200 mg)

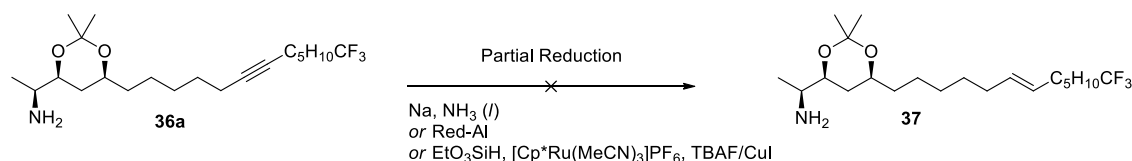
The newly developed 2-step methodology for oxidative cleavage of the *N,N*-dibenzyl group was implemented to yield compound **36** (Scheme 15), which after a simple acid mediated deprotection of the acetonide yielded the alkyne-enigmol derivatives **3** and **4**. To obtain the cis-alkene targets, a Lindlar reduction of alkynes **3** and **4** provided **7** and **8** in excellent yield with little no noticeable over-reduction. However, the radical reduction using Birch-type conditions to access the trans-alkenes was found to be problematic. Initially, compound **36b** underwent the

reduction as envisioned to give **5**, however in the presence of radicals, the fluorines proved troublesome.



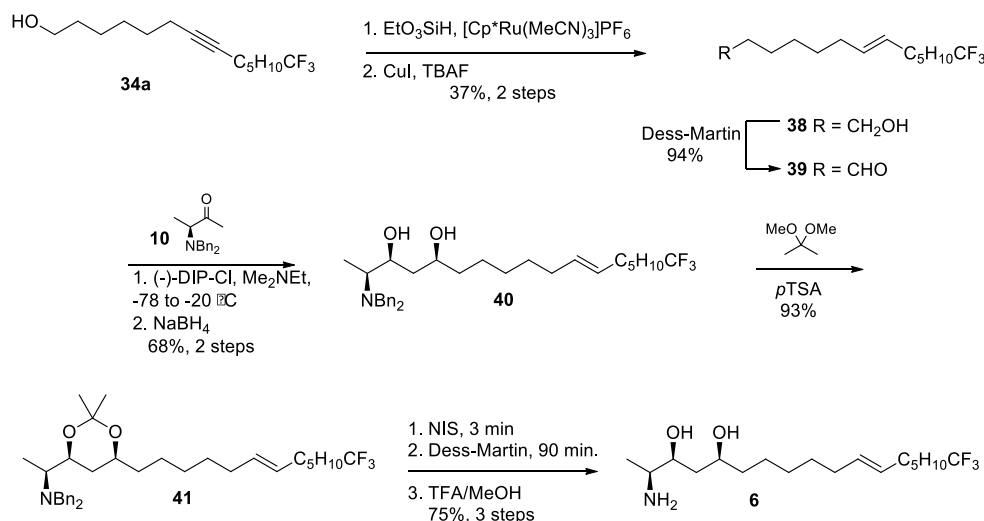
Scheme 15: Completion of synthesis for tail modified enigmols **3**, **4**, **5**, **7**, and **8** with optimized oxidative removal of the *N,N*-dibenzyl protecting groups.

Utilizing LCMS to monitor the reaction of trifluoromethyl containing **36a** under radical conditions, de-fluorination was evident prior to reduction of the alkyne. I attempted to circumvent this problem with hydride reduction by various reagents, but these showed no reaction. Intrigued by the reduction reported by both Trost and Fürstner to give exclusively the trans-alkene by hydrosilylation followed by protodesilylation, we subjected our alkyne containing compounds to this ruthenium mediated reaction.⁴³ However, when applied to the advanced intermediate **36a**, the reaction failed to give more than trace amounts of the desired alkene **37**. The failure was thought to originate from the free nitrogen poisoning the ruthenium catalyst, but the *N,N*-dibenzyl intermediate **25** also gave no isolated trans-product.



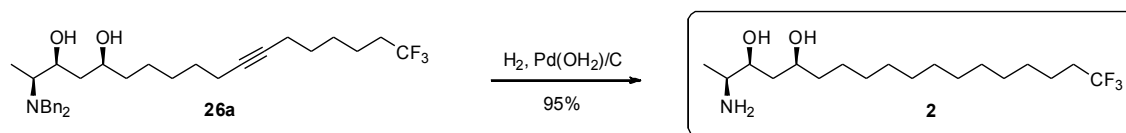
Scheme 16: Reductive conditions attempted for the transformation of alkyne **36a** to the trans-alkene **37**.

In order to attain the final alkene product **6**, the hydrosilylation procedure was applied to the much simpler substrate **34a**. To our satisfaction, the hydrosilylation and protodesilylation did furnish the desired trans-alkene, although in mediocre yields. The trans alcohol was carried through the same sequence as outlined previously to give the trans product **6** in 45% yield (Scheme 17), a vast increase from the more reactive alkynyl compounds (compare with 18-21%).



Scheme 17: Furnishing **6** by application of hydrosilylation/protodesilylation of internal alkyne **34a**, followed by application of our newly developed procedure.

To obtain the final, saturated analog, the *N,N*-dibenzyl alkynyl trifluoromethyl intermediate **26a** was subjected to standard hydrogenolysis conditions to give the C-18 trifluoromethyl-enigmol **2** (Scheme 18). This final reaction was scaled up to 2 grams in anticipation of advanced biological evaluation.



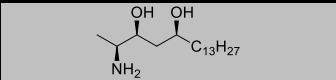
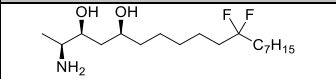
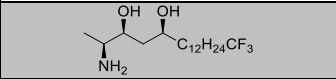
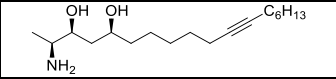
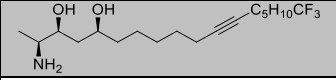
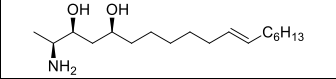
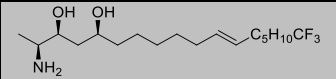
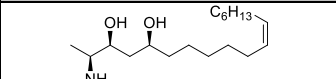
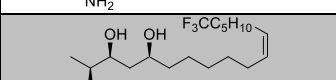
Scheme 18: Reduction of advanced intermediate **26a** was performed to attain the C-18 trifluoromethyl-enigmol **2**.

1.3 Biological Evaluation

1.3.1 *In vitro* Evaluation of Enigmol Analogs Against Prostate Cancer

Enigmol analogs with fluorination and varying levels of unsaturation in the tail were subjected to an *in vitro* prostate cancer cell toxicity assay (WST-1) as previously described.²³ All compounds were tested against androgen-dependant (LNCaP) and androgen-independent (PC-3) cell lines. These assays were performed by Suzanne Mays, a member of the Petros laboratory at the Winship Cancer Institute. The cells were incubated for 24 hours with a 1:1 stoichiometric mixture of the **Enigmol** analogs and bovine serum albumin (BSA) which we have found increases solubility of our compounds. After this time period, cell viability was assessed. IC₅₀ values based on a dose response are reported in Table 4.

Table 4: Efficacy of **Enigmol** analogs against prostate cancer cells for 24 h, and cytotoxicity was assessed by WST-1 assay. cLogP calculated with QuikProp on Maestro.

Compound	Structure	cLogP	LNCaP IC ₅₀ (μM)	PC-3 IC ₅₀ (μM)
Enigmol		3.47	13	10
1		3.82	18	13
2		4.13	13	13
3		3.42	>100	>100
4		3.70	>100	92
5		3.38	19	33
6		4.10	14	27
7		3.49	19	25
8		4.17	22	43

1.3.2 Pharmacokinetic Evaluation

To determine if a full pharmacokinetic (PK) study was justified, a preliminary PK study was performed with the trifluoromethyl-enigmol **2** in rats (n = 2, 30 mg/kg oral gavage dose). This study hinted that the peak plasma concentration of the enigmol-derivative was 2 to 3 fold higher than **Enigmol**.⁴⁴

Energized by this preliminary pharmacokinetic data, we proceeded to establish a full PK study on this compound. These studies were designed in collaboration with, and carried out by, the Emory Institute for Drug Discovery (EIDD) DMPK lab (Drs. Rick Arrendale, Randy Howard, Prabhakar Reddy, with the assistance of Deborah Culver and Taylor Evers). The goal of this study was to directly compare the pharmacokinetic properties of **Enigmol** with our trifluoromethyl-enigmol analog **2**. We were interested in following the plasma concentration over 24 hours to determine the tissue concentrations of each of the compounds at 24 hours, and to calculate the bioavailability of each compound in the same study. Bioavailability describes how much of an oral dose of a drug reaches the plasma when compared to directly injecting the drug in to the body. Calculating this drug property requires both an oral (P.O.) and intravenous (I.V.) dose of a drug, from which the P.O. dose-corrected area under the curve (AUC) is divided by the I.V. AUC. This can be described by the equation $\text{Bioavailability} = (\text{AUC}_{\text{I.V.}} * \text{D}_{\text{P.O.}}) / (\text{AUC}_{\text{P.O.}} * \text{D}_{\text{I.V.}})$.

In this study, we directly compared **Enigmol** to compound **2**. Since we had previous data for the I.V. administration of **Enigmol**, this group did not need to be repeated. Our study therefore consisted of 3 groups of rats, each with n = 4 rats. Jugular pre-cannulated Sprague Dawley rats were purchased from Harlan (250-300 g). Group 1 received **Enigmol** by P.O., group 2 received **2** by P.O., and group 3 received **2** by I.V. All animals dosed by P.O. received 10 mg/kg of the compound in a 90:10 mixture of olive oil/ethanol while the I.V. group received a 2

mg/kg dose in PEG400/ethanol/Tween 80/Water; 40/10/3/47. This method is a direct replication of the I.V. data we collected from the previous **Enigmol** study. Figure 9 and Table 5 summarize the data from this study.

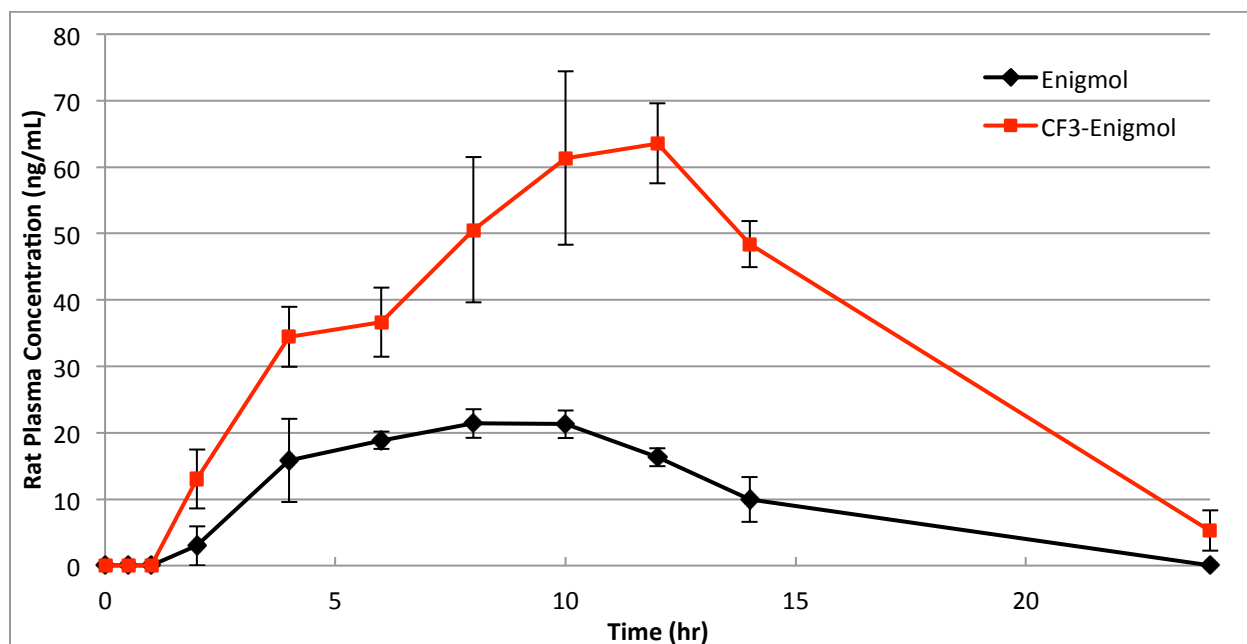


Figure 9: Pharmacokinetic data comparing mean plasma concentrations of **Enigmol** to CF₃-enigmol (**2**) over 24 hours.

Table 5: Mean pharmacokinetic parameters for **Enigmol** and CF₃-enigmol (**2**). Performed by the DMPK lab, EIDD.

Compound	Dosing Route	T _{max} (hrs)	C _{max} (ng/mL)	T _{1/2} (hrs)	AUC (0-t) (hrs*ng/mL)	AUC (0-∞) (hrs*ng/mL)	AUC Extrap. (%)	V _z _F (L/kg)	C ₁ (L/kg/hr)	BioAvail (%)
Enigmol	P.O.	9.0	25	4	198	278	29	221	36	11
	I.V.	0.8	737	4	437	515	15	22	0.8	
2	P.O.	12	69	6	725	970	25	82	11	76
	I.V.	0.8	597	1.3	229	225	10	15	8.0	

From this data, we can see an approximate 3 fold increase in plasma concentration from **Enigmol** to **2** (see also Figure 9). Specifically, the C_{max} and AUC (0-∞) are 2.8 and 3.5 fold higher respectively for **2** than **Enigmol**. The introduction of fluorination at the end of the tail on **Enigmol** clearly increases the amount of the compound that is absorbed into the blood stream. More astonishing is the increase in bioavailability, which for **Enigmol** was found to be 11% (18% found in previous study)⁴⁵ as compared to 76% for **2**.⁴⁶ This startling difference between

these two compounds may offer great promise in terms of druggability of **2** as a cancer therapeutic. By achieving over 3 fold higher concentrations in the plasma, the quantity of the compound required for dosing drops significantly, reducing therapeutic costs. Additionally, a therapeutic effect for **Enigmol** has been observed in prostate cancer xenograft models with a 10 mg/kg oral dose in this vehicle. From this data we may extrapolate that a dose as low as 2 mg/kg of **2** could achieve the desired clinical effect of tumor suppression. Alternatively, if the compound is well tolerated at 10 mg/kg, this could lead to an increased effective dose to the tumor, which ultimately may lead to greater efficacy than previously observed with **Enigmol**.

Organs from the animals in the PK study were analyzed to answer two separate questions. First, we wanted to determine if the trend for increased plasma concentrations of **2** in relation to **Enigmol** translated to increased tissue accumulation. Table 1 shows the absolute tissue concentrations as determined by LC-MS/MS ESI analysis for Red Blood Cells (RBC's) and tissue homogenate from five organs (liver, lung, brain, prostate and kidney) harvested at 24 hours after dosing. To our elation, the increase in plasma concentration of **2** in comparison to **Enigmol** also translated to an increase in tissue levels. Liver and brain showed a 1.8 fold increase in concentration of **2**, lung, kidney and RBC's showed a 3.5 fold increase, while prostate showed maximal differentiation at 4.5 fold increase in relative concentration.

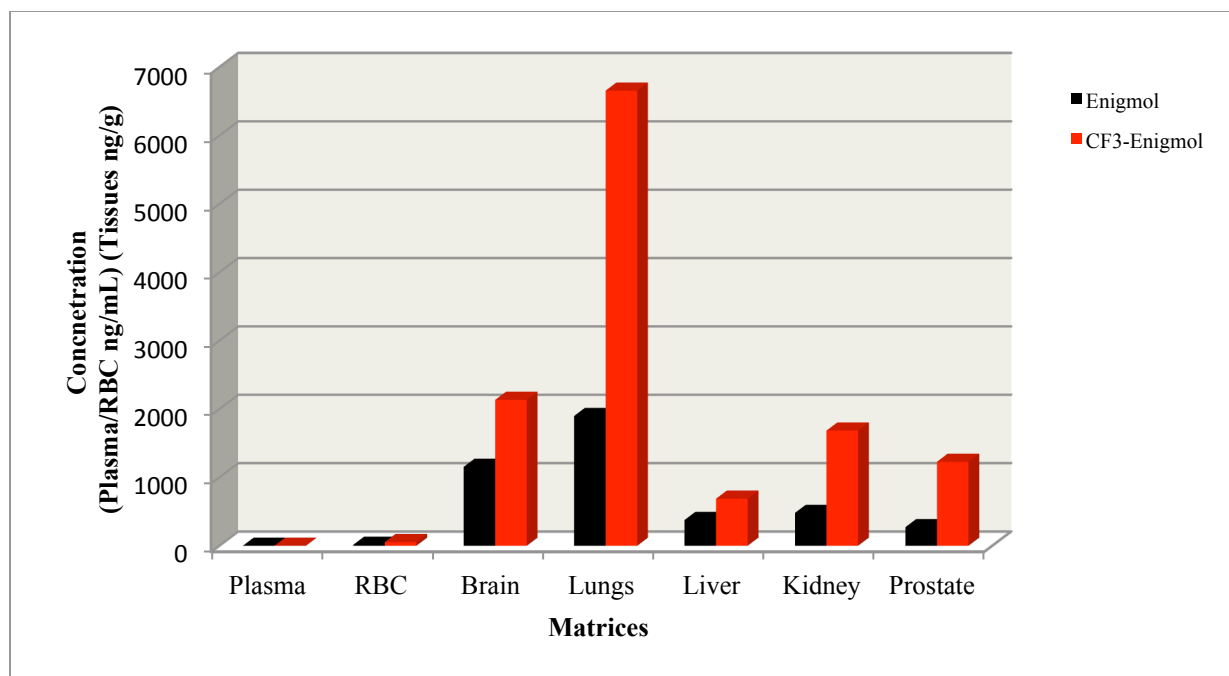


Figure 10: Mean rat tissue, plasma, and RBC concentrations at 24 hours post administration of **Enigmol** versus trifluoromethyl-enigmol **2** (10 mg/kg P.O. dose). Analysis performed by the DMPK lab, EIDD.

Table 6: Mean rat tissue concentrations of **Enigmol** and trifluoromethyl-enigmol **2** shown in **Figure 10**.

Compound	Dosing Route	Liver (ng/g)	Lung (ng/g)	Brain (ng/g)	Prostate (ng/g)	Kidney (ng/g)	RBC's (ng/mL)
Enigmol	P.O.	377	1899	1155	272	481	14.5
2	P.O.	689	6659	2135	1229	1685	54.6
	I.V.	87	562	244	296	156	0

1.3.3 ¹⁹F MRI Study Results

To determine the minimal detectable level of our compound **2**, Jaekeun Park in the laboratory of Xiaoping Hu at the Emory/Georgia Institute of Technology Biomedical Engineering organization tuned the small animal 9.4 T MRI scanner to detect the fluorine signal of this compound. We then performed a series of scans on solutions of varying concentrations of **2** in a phantom to determine the minimal detectable level of our compound. From these initial studies, we found that **2** at a concentration of 3 mM was weakly visible over the background (data not shown). However, 10 mM and 30 mM were quite visible. Hence, I was aware that we

would need to achieve incredibly high concentrations of **2** in the brain before we would be able to visualize its localization.

My primary goal for the animal ^{19}F MRI study was to achieve the maximum quantity of fluorinated compound in the animals in order to visualize the spatial localization. Since we had determined that the minimal detectable concentration of **2** was 3 mM in a phantom, I designed the experiment to deliver what we predicted to be the maximum tolerated dose. To do this, the rats ($n = 4$) were scheduled to be dosed by oral gavage (P.O.) at 30 mg/kg twice daily for five days. However, after a successful initial morning dose (day 1), Randy Howard encountered problems during the second dose given that evening. When attempting to administer the oral gavage, fluid was not able to reach the stomach, and instead was visible in the mouth of the rat. This suggests either that the stomach still contained an excess of fluid or that the esophagus was closed just above the stomach. This same phenomenon was observed on a second animal that was in the treatment group, although a control animal receiving vehicle alone showed no such issue. The other 2 non-control animals were not dosed at the end of the first day. Dosing on the morning of day 2 was changed to inter peritoneal (i.p.) injection of $1/5^{\text{th}}$ of the dose (based on an estimated 20% oral bioavailability from previous studies with **Enigmol**). This dosing regimen was continued for the remainder of the trial (4 days) on all of the animals.

On day 6, Park put the first rat under consciousness with isoflurane anesthesia, and then proceeded to take an initial ^1H MRI image for spatial reference of the brain. Once this was complete, he utilized a specially designed ^{19}F brain coil for increased resolution. Figure 11 shows the ^1H MRI image next to the ^{19}F MRI image obtained during the scanning of animal 1. Unfortunately, the only signal detected from the ^{19}F MRI was ever so slight in the fatty tissue

around the base of the neck. Due to the lack of signal and the time required to image each animal, we did not image the remaining 3 animals.

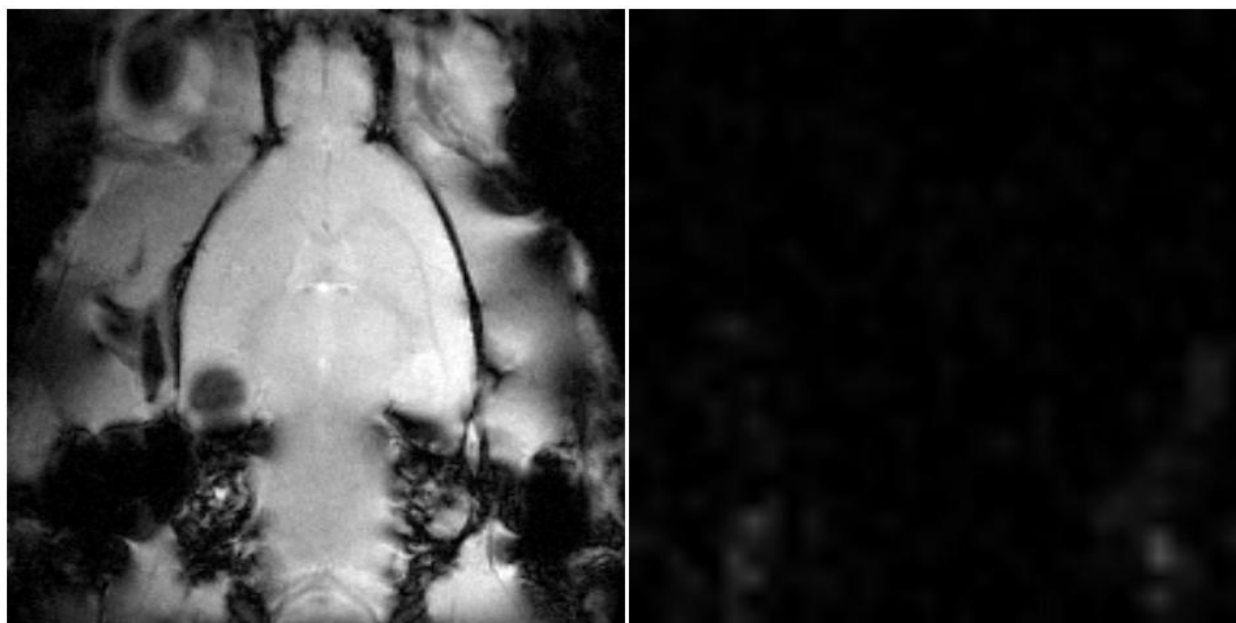


Figure 11: ^1H (left) and ^{19}F (right) MRI images of rat brain, dosed with **2**.

To change the dosing regimen in the middle of the study, we had assumed that the bioavailability of **2** was on par with **Enigmol** at $\sim 20\%$ instead of $\sim 75\%$ which it was subsequently determined to be two months after this study (reported in Section 4.2). If this study were to be repeated to increase the odds of obtaining a visual understanding of the distribution of **2**, we would either use a smaller oral dose of **2** (10-20 mg/kg) for the duration of the study, or give an i.p. injection that was 75% of the oral dose ($0.75 \times 30 \text{ mg/kg} = 22.5 \text{ mg/kg}$). With either of these changes, there is a much greater chance that we would have been able to obtain an image of this compound in the brain, and possibly other organs in the animals. However, from the data we did obtain, we can conclude that the concentration in the brain of these rats, which were dosed once at 30 mg/kg orally, then at 6 mg/kg i.p. for days two through five did not reach the minimal required concentration of 3 mM for visualization by ^{19}F MRI.

1.4 Discussion

We set out to probe the effect of modifications in the tail of **Enigmol** to determine how this would alter the anti-cancer activity and drug properties of this series. We hypothesized that the pluripotent activity of **Enigmol** imparts an influence on the **ceramide/S1P** rheostat by reinstating the careful balance between cell survival and apoptosis. Partial sphingosine kinase inhibition with **Enigmol** has been previously reported, which may also contribute to cellular toxicity.²² However, this affect should be accompanied by a relative increase in the ratio of **sphingosine** to **S1P** to balance the rheostat, which has not been observed *in vitro* in two previous studies.⁴⁷

When deciding what modifications to perform on the tail of **Enigmol**, we first selected an approach common to medicinal chemistry, which was to replace hydrogen atoms with fluorines in order to decrease potential metabolism, as well as to impart that portion of the molecule with a slight increase in hydrophobicity. With the swapping a methyl or methylene group for the per-fluorinated equivalent, we would impart the whole molecule with a relatively moderate increase in hydrophobicity. In our case, the calculated Log P (cLogP, reported in Table 4) shifted from 3.47 for **Enigmol**, to 3.82 for the difluoromethylene containing derivative **1**, to 4.13 for the trifluoromethyl derivative **2**. A drastic increase in lipophilicity could significantly decrease solubility, and would likely influence partitioning into cell membranes of the gut and not release into the circulating bloodstream. However, a moderate increase in lipophilicity may impart the molecule with more staying power, allowing a larger portion of the compound to be absorbed through the gut, while being released into the blood stream. Additionally, the compound may then partition to a higher degree from plasma into fatty tissue resulting in higher therapeutic dose to organs of interest such as lung, brain, and prostate.

Our structurally novel fluorinated analogs performed equally as well as **Enigmol** against cancer cells in our prostate cancer cell based assays (Table 4). This initial result was not in itself reason for celebration, but it did open the door for determining if the drug properties of this series would be improved with fluorination. A subsequent PK study of the trifluoromethyl containing compound **2** showed a significant increase in the plasma and tissues concentrations when directly compared with **Enigmol**. In addition to a three fold increase in plasma and tissue concentrations, bioavailability jumped from 11% for **Enigmol** to 76% for **2**. These values do not translate directly to what I expect to see in human patients, but they give us an idea of the trends I would expect to see. Conservatively, I may predict that we would see a three to four fold increase in patient plasma concentration. This increase would induce a potency boost of the compound, or alternatively, a decrease in the dose required for therapeutic efficacy.

I speculate that the boost in absorption occurs due to the increase in lipophilicity, which may lead to a slight improvement in uptake of the compound through the gut into the plasma. With an increased plasma concentration, it is logical that the lipophilic compound will partition into the tissues at proportionately increased levels. Further investigation of stability and metabolism would be required to better understand how this fluorinated analog manages to accumulate at such high levels in these animals.

The second major set of modifications we implemented in the tail of **Enigmol** was varying the level of unsaturation between C-11 and C-12. These changes not only altered the geometric configuration of the molecule, but also imparted rigidification on a part of the molecule that was previously flexible part of the molecule. Since a singular target has not been identified for these compounds, we hypothesized that they may share a binding pocket with **sphingosine** on an enzyme that is involved in the **ceramide/S1P** rheostat. In order to fit into this

binding pocket, a geometric kink in the middle of the tail was expected to keep the **Enigmol** analog from being able to enter or orient properly. Also, the alkyne-containing analog includes a 4-carbon rigid bar in the middle of what was previously a flexible tail. This could keep the molecule from changing conformation to fit into the pocket of an enzyme. Out of all of these modifications, it was hypothesized that the *trans*-alkene would maintain potency due to its relatively benign conformational change from when the tail is stretched out. However, we found that both the *cis* and *trans* derivatives, regardless of fluorination at the C-18 carbon, performed more poorly than **Enigmol** with IC₅₀ values ranging from 14-22 μM in LNCaP cells and 25-43 μM in PC-3 cells as compared to 10 μM for **Enigmol** in both cell lines. Alkyne containing compounds **3** and **4** showed nearly no detectable activity in our cancer cell assays even at concentrations as high as 100 μM. This body of data suggests that there is a cellular target that does not allow for geometric constraint and rigidification of the long tail. Removing the flexibility in this portion of our molecule decreased or completely removed the ability of the compounds to reregulate apoptosis in cancer cells. We hope that the targets for this series of compounds will be elucidated in the near future, as this will allow us to develop a computational model to design analogs with more tolerable modifications.

1.5 Conclusions

Little was previously known about the effect on potency of modifications to the long alkyl tail of **Enigmol**. To probe tail modifications, we successfully synthesized derivatives **1-8**. These compounds contained a CF₂ at C-11 (**1**) or CF₃ group at C-18 (**2**), a *cis*-alkene between C-11 and C-12 (**3**) in concert with a CF₃ at C-18 (**4**), a *trans*-alkene between C-11 and C-12 (**5**) in concert with a CF₃ at C-18 (**6**), and finally an alkyne between C-11 and C-12 (**7**) in concert with a CF₃ at C-18 (**8**). Although the unsaturation in the middle of the tail reduced the potency of

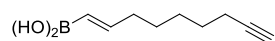
these **Enigmol** analogs, the fluorinated analogs retained efficacy against prostate cancer cells. The CF₃-containing analog **2** was further evaluated for PK properties, where we saw a drastic increase in plasma and tissue levels after a 10 mg/kg P.O. dose, as compared to **Enigmol**. Especially exciting was the increase in bioavailability from 11% to 76%. The novel compound **2** shows great promise and will be further evaluated for its effectiveness as a potentially low-toxicity chemotherapeutic agent for prostate cancer.

1.6 Methods and Experimental Protocol

1.6.1 Experimental Procedure for the Synthesis of Tail-modified Enigmols:

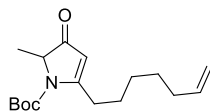
General: All solvents were dried and degassed by the SG Waters Glass Contour System unless otherwise specified. The ¹H, ¹⁹F, and ¹³C NMR spectra were recorded on Varian Inova 400 MHz spectrometer in deuterated chloroform (CDCl₃) with the solvent residual peak (CDCl₃: ¹H = 7.27 ppm, ¹³C = 77.2 ppm) as internal references and trifluoroacetic acid as external reference (¹⁹F, TFA = -75.8 ppm) unless otherwise specified. Data are reported in the following order: chemical shifts are given (δ); multiplicities are indicated as br (broadened), s (singlet), d (doublet), t (triplet), q (quartet), m (multiplet), app (apparent); coupling constants, *J*, are reported (Hz); integration is provided. Infrared absorption spectra were obtained on a Thermo Scientific Nicolet 370 FT-IR spectrophotometer via the Smart Orbit Diamond Attenuated Total Reflectance accessory. Peaks are reported (cm⁻¹). Elemental analyses were performed by Atlantic Microlab, Inc (Norcross, Ga.). High resolution mass spectrometry was performed by the Emory University Mass Spectrometry Center (Dr. Fred Strobel). Optical rotation was measured on a Perkin Elmer 341 Polarimeter. Microwave reactions were performed in a Biotage Initiator EXP microwave synthesizer. Melting points (mp) were taken in open capillary tubes on a 200W MelTemp capillary melting points apparatus and are not corrected. Analytical thin-layer chromatography

(TLC) was carried out on commercial Aldrich aluminum-supported silica gel plates (thickness: 200 μm) with fluorescent indicator (F-254). Visualization was accomplished by UV light or stained with ninhydrin, potassium permanganate, or sulfuric acid (4% aqueous). Flash column chromatography was done with a Teledyne ISCO CombiFlash Companion automated flash column system with silica packed columns from Silicycles unless otherwise specified. LCMS was performed on an Agilent 1200 HPLC with a 150 x 4.6 mm or 50 x 4.6 cm C18 XDB eclipse 5 μm column coupled to a 6120 Quadrupole mass spectrometer (HPLC grade water and methanol were used).



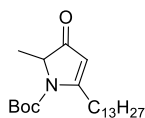
(E)-Non-1-en-8-yn-1-ylboronic acid (46): Concepts applied from literature procedures.⁴⁸ In a dried and argon purged flask with a condenser and argon inlet, catecholborane (0.421 ml, 3.95 mmol) was added to nonadiyne dissolved in dry THF (5.0 ml) at RT over 5 minutes. The mixture was warmed to reflux (70 °C) and held for 12 hours. At this point heat was removed and mixture left to cool overnight. TLC showed complete consumption of starting material, and new UV active spot ($R_f = 0.20$ in 2:1 H/EA). The solution was cooled and concentrated *in vacuo* to leave a cloudy colorless oil. The oil was purified by Kugelrohr distillation in a Buchi oven at full vacuum (0.1 mm Hg) and 120 °C oven temperature to remove byproducts, then 240 °C to obtain the catechol alkenal borane as a clear slightly yellow oil. The catechol was then hydrolyzed by stirring vigorously with water (25 mL) at RT for 4 hours. The resulting precipitate was filtered, brought up in EtOAc (25 mL) and washed with brine (10 mL). The organic fraction was dried with MgSO_4 and concentrated *in vacuo* to give the boronic acid, which was recrystallized from water (25 mL) at 4 °C overnight to yield the final product as a white solid (230 mg, 30%). $R_f = 0.45$ (2:1, hexanes:EtOAc). $^1\text{H NMR}$ (400 MHz, CDCl_3) δ 6.96 (dt, $J = 17.6, 6.41$ Hz, 1 H), 5.54

(d, $J = 17.6$ Hz, 1 H), 2.21 (m, 4 H), 1.95 (t, $J = 2.60$ Hz, 1 H), 1.62 – 1.20 (m, 8 H). ^{13}C NMR (125 MHz, CDCl_3) δ 157.6, 122.4, 84.8, 68.4, 35.7, 28.5 (2 C), 27.8, 18.5.

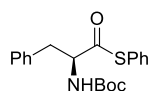


Tert-butyl 5-(hept-6-en-1-yl)-2-methyl-3-oxo-2,3-dihydro-1H-pyrrole-1-carboxylate 48:

Following literature procedure.²³ To a suspension of pure (E)-non-1-en-8-ynylboronic acid **46** (190 mg, 1.14 mmol), (*S*)-*S*-phenyl 2-(tert-butoxycarbonylamino)propanethioate **20** (189 mg, 0.673 mmol), $\text{Pd}_2(\text{dba})_3$ (15.4 mg, 0.017 mmol), and Copper Tc (218 mg, 1.14 mmol) in dry DMF (5 ml) was added triethyl phosphite (0.024 ml, 0.14 mmol). The mixture was stirred at room temperature for 7 days. DMF was removed under reduced pressure, then the mixture was brought up in EtOAc (20 mL) and filtered on Buchner funnel. The solution was washed with 2% NH_4OH until wash is clear (1 x 20 mL), then with 0.1 N HCl (20 mL), sat'd NaHCO_3 (20 mL), and finally with brine. Organic layer was dried with MgSO_4 , then solvent was removed under reduced pressure leaving a black oil. This crude product was purified by column chromatography (ISCO, 12 g SiO_2 , 0 - 20 % EtOAc in Hex) to yield the product as a yellow oil (61 mg, 31%). $R_f = 0.55$ (2:1, hexanes:EtOAc). $[\alpha]_D^{24} = -0.13^\circ$ ($c = 3.5$ in CHCl_3). ^1H NMR (400 MHz, CDCl_3) δ 5.77 (m, 1 H), 5.35 (s, 1 H), 4.98 (m, 1 H), 4.92 (m, 1 H), 4.00 (q, $J = 7.01$ Hz, 1 H), 2.89 (m, 2 H), 2.04 (m, 2 H), 1.61 (m, 2 H), 1.51 (s, 9 H), 1.44 (d, $J = 7.00$ Hz, 3 H), 1.41 (m, 4 H). ^{13}C NMR (125 MHz, CDCl_3) δ 201.1, 176.7, 149.4, 138.8, 114.7, 108.0, 82.9, 62.8, 33.7, 31.1, 28.8, 28.7, 28.3, 27.4, 17.4. HRMS $m/z = 294.20623$ (Theo. for $\text{C}_{17}\text{H}_{27}\text{NO}_3 + \text{H}$: 294.20637).

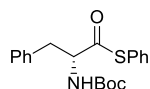


Tert-butyl 2-methyl-3-oxo-5-tridecyl-2,3-dihydro-1H-pyrrole-1-carboxylate (55): To a suspension of pentadec-1-yne (100 mg, 0.480 mmol), (*S*)-*S*-phenyl 2-(tert-butoxycarbonylamino)propanethioate **20** (79 mg, 0.28 mmol), Pd₂(dba)₃ (6.5 mg, 7.1 μmol), and Copper Tc (92 mg, 0.48 mmol) in dry DMF (2.5 ml) was added triethyl phosphite (9.9 μl, 0.06 mmol). The mixture was stirred at room temperature overnight. The reaction mixture was transferred to larger flask and the DMF removed under reduced pressure. The brown mixture was brought up in EtOAc (20 mL), and filtered on Buchner funnel. The solution was washed with 2% NH₄OH until wash is clear (1 x 20, 1 x 5 mL), then with 0.1 N HCl (10 mL), sat'd NaHCO₃ (10 mL), and finally with brine. Organic layer was dried with MgSO₄, then solvent was removed under reduced pressure leaving a light brown oil. The crude material was purified via column chromatography (ISCO, 4 g SiO₂, 0 - 20% EtOAc in Hex) to yield the product as a slightly yellow oil (3.3 mg, 3%). R_f = 0.67 (3:1 hexanes:EtOAc). ¹H NMR (400 MHz, CDCl₃) δ 5.19 (s, 1 H), 4.40 (m, 1 H), 2.39 (t, *J* = 7.15 Hz, 2 H), 2.89 (m, 2 H), 2.04 (m, 2 H), 1.61 (m, 2 H), 1.68 – 1.20 (m, 35 H), 0.89 (t, *J* = 6.85 Hz, 3 H). HRMS *m/z* = 380.31580 (Theo. for C₂₃H₄₁NO₃+H: 380.31592).

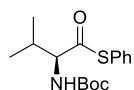


(*S*)-*S*-Phenyl 2-((tert-butoxycarbonyl)amino)-3-phenylpropanethioate (58a): Under argon, at 0 °C, to a solution of (*S*)-2-(tert-butoxycarbonylamino)-3-phenylpropanoic acid (15.0 g, 56.5 mmol) and 1H-benzo[d][1,2,3]triazol-1-ol (7.64 g, 56.5 mmol) in dry EtOAc (160 ml) (dried over M.S.) was added benzenethiol (11.6 ml, 113 mmol). After 5 minutes, *N,N'*-methanediylidenedicyclohexanamine (12.3 g, 59.4 mmol) was added portion wise. The reaction was allowed to warm to RT with stirring overnight, when LCMS shows complete conversion to product. The reaction was quenched by addition of a 50% solution of acetic acid in EtOAc (15

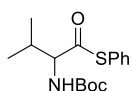
mL) with stirring continued for 30 minutes. The reaction mixture was filtered through a pad of Celite, which was washed with additional EtOAc (150 mL). Solvent was removed under reduced pressure to yield the crude product as an off white solid. Thiophenol was extracted from the solid by multiple hexanes washes (3 x 150 mL). The crude product was purified by column chromatography (250 g SiO₂, 0 – 5% MeOH in DCM) to yield the product as a white solid (15.8 g, 78%). NMR's closely match literature spectrum.⁴⁹ $R_f = 0.60$ (4:1, hexanes:EtOAc). $[\alpha]_D^{24} = -81.7^\circ$ ($c = 1.3$ in CHCl₃). ¹H NMR (400 MHz, CDCl₃) δ 7.42-7.32 (m, 7 H), 7.29 - 7.19, (m, 3 H), 4.99 (d, $J = 9.0$ Hz, 1 H), 4.76 (m, 1 H), 3.19-3.10 (m, 2 H), 1.44 (s, 9 H). ¹³C NMR (125 MHz, CDCl₃) δ 199.5, 155.1, 135.7, 134.8, 129.7, 129.6, 129.4, 128.8, 127.4, 127.3, 80.6, 61.1, 38.5, 28.4. HRMS $m/z = 358.14716$ (Theo. for C₂₀H₂₃NO₃S+H: 358.14714).



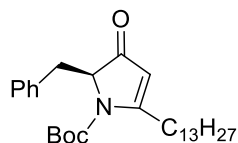
(R)-S-Phenyl 2-((tert-butoxycarbonyl)amino)-3-phenylpropanethioate (58b): This compound was synthesized using the same method as described for **58a** only utilizing (*R*)-2-(tert-butoxycarbonylamino)-3-phenylpropanoic acid as the starting material. (1.07 g, 79%). $R_f = 0.60$ (4:1, hexanes:EtOAc). $[\alpha]_D^{24} = +81.4^\circ$ ($c = 1.0$ in CHCl₃). ¹H NMR (400 MHz, CDCl₃) δ 7.42-7.32 (m, 7 H), 7.29 - 7.19, (m, 3 H), 4.99 (d, $J = 9.0$ Hz, 1 H), 4.76 (m, 1 H), 3.19-3.10 (m, 2 H), 1.44 (s, 9 H). ¹³C NMR (125 MHz, CDCl₃) δ 199.5, 155.1, 135.7, 134.8, 129.7, 129.6, 129.4, 128.8, 127.4, 127.3, 80.6, 61.1, 38.5, 28.4. HRMS $m/z = 358.14716$ (Theo. for C₂₀H₂₃NO₃S+H: 358.14714).



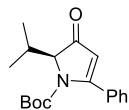
(S)-S-Phenyl 2-((tert-butoxycarbonyl)amino)-3-methylbutanethioate (62): This compound was synthesized using the same method as described for **58a** only utilizing (*S*)-2-((tert-butoxycarbonyl)amino)-3-methylbutanoic acid as the starting material. (1.25 g, 50%). >99.9% e.e. by chiral HPLC: Retention time of 2 enantiomers is 9.2 and 14.9 min in 10% iPrOH in hexanes isocratic run (AD-H 4.6 x 250 mm column, 1 mL/min, 5 μ L of a 1 mg/mL solution), and the *S*-enantiomer has a retention time of 15.1 min as a single peak. $R_f = 0.60$ (4:1, hexanes:EtOAc). $[\alpha]_D^{24} = -59.6^\circ$ ($c = 2.8$ in CHCl_3). $^1\text{H NMR}$ (400 MHz, CDCl_3) δ 7.40 (s, 5 H), 5.11 (d, $J = 9.4$ Hz, 1 H), 4.42 (dd, $J = 9.5, 4.6$ Hz, 1 H), 2.34 (m, 1 H), 1.50 (s, 9 H), 1.04 (d, $J = 7.0$ Hz, 1 H), 0.93 (d, $J = 7.0$ Hz, 1 H). $^{13}\text{C NMR}$ (125 MHz, CDCl_3) δ 199.4, 155.7, 134.7, 129.5, 129.3, 127.6, 80.4, 65.4, 31.2, 28.5, 19.6, 17.1. HRMS $m/z = 310.14729$ (Theo. for $\text{C}_{16}\text{H}_{23}\text{NO}_3\text{S}+\text{H}$: 310.14714).



S-Phenyl 2-((tert-butoxycarbonyl)amino)-3-methylbutanethioate (62+/-): This compound was synthesized using the same method as described for **58a** only utilizing racemic 2-((tert-butoxycarbonyl)amino)-3-methylbutanoic acid as the starting material. (200 mg, 14%). $R_f = 0.60$ (4:1, hexanes:EtOAc). $^1\text{H NMR}$ (400 MHz, CDCl_3) δ 7.40 (s, 5 H), 5.11 (d, $J = 9.4$ Hz, 1 H), 4.42 (dd, $J = 9.5, 4.6$ Hz, 1 H), 2.34 (m, 1 H), 1.50 (s, 9 H), 1.04 (d, $J = 7.0$ Hz, 1 H), 0.93 (d, $J = 7.0$ Hz, 1 H). $^{13}\text{C NMR}$ (125 MHz, CDCl_3) δ 199.4, 155.7, 134.7, 129.5, 129.3, 127.6, 80.4, 65.4, 31.2, 28.5, 19.6, 17.1. HRMS $m/z = 310.14737$ (Theo. for $\text{C}_{16}\text{H}_{23}\text{NO}_3\text{S}+\text{H}$: 310.14714).

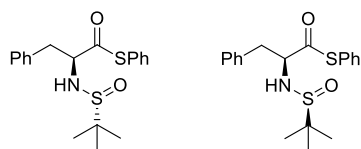


(S)-Tert-butyl 2-benzyl-3-oxo-5-tridecyl-2,3-dihydro-1H-pyrrole-1-carboxylate (60): (S)-S-phenyl 2-(tert-butoxycarbonylamino)-3-phenylpropanethioate **58a** (91 mg, 0.26 mmol) was dissolved in dry DMF (2.5 ml) under an atmosphere of argon, to which Pd₂(dba)₃ (5.83 mg, 6.36 μmol), Copper Tc (83 mg, 0.43 mmol), and pentadec-1-yne (0.117 ml, 0.433 mmol) were. Finally, triethylphosphite (8.9 μl, 0.051 mmol) was added. The mixture was warmed to 60 °C with continuous stirring. After 2 hours, the reaction mixture was transferred to larger flask and the solvent was removed under reduced pressure leaving a brown paste. The mixture was brought up in EtOAc (20 mL) and filtered on Buchner funnel. The solution was washed with 2% NH₄OH until wash it was clear (1 x 10, 3 x 5 mL), then with 0.1 N HCl (10 mL), sat'd NaHCO₃ (10 mL), and finally with brine (2 x 10 mL). The organic layer was dried with MgSO₄, then solvent was removed under reduced pressure leaving a light brown oil. The crude product was subject to column chromatography (ISCO, 4 g SiO₂, 0 - 7% EtOAc in Hex) to yield the product as a slightly yellow oil (32.8 mg, 28%). 13% e.e. by chiral HPLC: Retention time of 2 enantiomers is 6.0 and 6.8 min in 1% iPrOH in hexanes isocratic run (AD-H 4.6 x 250 mm column, 1 mL/min, 5 μL of a 1 mg/mL solution). R_f = 0.20 (6:1 hexanes:EtOAc). [α]_D²⁴ = -11.9 ° (c = 1.64 in CHCl₃). IR (ν_{max}, cm⁻¹): 2924, 2853, 1728, 1694, 1576, 1455, 1394, 1353, 1279, 1255, 1165, 1139, 1077, 1058, 548, 796, 755, 699. ¹H NMR (400 MHz, CDCl₃) δ 7.17 (m, 3 H), 7.04 (m, 2 H), 5.14 (s, 1 H), 4.26 (dd, *J* = 5.87, 3.52 Hz, 1 H), 3.44 (dd, *J* = 13.30, 6.62 Hz, 1 H), 3.29 (dd, *J* = 13.30, 2.35 Hz, 1 H), 2.75 (m, 1 H), 2.49 (m, 1 H), 1.60 (s, 9 H), 1.34 - 0.95 (m, 22 H), 0.88 (t, *J* = 7.04 Hz, 3 H). ¹³C NMR (100 MHz, CDCl₃) δ 200.1, 178.0, 149.4, 134.6, 129.9 (2 C), 128.1 (2 C), 127.1, 110.4, 83.2, 66.8, 36.8, 32.1, 31.2, 29.9 (3 C), 29.8, 29.6 (2 C), 29.5, 29.2, 28.5 (3 C), 27.8, 22.9, 14.3. HRMS (ESI) *m/z* = 456.34773 (Theo. for C₂₉H₄₅NO₃+H: 456.34722).



(S)-Tert-butyl 2-isopropyl-3-oxo-5-phenyl-2,3-dihydro-1H-pyrrole-1-carboxylate (52a): (S)-S-phenyl 2-(tert-butoxycarbonylamino)-3-methylbutanethioate (46.5 mg, 0.150 mmol) was first dissolved in dry DMF (1.25 ml) under an atmosphere of argon, to which Pd₂(dba)₃ (3.44 mg, 3.76 μmol), Copper Tc (48.7 mg, 0.255 mmol), and ethynylbenzene (26.1 mg, 0.255 mmol) were added. Finally, triethyl phosphite (5.26 μl, 0.030 mmol) was added. The mixture was warmed to 60 °C with continuous stirring for 2 hours at which time LCMS showed consumption of most of the starting material and small peak for product. The reaction mixture was transferred to larger flask and the DMF removed under reduced pressure leaving a brown paste. The mixture was brought up in EtOAc (10 mL) and filtered on Buchner funnel. The solution was washed with 2% NH₄OH until wash is clear (1 x 10, 1 x 5 mL), then with 0.1 N HCl (5 mL), sat'd NaHCO₃ (5 mL), and finally with brine (2 x 5 mL). The organic layer was dried with MgSO₄, then solvent was removed under reduced pressure leaving a light brown oil. The crude reaction mixture was subject to column chromatography (ISCO, 4 g SiO₂, 0 - 7% EtOAc in Hex) to yield the cyclic product as a yellow oil (2.3 mg, 5%). 84% e.e. by chiral HPLC: Retention time of 2 enantiomers (from racemic starting material) are 8.9 and 9.7 min in 2% iPrOH in hexanes isocratic run (AD-H 4.6 x 250 mm column, 1 mL/min, 5 μL of a 1 mg/mL solution), and the S-enantiomer from this reaction has a retention time of 9.7 min as the major peak. Characterization matches reported literature compound.⁵⁰ R_f = 0.35 (6:1 hexanes:EtOAc). [α]_D²⁴ = -4 ° (c = 0.24 in CH₂Cl₂), [α]_D²⁴ = -9 ° (c = 0.230 in CHCl₃). ¹H NMR *mixture of 2 rotamers in 90:10 ratio* (400 MHz, CDCl₃) δ 7.48 (m, 5 H), 5.14 (s, 1 H), 4.26 (dd, *J* = 5.87, 3.52 Hz, 1 H), 3.44 (dd, *J* = 13.30, 6.62 Hz, 1 H), 3.29 (dd, *J* = 13.30, 2.35 Hz, 1 H), 2.75 (m, 1 H), 2.49 (m, 1 H), 1.60 (s, 9 H), 1.34 - 0.95 (m, 22

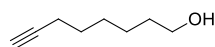
H), 0.88 (t, $J = 7.04$ Hz, 3 H). HRMS (ESI) $m/z = 302.17525$ (Theo. for $C_{18}H_{23}NO_3+H$: 302.17507).



S-Phenyl 2-((R)-1,1-dimethylethylsulfonamido)-3-phenylpropanethioates (69a & 69b)

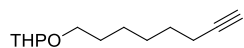
(separable but unassigned diastereomers): (*S*)-*S*-Phenyl 2-(tert-butoxycarbonylamino)-3-phenylpropanethioate **58** (500 mg, 1.40 mmol) was brought up in a 1:2 mixture of TFA (0.823 ml, 10.7 mmol) and DCM (2 ml). The mixture was stirred without an argon atmosphere for 15 min. TLC and LCMS at this point showed >95% deprotection. Solvent was removed under reduced pressure on a rotary evaporator, then the oily residue was brought up in DCM (3 mL) and evaporated multiple times (3-5) to remove all excess TFA. The crude oil was put under high vac for 20 min, and the resulting solid was used in the next reaction as the TFA salt. $R_f = 0.10$ (1:1 hexanes:EtOAc). The crude deprotected TFA salt was dissolved in dry DCM (18 mL) and 2-methylpropane-2-sulfinic chloride (0.182 mL, 1.54 mmol) was added. The mixture was cooled to 0 °C for 10 min, then Et_3N (0.976 mL, 7.00 mmol) was added drop-wise to the mixture. Once addition was complete, the mixture was stirred under an atmosphere of argon. LCMS at 10 showed complete conversion to product. The reaction mixture was diluted into DCM (90 mL), then washed with 0.1 N HCl (30 mL), water (30 mL), sat'd $NaHCO_3$ (30 mL), brine (60 mL), and the murky organic solution was finally dried with $MgSO_4$ and filtered to give a clear solution, which was evaporated to give the crude product. The crude material purified by column chromatography (ISCO, 40 g SiO_2 , 0 - 50% EtOAc in Hex for **long gradient**) to separate the two diastereomers as a white solid (a = 206 mg, 41%) and a clear colorless oil (b = 216 mg, 43%). Characterization for **69a**: $R_f = 0.52$ (1:1, hexanes:EtOAc). $[\alpha]_D^{24} = -158$. ° (c = 2.1 in $CHCl_3$). 1H

NMR (400 MHz, CDCl₃) δ 7.43 - 7.23 (m, 10 H), 4.40 (ddd, $J = 9.39, 5.87, 4.30$ 1 H), 3.86 (d, $J = 9.39$ Hz, 1 H), 3.50 (dd, $J = 13.7, 4.30$ Hz, 1 H), 3.20 (d, $J = 13.7, 5.87$ Hz, 1 H), 1.28 (s, 9 H). ¹³C NMR (125 MHz, CDCl₃) δ 200.5, 134.7, 134.4, 130.9 (2 C), 129.7, 129.4 (2 C), 128.9 (2 C), 128.0, 127.6, 65.7, 57.0, 39.7, 22.8. HRMS (ESI) $m/z = 362.12444$ (Theo. for C₁₉H₂₃NO₂S₂+H: 362.12430). Characterization for **69b**: $R_f = 0.43$ (1:1, hexanes:EtOAc). $[\alpha]_D^{24} = +33.4^\circ$ ($c = 2.2$ in CHCl₃). ¹H NMR (400 MHz, CDCl₃) δ 7.39 (s, 5 H), 7.32 - 7.16 (m, 5 H), 4.33 (ddd, $J = 9.00, 7.83, 5.48$ 1 H), 4.20 (d, $J = 9.00$ Hz, 1 H), 3.18 (dd, $J = 13.69, 5.48$ Hz, 1 H), 3.03 (d, $J = 13.69, 7.83$ Hz, 1 H), 1.11 (s, 9 H). ¹³C NMR (125 MHz, CDCl₃) δ 199.0, 134.7 (2 C), 129.8 (3 C), 129.3 (2 C), 128.6 (3 C), 127.2, 126.7, 65.7, 56.7, 40.6, 22.5 (3 C). HRMS (ESI) $m/z = 362.12441$ (Theo. for C₁₉H₂₃NO₂S₂+H: 362.12430).

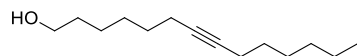


Oct-7-yn-1-ol (32): In an argon purged 3 neck flask (1 L) was added newly purchased ethylenediamine (100 ml, 1481 mmol), which was cooled to 0 °C, and newly purchased sodium hydride (95 %, 6.01 g, 238 mmol) was added in one portion keeping the reaction stirring.⁵¹ The mixture was slowly warmed to RT and bubbles were accompanied by a color change to a deep dark blue. The mixture was stirred at RT for one hour (turned brown, then purple, then brown again), then the mixture was slowly heated to 60 °C. After stirring at this temperature for one hour, the reaction was cooled to 45 °C and oct-3-yn-1-ol (8.52 ml, 59.4 mmol) was added drop wise. The brown mixture was again heated to 65 °C for one hour. The mixture was then cooled to 0 °C and water (100 ml) (reaction turned purple again) and aqueous HCl (1.0 M, 100 mL) were added slowly turning the slurry yellow. This mixture (small amount of oil on surface) was poured into a 2 L Erlenmeyer flask and aqueous HCl (1.0 M, 200 mL) was added. The mixture was extracted twice with Et₂O (100 ml), the aqueous layer was acidified with aqueous HCl (1.0

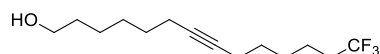
M, 100 mL), and again extracted twice with Et₂O (100 ml). The combined organic layers were washed with aqueous HCl (1.0 M, 100 mL), brine (2 x 100 mL), and dried over MgSO₄. TLC shows complete conversion to product. The solvent was removed under vacuum to give the crude product (5.705 g), the NMR of which shows >95% purity with water as main contaminant. The product was purified by chromatography (ISCO, 120 g SiO₂, 0 - 30% EtOAc in Hex). Product was obtained a clear slightly yellow oil (5.42 g, 72%). R_f = 0.35 (2:1, hexanes:EtOAc). ¹H NMR (400 MHz, CDCl₃) δ 3.63 (t, *J* = 6.7 Hz, 2 H), 2.19 (dt, *J* = 6.7, 2.4 Hz, 2 H), 1.94 (t, *J* = 2.4 Hz, 1 H), 1.56 (m, 4 H), 1.40 (m, 4 H). ¹³C NMR (125 MHz, CDCl₃) δ 84.8, 68.4, 63.1, 32.8, 28.7, 28.6, 25.4, 18.5. HRMS (ESI) *m/z* 127.11151 (Theo. for C₈H₁₄O+H: 127.11229)



2-(Oct-7-yn-1-yloxy)tetrahydro-2H-pyran (33): Oct-7-yn-1-ol (2.90 g, 23.01 mmol) was brought up in DCM (15 ml) and cooled to 0° C. To this solution was added tosic acid monohydrate (40 mg, 0.230 mmol), then dihydropyran (2.63 ml, 28.8 mmol) was added drop wise.⁵² Upon completion of addition, the reaction was removed from the ice bath and stirred for 15 minutes, at which time TLC showed complete conversion to the product. The mixture was diluted with Et₂O (200 ml) and washed with sat'd NaHCO₃. Dried organics over MgSO₄ and concentrated to give the crude orange oil, which was subject to purification via column chromatography (ISCO, 120 g SiO₂, 0 - 10% EtOAc in Hex) to give a clear colorless oil (4.05 g, 84%). R_f = 0.35 (9:1 H/EA). ¹H NMR (400 MHz, CDCl₃) δ 4.58 (dd, *J* = 4.3 Hz, 1 H, anomeric proton on THP), 3.87 (m, 1 H), 3.74 (dt, *J* = 9.4, 7.0 Hz, 1 H, CHaHb-O-THP), 3.50 (m, 1 H), 3.40 (dt, *J* = 9.4, 7.0 Hz, 1 H, CHaHb-O-THP), 2.19 (dt, *J* = 7.0, 2.7 Hz, 2 H), 1.94 (t, *J* = 2.7 Hz, 1 H), 1.90 - 1.32 (m, 14 H). ¹³C NMR (100 MHz, CDCl₃) δ 99.1, 84.9, 68.3, 67.7, 62.6, 31.0, 29.8, 28.8, 28.6, 26.0, 25.7, 19.9, 18.6.

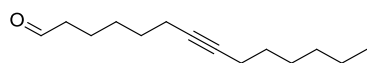


Tetradec-7-yn-1-ol (34b): To a solution of 2-(oct-7-yn-1-yloxy)tetrahydro-2H-pyran (4.05 g, 19.3 mmol) in THF (75.0 ml) at -40 °C was added *n*-butyl lithium (10.0 ml of 2.5 M in THF, 25.0 mmol) drop wise. The reaction was stirred for 1 hour and allowed to warm to -10 °C, then HMPA (6.70 ml, 38.5 mmol) and freshly distilled 1-bromohexane (6.70 ml, 38.5 mmol) were added slowly. The mixture was allowed to warm to RT and stirred for 24 hours. The reaction was quenched by pouring into ice water (75 mL), extracted with Et₂O (200 mL), which was subsequently washed with brine (50 mL), aqueous HCl (2.0 M, 3 x 50 mL), sat'd NaHCO₃ (50 mL), and brine (50 mL), then dried over MgSO₄. The solvent was evaporated on a rotovap giving a clear slightly yellow crude oil. The crude material was deprotected by dissolving in EtOH (175 ml), to which tosic acid monohydrate (1.83 g, 9.62 mmol) was added. The mixture was stirred open to air and heated to 55 °C for 30 minutes, at which time TLC showed a separable mixture of the two alcohols (10:1). The solvent was evaporated down to 20 mL, then brought up in EtOAc (200 mL), and washed with sat'd NaHCO₃ (50 mL), then brine (50 mL). The organic layer was then dried over MgSO₄ and evaporated to yield the crude product as a dark yellow oil. The product was purified by dry-loading the crude material on silica (15 g) and subjecting it to column chromatography (ISCO, 120 g SiO₂, 0 - 8 % EtOAc in hexanes). The product was isolated as a clear colorless oil (2.62 g, 65% over 2 steps). $R_f = 0.40$ (2:1 hexanes:EtOAc). IR (ν_{\max} , cm⁻¹): 3337, 2929, 2857, 1460, 1430, 1377, 1332, 1054, 1030, 907, 730. ¹H NMR (400 MHz, CDCl₃) δ 3.62 (t, $J = 6.7$ Hz, 2 H), 2.13 (m, 4 H), 1.64 (bs, 1 H), 1.60 - 1.22 (m, 14 H), 0.87 (t, $J = 7.0$ Hz, 3 H). ¹³C NMR (100 MHz, CDCl₃) δ 80.6, 80.2, 63.1, 32.8, 31.5, 29.3, 29.2, 28.8, 28.7, 25.5, 22.7, 18.9, 18.8, 14.2. HRMS (ESI) m/z 211.20576 (Theo. for C₁₄H₂₆O+H: 211.20564).

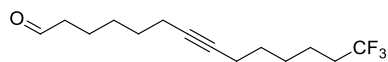


14,14,14-Trifluorotetradec-7-yn-1-ol (34a): To a solution of 2-(oct-7-ynyloxy)tetrahydro-2H-pyran (3.87 g, 18.4 mmol) in THF (75.0 ml) at -40 °C was added *n*-butyl lithium (9.57 ml of 2.5 M in THF, 23.9 mmol) drop wise. The reaction was stirred for 1 hour and allowed to warm to -10 °C, then HMPA (6.40 ml, 36.8 mmol) and 6-bromo-1,1,1-trifluorohexane (4.84 g, 22.08 mmol) (Oakwood Chemicals) were added slowly.⁵³ The mixture was allowed to warm to RT and stirred for 24 hours. The product and starting material co-eluted by TLC in multiple solvent systems, so the protecting group was removed after a short workup and before purification. The reaction was quenched by pouring into ice water (75 mL), extracted with Et₂O (200 mL), which was subsequently washed with brine (50 mL), aqueous HCl (2.0 M, 3 x 50 mL), sat'd NaHCO₃ (50 mL), and brine (50 mL), then dried over MgSO₄. The solvent was evaporated on a rotovap giving a clear slightly yellow crude oil. The crude material was deprotected by dissolving in EtOH (175 ml), to which tosic acid monohydrate (1.75 g, 9.20 mmol) was added. The mixture was stirred open to air and heated to 55 °C for 90 minutes, at which time TLC showed a separable mixture of the two alcohols (10:1). The solvent was evaporated down to 20 mL, then brought up in EtOAc (200 mL), and washed with sat'd NaHCO₃ (50 mL), then brine (50 mL). The organic layer was then dried over MgSO₄ and evaporated to yield the crude product as a dark yellow oil. The product was purified by dry-loading the crude material on silica (15 g) and subjecting it to column chromatography (ISCO, 120 g SiO₂, 0 - 30 % EtOAc in hexanes). The product was isolated as a clear colorless oil (3.70 g, 76% over 2 steps). R_f = 0.45 (2:1 hexanes:EtOAc). IR (ν_{max}, cm⁻¹): 3335, 2933, 2860, 1463, 1439, 1389, 1334, 1253, 1190, 1133, 1034, 729, 653. ¹H NMR (400 MHz, CDCl₃) δ 3.63 (t, *J* = 6.7 Hz, 2 H), 2.20 - 2.00 (m, 6 H), 1.68 (bs, 1 H), 1.60 - 1.22 (m, 14 H). ¹³C NMR (100 MHz, CDCl₃) δ 127.4 (q, *J* = 267 Hz, 1 C),

80.7, 79.8, 63.1, 33.7 (q, $J = 28.2$ Hz, 1 C), 32.8, 29.2, 28.8 (2 C), 28.0, 25.4, 21.6 (q, $J = 3.1$ Hz, 1 C), 18.8, 18.7. ^{19}F NMR (400 MHz, CDCl_3) δ -66.76 (t, $J = 11.0$ Hz, 3 F). HRMS (ESI) m/z 265.17740 (Theo. for $\text{C}_{14}\text{H}_{23}\text{F}_3\text{O}+\text{H}$: 265.17792). Anal. calcd. for $\text{C}_{14}\text{H}_{23}\text{F}_3\text{O}$: C, 63.61; H, 8.77; F, 21.56. Found: C 63.74; H 8.94; F 21.27.



Tetradece-7-ynal (27b): A solution of tetradece-7-yn-1-ol (2.53 g, 12.0 mmol) in DCM (100 ml) was added to a solution of Dess-Martin periodinane⁵⁴ (6.11 g, 14.4 mmol) in DCM (150 ml). The reaction was stirred at room temperature under argon over 3 hours until TLC showed complete conversion to product. At this time, the homogenous reaction mixture was diluted with Et_2O (500 ml), and the resulting suspension of iodine was added to an aqueous solution of NaOH (1.3 M, 25 mL) to hydrolyze the iodine to the water soluble 2-iodobenzoate. The mixture was stirred vigorously for 10 minutes, then the organic layer was extracted with aq. NaOH (1.3 M, 25 mL), water (16 mL), and brine (2 x 100 mL). The organic layer was then dried over MgSO_4 and evaporated to give the crude product, which did not require any purification for use in next reaction (2.18 g, 87%). $R_f = 0.80$ (2:1, hexanes:EtOAc). IR (ν_{max} , cm^{-1}): 2938, 2858, 1707, 1459, 1413, 1278, 1225, 935, 728. ^1H NMR (400 MHz, CDCl_3) δ 9.73 (m, 1 H), 2.42 (dt, $J = 7.6, 1.5$ Hz, 2 H), 2.14 (m, 4 H), 2.08 (m, 2 H), 1.64 (m, 2 H), 1.54 - 1.20 (m, 10 H), 0.88 (t, $J = 7.3$ Hz, 3 H). ^{13}C NMR (125 MHz, CDCl_3) δ 202.8, 80.8, 79.8, 44.0, 31.5, 29.3, 29.0, 28.7, 28.5, 22.8, 21.8, 18.9, 18.7, 14.2. HRMS (ESI) $m/z = 209.19014$ (Theo. for $\text{C}_{14}\text{H}_{24}\text{O}+\text{H}$: 209.18999).



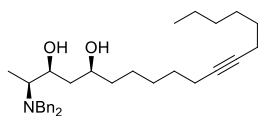
14,14,14-Trifluorotetradece-7-ynal (27a): A solution of 14,14,14-trifluorotetradece-7-yn-1-ol (3.67 g, 13.9 mmol) in DCM (200 ml) was added to a solution of Dess-Martin periodinane (7.06 g, 16.6 mmol) in DCM (300 ml). The reaction was stirred at room temperature under argon over

3 hours until TLC showed complete conversion to product. At this time, the homogenous reaction mixture was diluted with Et₂O (1500 ml), and the resulting suspension of iodine was added to an aqueous solution of NaOH (1.3 M, 50 mL) to hydrolyze the iodine to the water soluble 2-iodobenzoate. The mixture was stirred for 10 minutes, then the ether layer was extracted aq. NaOH (1.3 M, 50 mL), washed with water (16 mL), and dried with brine (2 x 100 mL). The organic layer was then dried over MgSO₄ and evaporated to give the crude product, which did not require any purification for use in next reaction (3.29 g, 86%). $R_f = 0.70$ (2:1, hexanes:EtOAc). IR (ν_{max} , cm⁻¹): 2938, 2858, 1708, 1433, 1389, 1333, 1252, 1191, 1132, 1035, 934, 655. ¹H NMR (400 MHz, CDCl₃) δ 9.78 (t, $J = 1.8$ Hz, 1 H), 2.45 (dt, $J = 7.3, 1.8$ Hz, 2 H), 2.16 (m, 4 H), 2.08 (m, 2 H), 1.70 - 1.40 (m, 14 H). ¹⁹F NMR (400 MHz, CDCl₃) δ -66.70 (t, $J = 11.6$ Hz, 3 F). ¹³C NMR (125 MHz, CDCl₃) δ 202.6, 127.4 (q, $J = 276$ Hz, 1 C), 80.2, 80.0, 43.9, 33.7 (q, $J = 28.6$ Hz, 1 C), 28.9, 28.7, 28.4, 27.9, 21.7, 21.6 (q, $J = 2.7$ Hz, 1 C), 18.6 (2 C). HRMS (ESI) $m/z = 263.16171$ (Theo. for C₁₄H₂₁F₃O+H: 263.16227).



(S)-3-(Dibenzylamino)butan-2-one (10): To a stirred solution of (2S)-2-dibenzylamino-N-methoxy-N-methylpropanamide (16.9 g, 54 mmol) in THF (200 mL) under argon at -78 °C was added methyl lithium (1.6 M in Et₂O, 58.1 mL, 93 mmol) over a period of 15 minutes maintaining the temperature below -70 °C.³⁶ The resulting solution was stirred for another 30 minutes. TLC showed complete conversion to. The reaction was quenched with saturated aq. NH₄Cl (40 mL) and concentrated to remove THF. The aq. solution was extracted with Et₂O (600 mL). The ether solution was washed with brine (200 mL), dried over MgSO₄ and concentrated *in vacuo* to give the product as a pale yellow oil (13.8 g, 95%). Characterization matched reported

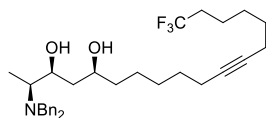
literature values.³⁶ This material was used without further purification in the next step. $R_f = 0.42$ in 9:1 H/EA. $[\alpha]_D^{24} = -52.3^\circ$ ($c = 3.2$ in CHCl_3).



(2*S*,3*S*,5*S*)-2-(Dibenzylamino)octadec-11-yne-3,5-diol (26b): To a stirred solution of (-)-DIP-Cl (50-65% wt. in hexanes, 9.77 ml, 13.6 mmol) in a flame dried 250 mL flask with THF (40 ml), *N,N*-dimethylethylamine (4.41 ml, 40.7 mmol), was added drop wise at RT. The clear reaction mixture was cooled to -30°C , and a solution of (*S*)-3-(dibenzylamino)butan-2-one (3.26 g, 12.2 mmol) in THF (20.0 ml) was added drop wise over a 2 minute period at -30°C . The resulting cloudy white mixture was stirred for 1.5 hrs more at -30°C turning yellow and then was cooled to -78°C . A solution of freshly prepared tetradec-7-ynal (2.12 g, 10.2 mmol) in THF (20.0 ml) was added drop wise over the next 5 minutes. The reaction vessel was kept stirring at -78°C for 4 hours, then allowed to warm to -20°C overnight. TLC and LCMS showed complete conversion to the product, so the reaction was quenched by the addition of a phosphate buffer (20 mL, pH = 7) over 3 minutes at -20°C , and stirring was continued over the next hour while the reaction was allowed to warm to RT. The mixture was then cooled to -20°C , and hydrogen peroxide (30% aq., 2.83 ml, 27.5 mmol) was added drop wise to the stirring mixture. After stirring for an additional hour and warming back to RT, the reaction mixture was diluted into Et_2O (200 mL), washed with brine (200 mL), dried over MgSO_4 , filtered, and concentrated under vacuum to yield a clear, colorless oil that was immediately used. The beta-ketone (2*S*,5*S*)-2-(dibenzylamino)-5-hydroxyoctadec-11-yn-3-one was brought up in MeOH (125 ml) and brought to -20°C , where powdered SODIUM BOROHYDRIDE (0.585 g, 25.4 mmol) was added in portions of ~ 100 mg each until the no more bubbles were formed and TLC showed no more

starting material. Reaction is complete within minutes of the addition of sodium borohydride. The resulting mixture was quenched by the drop wise addition of acetic acid (1 mL) until bubbling ceases, then concentrated in vacuum, diluted with Et₂O (500 mL) to which HCl (1 N, 10 mL) was added, then was neutralized with a sat'd NaHCO₃ wash (500 mL). The organic layer was then separated and washed with water (500 mL), then brine (500 mL), dried over MgSO₄, and finally concentrated under vacuum to give a clear colorless oil.

Pinene byproducts were removed by sublimation overnight at 50 °C and full vacuum. The crude product was purified by column chromatography (ISCO, 120 g SiO₂, 0 - 20 % EtOAc in Hex (each with 1.5 % Et₃N present)) to give a clear colorless oil (3.26 g, 67% over 2 steps). LCMS $m/z = 478.5$. $R_f = 0.33$ (4:1, hexanes:EtOAc). $[\alpha]_D^{24} = +24.3^\circ$ ($c = 2.73$ in CHCl₃). IR (ν_{\max} , cm⁻¹): 3433, 3025, 2930, 2855, 2237, 1453, 1427, 1296, 1142, 1099, 1057, 909, 837, 731, 698. ¹H NMR (400 MHz, CDCl₃) δ 7.34 - 7.24 (m, 10 H), 4.77 (bs, 1 H), 4.05 (bs, 1 H), 3.84 (m, 1 H), 3.80 (d, $J = 13.3$ Hz, 2 H), 3.65 (dt, $J = 10.4, 2.4$ Hz, 1 H), 3.30 (d, $J = 13.3$ Hz, 2 H), 2.54 (m, 1 H), 2.13 (m, 6 H), 1.60 - 1.10 (m, 16 H), 1.01 (d, $J = 6.7$ Hz, 3 H), 0.88 (t, $J = 7.0$ Hz, 3 H). ¹³C NMR (100 MHz, CDCl₃) δ 138.8 (2 C), 129.2 (4 C), 128.7 (4 C), 127.6 (2 C), 80.4, 80.3, 72.2, 72.0, 59.0, 53.4 (2 C), 40.3, 37.7, 31.6, 29.3 (2 C), 29.1, 28.7, 25.2, 22.8, 18.9 (2 C), 14.3 8.2. HRMS (ESI) $m/z = 478.36785$ (Theo. for C₃₂H₄₄F₃NO₂+H: 478.36796). Anal. calcd. for C₃₂H₄₇NO₂: C, 80.45; H, 9.92; N, 2.93. Found: C 80.37; H 9.93, N 2.99.

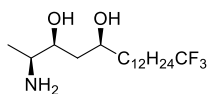


(2S,3S,5S)-2-(Dibenzylamino)-18,18,18-trifluorooctadec-11-yne-3,5-diol (26a): To a stirred solution of (-)-DIP-Cl (11.3 ml, 15.8 mmol) in a flame dried 250 mL flask with dry THF (50 ml), N,N-dimethylethylamine (5.11 ml, 47.1 mmol), was added drop wise at room temperature. The

clear reaction mixture was cooled to $-30\text{ }^{\circ}\text{C}$, and a solution of (S)-3-(dibenzylamino)butan-2-one (3.78 g, 14.1 mmol) in THF (25.00 ml) was added drop wise over a 2 minute period at $-30\text{ }^{\circ}\text{C}$. The resulting cloudy white mixture was stirred for 1.5 hrs more at $-30\text{ }^{\circ}\text{C}$ turning yellow, then was cooled to $-78\text{ }^{\circ}\text{C}$. A solution of freshly prepared 14,14,14-trifluorotetradec-7-ynal (3.09 g, 11.78 mmol) in THF (25.0 ml) was added drop wise over the next 5 minutes. The reaction was stirred at $-78\text{ }^{\circ}\text{C}$ for 4 hours, then at $-20\text{ }^{\circ}\text{C}$ overnight.

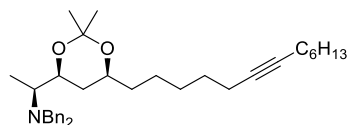
TLC and LCMS showed complete conversion to the product, so the reaction was quenched by the addition of a phosphate buffer (30 mL, pH = 7) over 3 minutes at $-20\text{ }^{\circ}\text{C}$, and stirring was continued over the next hour while the reaction was allowed to warm to RT. The mixture was then cooled to $-20\text{ }^{\circ}\text{C}$, and hydrogen peroxide (30% aq., 3.28 ml, 31.8 mmol) was added drop wise to the stirring mixture. After stirring for an additional hour and warming back to RT, the reaction mixture was diluted into Et₂O (300 mL), washed with brine (300 mL), dried over MgSO₄, filtered, and concentrated under vacuum to yield a clear, colorless oil that was immediately used. The beta-ketone (2S,5S)-2-(dibenzylamino)-5-hydroxyoctadec-11-yn-3-one was brought up in MeOH (175 ml) and brought to $-20\text{ }^{\circ}\text{C}$, where powdered SODIUM BOROHYDRIDE (0.677 g, 29.5 mmol) was added in portions of ~100 mg each until the no more bubbles were formed and TLC showed no more starting material. Reaction is complete within minutes of the addition of sodium borohydride. The resulting mixture was quenched by the drop wise addition of acetic acid (1 mL) until bubbling ceases, then concentrated in vacuum, diluted with Et₂O (500 mL) to which HCl (1 N, 10 mL) was added, then was neutralized with a sat'd NaHCO₃ wash (500 mL). The organic layer was then separated and washed with water (500 mL), then brine (500 mL), dried over MgSO₄, and finally concentrated under vacuum to give a clear colorless oil. Pinene byproducts were removed by sublimation overnight at $50\text{ }^{\circ}\text{C}$

and full vacuum. The crude product was purified by column chromatography (ISCO, 120 g SiO₂, 0 - 20 % EtOAc in Hex (each with 1.5 % Et₃N present)) to give a clear colorless oil (4.33 g, 69% over 2 steps). $R_f = 0.37$ (4:1, hexanes:EtOAc). $[\alpha]_D^{24} = +22.1^\circ$ ($c = 1.72$ in CHCl₃). IR (ν_{\max} , cm⁻¹): 3492, 3387, 3025, 2935, 2857, 1602, 1453, 1253, 1134, 1056, 1033, 845, 748, 733, 699. ¹H NMR (400 MHz, CDCl₃) δ 7.24 - 7.34 (m, 10 H), 4.77 (bs, 1 H), 4.06 (bs, 1 H), 3.85 (m, 1 H), 3.81 (d, $J = 13.3$ Hz, 2 H), 3.65 (dt, $J = 10.4, 2.4$ Hz, 1 H), 3.30 (d, $J = 13.3$ Hz, 2 H), 2.55 (m, 1 H), 2.00 - 2.19 (m, 6 H), 1.30 - 1.60 (m, 16 H), 1.01 (d, $J = 6.4$ Hz, 3 H). ¹³C NMR (100 MHz, CDCl₃) δ 138.9 (2 C), 129.2 (4 C), 128.8 (4 C), 127.6 (2 C), 127.5 (q, $J = 267$ Hz, 1 C), 80.9, 79.8, 72.2, 72.0, 59.0, 53.4 (2 C), 40.4, 37.8, 33.9 (q, $J = 28.2$ Hz, 1 C), 29.3, 29.2, 28.8, 28.0, 25.2, 21.7 (q, $J = 3.1$ Hz, 1 C), 18.9, 18.7, 8.2. ¹⁹F NMR (400 MHz, CDCl₃) δ -66.64 (t, $J = 12.0$ Hz, 3 F). HRMS (ESI) $m/z = 532.33969$ (Theo. for C₃₂H₄₄F₃NO₂+H: 532.33969). Anal. calc'd. for C₃₂H₄₄F₃NO₂: C, 72.29; H, 8.34; N, 2.63; F 10.72. Found: C 72.19; H 8.35, N 2.66, F 10.65.



(2S,3S,5S)-2-Amino-18,18,18-trifluorooctadecane-3,5-diol (2): (2S,3S,5S)-2-(dibenzylamino)-18,18,18-trifluorooctadec-11-yne-3,5-diol (3.21 g, 6.03 mmol) was dissolved in EtOH (100 mL), to which Pearlman's catalyst (166 mg, 1.18 mmol) was added. The heterogeneous solution was purged of air 3 times with aspiration vacuum and stirring, filling with argon each time. On the fourth and fifth purges the flask was filled with hydrogen gas (1 atm.). The reaction was stirred vigorously with a balloon of hydrogen for 24 hours, at which time only product was observed by TLC and LCMS. The crude mixture was filtered over Celite, which was washed with EtOH (500 mL). The solution was evaporated under reduced pressure, then DCM was added to co-evaporate the remaining ethanol to give the crude material. The product was purified by column chromatography on neutralized silica (ISCO, 120 g SiO₂, 10 - 100% B (70:30:2 of

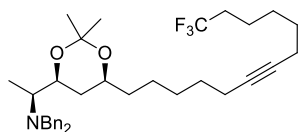
DCM:MeOH:NH₄OH) in DCM) to give a white solid (1.89 g, 88%). $R_f = 0.25$ (79:20:1 of CH₂Cl₂:MeOH:NH₄OH (30% aq.)). MP: 69 – 70 °C. IR (ν_{\max} , cm⁻¹): 3424, 3338, 2917, 2847, 2795, 1585, 1462, 1325, 1252, 1129, 1051, 976, 818, 719, 657. $[\alpha]_D^{24} = +2.4^\circ$ (c = 1.19 in CHCl₃), $[\alpha]_D^{24} = -8.8^\circ$ (c = 1.26 in MeOH). ¹H NMR (400 MHz, CDCl₃) δ 3.82 (m, 1 H), 3.44 (m, 1 H), 2.95 (bs, 2 H) 2.73 (ap, $J = 6.4$ Hz, 1 H), 2.02 (m, 2 H), 1.61 (dt, $J = 14.3, 2.1$ Hz, 1 H), 1.56 - 1.89 (m, 25 H), 1.07 (d, $J = 6.4$ Hz, 3 H). ¹³C NMR (100 MHz, CD₃OD) δ 127.5 (q, $J = 276$), 76.7, 72.1, 51.8, 40.2, 38.2, 33.8 (q, $J = 28.2$ Hz), 29.9, 29.8, 29.7 (2 C), 29.5, 29.3, 28.8, 25.7, 22.9, 22.0 (q, $J = 3.0$ Hz), 20.8. ¹⁹F NMR (400 MHz, CDCl₃) δ -66.37 (t, $J = 11.1$ Hz, 3 F). HRMS (ESI) $m/z = 356.27688$ (Theo. for C₁₈H₃₆F₃NO₂+H: 356.27709). Anal. calcd. for C₁₈H₃₆F₃NO₂: C, 60.82; H, 10.21; N, 3.94; F, 16.03. Found: C 61.01; H 10.08; N 3.83; F 15.90.



(S)-N,N-Dibenzyl-1-((4S,6S)-2,2-dimethyl-6-(tridec-6-ynyl)-1,3-dioxan-4-yl)ethanamine

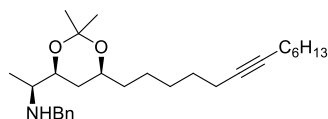
(25b): (2*S*,3*S*,5*S*)-2-(dibenzylamino)octadec-11-yne-3,5-diol (3.26 g, 6.83 mmol) was dissolved in 2,2-dimethoxypropane (33.5 ml, 273 mmol), to which tosic acid monohydrate (236 mg, 1.37 mmol) was added. The reaction was heated to 40 °C with stirring. After 12 hours, the TLC showed complete conversion to product. The reaction was worked up by diluting with Et₂O (300 mL), washing with sat'd NaHCO₃ (100 mL), and the aqueous layer was back extracted with Et₂O (100 mL). The combined organic layers were dried over MgSO₄ and evaporated to dryness. To remove remaining dimethoxypropane, the mixture was brought back up in Et₂O (2 x 20 mL) and rotovapped down again. The crude slightly yellow was purified by column chromatography on neutralized silica (ISCO, 120 g SiO₂, 0 - 15% EtOAc in hexanes, each with 1.5% Et₃N) to yield the product as a clear colorless oil (3.14 g, 89%). $R_f = 0.85$ (4:1, hexanes:EtOAc). IR (ν_{\max} , cm⁻¹

¹): 3025, 2930, 1601, 1489, 1450, 1376, 1257, 1199, 1175, 1109, 1072, 1028, 970, 945, 872, 744, 729, 698. $[\alpha]_D^{24} = -8.0^\circ$ ($c = 4.5$ in CHCl_3). ¹H NMR (400 MHz, CDCl_3) δ 7.40 (m, 4 H), 7.27 (m, 4 H), 7.19 (m, 2 H), 3.92 (d, $J = 13.7$ Hz, 2 H), 3.85 (m, 1 H), 3.76 (m, 1 H), 3.50 (d, $J = 13.7$ Hz, 2 H), 2.67 (m, 1 H), 2.13 (m, 4 H), 1.55 - 1.45 (m, 5 H), 1.43 (s, 3 H), 1.43 (s, 3 H), 1.40 - 1.15 (m, 13 H), 1.02 (d, $J = 7.02$ Hz, 3 H), 0.88 (t, $J = 7.32$ Hz, 3 H). ¹³C NMR (125 MHz, CDCl_3) δ 141.3 (2 C), 129.0 (4 C), 128.1 (4 C), 126.7 (2 C), 98.3, 80.5, 80.3, 72.6, 69.2, 56.3, 54.8 (2 C), 36.7, 34.7, 31.6, 30.5, 29.3, 29.3, 29.0, 28.7, 24.7, 22.8, 19.7, 19.0, 18.9, 14.3, 11.4. HRMS (ESI) $m/z = 518.39965$ (Theo. for $\text{C}_{35}\text{H}_{51}\text{NO}_2 + \text{H}$: 518.39926). Anal. calcd. for $\text{C}_{35}\text{H}_{51}\text{NO}_2$: C, 81.19; H, 9.93; N, 2.45. Found: C 80.93; H 9.96; N 2.71.



(S)-N,N-Dibenzyl-1-((4S,6S)-2,2-dimethyl-6-(13,13,13-trifluorotridec-6-ynyl)-1,3-dioxan-4-yl)ethanamine (25a): (2*S*,3*S*,5*S*)-2-(dibenzylamino)-18,18,18-trifluorooctadec-11-yne-3,5-diol (2.24 g, 4.21 mmol) was dissolved in 2,2-dimethoxypropane (15.4 ml, 126 mmol), to which tosic acid monohydrate (344 mg, 2.00 mmol) was added. The reaction was heated to 40 °C. After 12 hours, the TLC showed complete conversion to product. The reaction was worked up by diluting with Et_2O (300 mL), washing with sat'd NaHCO_3 (100 mL), and the aqueous layer was back extracted with Et_2O (100 mL). The combined organic layers were dried over MgSO_4 and evaporated to dryness. To remove remaining dimethoxypropane, the mixture was brought back up in Et_2O (2 x 20 mL) and evaporated again. The crude slightly yellow was purified by column chromatography on neutralized silica (ISCO, 120 g SiO_2 , 0 - 15% EtOAc in Hex, each with 1.5% Et_3N) to yield the product as a clear colorless oil (2.36 g, 98%). $R_f = 0.75$ (4:1, hexanes: EtOAc). $[\alpha]_D^{24} = -8.8^\circ$ ($c = 3.7$ in CHCl_3). IR (ν_{max} , cm^{-1}): 3025, 2989, 2935, 2854, 1601, 1489, 1454,

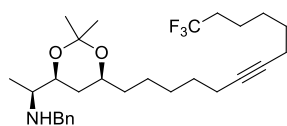
1377, 1253, 1199, 1180, 1134, 1033, 968, 949, 872, 745, 730, 698, 652. ^1H NMR (400 MHz, CDCl_3) δ 7.45 - 7.20 (m, 10 H), 4.77 (bs, 1 H), 3.81 (d, $J = 13.3$ Hz, 2 H), 3.88 (m, 1 H), 3.80 (m, 1 H), 3.54 (d, $J = 13.3$ Hz, 2 H), 2.72 (m, 1 H), 2.21 - 2.02 (m, 6 H), 1.64 - 1.47 (m, 8 H), 1.46 (s, 6 H), 1.45 - 1.19 (m, 7 H), 1.05 (d, $J = 6.4$ Hz, 3 H). ^{13}C NMR (100 MHz, CDCl_3) δ 141.3 (2 C), 129.0 (4 C), 128.2 (4 C), 127.4 (q, $J = 267$ Hz, 1 C), 126.7 (2 C), **98.4**, 80.8, 79.8, 72.6, 69.2, 56.3, 54.8, 36.7, 34.7, 33.9 (q, $J = 28.2$ Hz, 1 C), **30.6**, 29.2, 29.0, 28.8, 28.0, 24.8, 21.7 (q, $J = 3.1$ Hz, 1 C), **19.7**, 18.9, 18.7, 11.4. ^{19}F NMR (400 MHz, CDCl_3) δ -66.60 (t, $J = 10.9$ Hz, 3 F). HRMS (ESI) $m/z = 572.37189$ (Theo. for $\text{C}_{32}\text{H}_{44}\text{F}_3\text{NO}_2 + \text{H}$: 532.34024). Anal. calcd. for $\text{C}_{35}\text{H}_{48}\text{F}_3\text{NO}_2$: C, 73.52; H, 8.46; N, 2.45; F 9.97. Found: C 73.69; H 8.48; N, 2.43; F, 9.85.



(S)-N-Benzyl-1-((4S,6S)-2,2-dimethyl-6-(tridec-6-ynyl)-1,3-dioxan-4-yl)ethanamine (35b):

Utilizing literature precedence, (*S*)-*N,N*-dibenzyl-1-((4*S*,6*S*)-2,2-dimethyl-6-(tridec-6-ynyl)-1,3-dioxan-4-yl)ethanamine (3.06 g, 5.90 mmol) was dissolved in DCM (100 ml) (not dry or under argon), to which *N*-iodosuccinimide (3.98 g, 17.7 mmol) was added all in one portion.⁵⁵ The reaction was stirred vigorously for 3 minutes, at which point it was quenched by the addition of sat'd sodium thiosulfate (20 mL). The mixture was then diluted with DCM (300 mL), washed with sat'd NaHCO_3 (100 mL), water (100 mL), then brine (100 mL), and finally dried over MgSO_4 and evaporated to give the crude product as a yellow oil. The product was purified by column chromatography on neutralized silica (ISCO, 120 g SiO_2 , 10 - 40% B (90:10:1 of DCM:MeOH: HN_4OH) in DCM) to give the desired intermediate as a yellow oil (2.55 g, 99%).

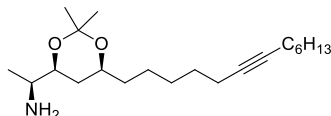
$R_f = 0.05$ (4:1, hexanes:EtOAc). $^1\text{H NMR}$ (400 MHz, CDCl_3) δ 7.34 - 7.22 (m, 5 H), 3.89 (d, $J = 13.1$ Hz, 1 H), 3.79 (m, 1 H), 3.68 (d, $J = 13.1$ Hz, 1 H), 3.67 (m, 1 H), 2.63 (m, 1 H), 2.22 (bs, 1 H), 2.14 (m, 4 H), 1.55 - 1.42 (m, 7 H), 1.41 (s, 3 H), 1.38 (s, 3 H), 1.42 - 1.24 (m, 11 H), 1.02 (d, $J = 7.0$ Hz, 3 H), 0.89 (t, $J = 7.3$ Hz, 3 H). $^{13}\text{C NMR}$ (125 MHz, CDCl_3) δ 140.9, 128.6 (2 C), 128.3 (2 C), 127.0, 98.7, 80.5, 80.2, 72.9, 68.9, 57.2, 51.3, 36.6, 33.5, 31.6, 30.4, 29.3, 29.2, 28.9, 28.7, 24.7, 22.8, 20.1, 19.0, 18.9, 15.3, 14.3. HRMS (ESI) $m/z = 428.35242$ (Theo. for $\text{C}_{28}\text{H}_{45}\text{NO}_2 + \text{H}$: 428.35231).



(S)-N-Benzyl-1-((4S,6S)-2,2-dimethyl-6-(13,13,13-trifluorotridec-6-ynyl)-1,3-dioxan-4-

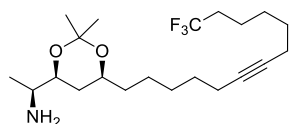
yl)ethanamine (35a): (S)-N,N-dibenzyl-1-((4S,6S)-2,2-dimethyl-6-(13,13,13-trifluorotridec-6-ynyl)-1,3-dioxan-4-yl)ethanamine (52 mg, 0.091 mmol) was dissolved in DCM (2 mL) (not dry or under argon), to which N-iodosuccinimide (61.4 mg, 0.273 mmol) was added all in one portion. The reaction was stirred for 3 minutes, at which point it was quenched by the addition of saturated sodium thiosulfate (1 mL). The mixture was then diluted with DCM (3 mL), washed with sat'd NaHCO_3 (3 mL), water (3 mL), then brine (3 mL), and finally dried over MgSO_4 and evaporated to yield a clear yellow oil which LCMS confirms to be product. The crude product was purified by column chromatography on neutralized silica (ISCO, 4 g, 10 - 60% B (90:10:1 of DCM:MeOH: HN_4OH) in DCM) to give the free amine as a clear yellow oil (41 mg, 94%). $R_f = 0.05$ (4:1, hexanes:EtOAc), 0.78 (89:10:1, DCM:MeOH: NH_4OH). $^1\text{H NMR}$ (400 MHz, CDCl_3) δ 7.34 - 7.22 (m, 5 H), 3.89 (d, $J = 13.1$ Hz, 1 H), 3.79 (m, 1 H), 3.68 (d, $J = 13.1$ Hz, 1 H), 3.66 (m, 1 H), 2.63 (m, 1 H), 2.22 (bs, 1 H), 2.14 (m, 4 H), 2.08 (m, 2 H), 1.61 - 1.42 (m, 11 H), 1.41 (s, 3 H), 1.38 (s, 3 H), 1.42 - 1.24 (m, 5 H), 1.02 (d, $J = 7.0$ Hz, 3 H). $^{13}\text{C NMR}$ (125 MHz,

CDCl₃) δ 140.9, 128.6 (2 C), 128.3 (2 C), 127.4 (q, $J = 267$ Hz, 1 C), 127.0, 98.7, 80.7, 79.8, 72.9, 68.9, 57.2, 51.3, 36.6, 33.9 (q, $J = 28.2$ Hz), 33.5, 30.4, 29.2, 29.0, 28.8, 28.0, 24.7, 21.6 (q, $J = 3.0$ Hz), 20.1, 18.8, 18.7, 15.3. ¹⁹F NMR (400 MHz, CDCl₃, ref to TFA ext. at -75.8p) δ -66.78 (t, $J = 11.8$ Hz, 3 F). HRMS (ESI) $m/z = 482.32408$ (Theo. for C₂₈H₄₂F₃NO₂+H: 482.32404).



(S)-1-((4S,6S)-2,2-Dimethyl-6-(tridec-6-ynyl)-1,3-dioxan-4-yl)ethanamine (36b): (*S*)-*N*-benzyl-1-((4S,6S)-2,2-dimethyl-6-(tridec-6-ynyl)-1,3-dioxan-4-yl)ethanamine (243 mg, 0.568 mmol) was brought up in DCM (10 mL) in a round bottom flask (not under argon), to which Dess-Martin periodinane (723 mg, 1.71 mmol) was added all at once.⁵⁶ The reaction vessel was stirred at RT for 105 minutes, at which time LCMS showed nearly complete conversion (>13:1) to product with no byproducts formed. The reaction was diluted into Et₂O (90 mL), to which aq. NaOH (1.0 M, 30 mL) was added to hydrolyze the periodinane. The mixture was stirred vigorously for 10 minutes, then the organic layer was washed with aq. NaOH (1.0 M, 25 mL), water (40 mL), brine (40 mL), dried over MgSO₄, and evaporated to give a cloudy yellow oil. The product was purified crude product by non-automated column chromatography on neutralized silica (15 g SiO₂, 0 - 100% B (90:10:1 of DCM:MeOH:NH₄OH) in DCM after neutralizing column in 10% B) to give the product as a brown oil (108 mg, 56 %). $R_f = 0.38$ (90:10:1 of DCM:MeOH:NH₄OH). IR (ν_{\max} , cm⁻¹): 3375, 2993, 2930, 2858, 1643, 1585, 1460, 1378, 1262, 1199, 1174, 1104, 971, 929, 870, 735, 629. $[\alpha]_D^{24} = -0.9^\circ$ ($c = 1.50$ in CHCl₃). ¹H NMR (400 MHz, CDCl₃) δ 3.79 (m, 1 H), 3.49 (m, 1 H), 2.80 (m, 1 H), 2.25 (bs, 2 H), 2.13 (m, 4 H), 1.59 - 1.21 (m, 18 H), 1.42 (s, 3 H), 1.39 (s, 3 H), 1.04 (d, $J = 7.02$ Hz, 3 H), 0.89 (t, $J =$

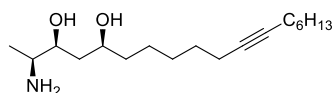
6.85 Hz, 3 H). ^{13}C NMR (125 MHz, CDCl_3) δ 98.7, 80.5, 80.3, 74.6, 68.8, 51.5, 36.6, 33.6, 31.6, 30.4, 29.3, 29.2, 28.9, 28.7, 24.7, 22.8, 20.1, 19.0, 18.9, 18.5, 14.3. HRMS (ESI) m/z = 338.30560 (Theo. for $\text{C}_{21}\text{H}_{36}\text{F}_3\text{NO}_2+\text{H}$: 338.30536). Anal. calcd. for $\text{C}_{21}\text{H}_{39}\text{NO}_2 + 0.20\cdot\text{DCM}$: C, 71.82; H, 11.20; N, 3.95. Found: C 72.20; H 10.95; N, 3.96.



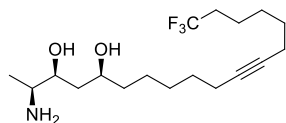
(S)-1-((4S,6S)-2,2-Dimethyl-6-(13,13,13-trifluorotridec-6-ynyl)-1,3-dioxan-4-yl)ethanamine

(36a): (*S*)-*N*-benzyl-1-((4*S*,6*S*)-2,2-dimethyl-6-(13,13,13-trifluorotridec-6-ynyl)-1,3-dioxan-4-yl)ethanamine (575 mg, 1.19 mmol) was brought up in DCM (20 mL) in a round bottom flask (not under argon), to which Dess-Martin periodinane (760 mg, 1.79 mmol) was added all at once. The reaction vessel was stirred at RT for 100 minutes, at which time LCMS showed 90% conversion to product. The reaction was diluted into Et_2O (160 mL), to which aq. NaOH (1.0 M, 60 mL) was added to hydrolyze the periodinane. The mixture was stirred vigorously for 10 minutes, then the organic layer was washed with aq. NaOH (1.0 M, 60 mL), water (80 mL), brine (2 x 60 mL), dried over MgSO_4 , and evaporated to give a cloudy yellow oil, which was dry-loading on 1.5 g of silica, then purified by column chromatography on neutralized silica (ISCO, 40 g SiO_2 , 0 - 100% B (90:10:1 of DCM:MeOH: NH_4OH) in DCM after neutralizing column in 10% B) to give the product as a brown oil (200 mg, 39%). R_f = 0.38 (90:10:1 of DCM:MeOH: NH_4OH). IR (ν_{max} , cm^{-1}): 3367, 2993, 2939, 2862, 2202, 1581, 1458, 1435, 1385, 1331, 1254, 1198, 1177, 1132, 1035, 968, 910, 868, 732, 648. $[\alpha]_{\text{D}}^{24} = +0.9^\circ$ ($c = 3.4$ in CHCl_3). ^1H NMR (400 MHz, CDCl_3) δ 3.77 (m, 1 H), 3.45 (m, 1 H), 2.76 (m, 1 H), 2.12 (m, 4 H), 2.06 (m, 2 H), 1.94 (bs, 2 H), 1.59 - 1.21 (m, 16 H), 1.40 (s, 3 H), 1.37 (s, 3 H), 1.01 (d, $J = 7.0$ Hz, 3 H). ^{13}C NMR (125 MHz, CDCl_3) δ 127.4 (q, $J = 267$ Hz, 1 C), 98.7, 80.7, 79.8, 74.7, 68.8, 51.3,

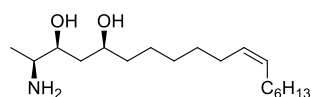
36.6, 33.8 (q, $J = 28.2$ Hz), 33.6, 30.3, 29.1, 28.9, 28.7, 28.0, 24.7, 21.6 (q, $J = 3.0$ Hz), 20.0, 18.8, 18.7, 18.6. ^{19}F NMR (400 MHz, CDCl_3) δ -66.84 (t, $J = 10.8$ Hz, 3 F). HRMS (ESI) $m/z = 392.27718$ (Theo. for $\text{C}_{21}\text{H}_{36}\text{F}_3\text{NO}_2 + \text{H}$: 392.27709). Anal. calcd. for $\text{C}_{21}\text{H}_{36}\text{F}_3\text{NO}_2$: C, 64.42; H, 9.27; N, 3.58; F, 14.56. Found: C 64.16; H 9.07; N, 3.58; F, 14.30.



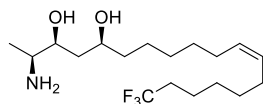
(2S,3S,5S)-2-Aminooctadec-11-yne-3,5-diol (3) (*S*)-1-(((4*S*,6*S*)-2,2-dimethyl-6-(tridec-6-ynyl)-1,3-dioxan-4-yl)ethanamine (216 mg, 0.640 mmol) was dissolved in MeOH (4 mL), to which tosic acid monohydrate (487 mg, 2.83 mmol) was added. The reaction was stirred at RT for 100 minutes. The solvent was evaporated down to 1 mL, then the mixture was diluted with DCM (100 mL), which was neutralized with sat'd NaHCO_3 (10 mL). The aqueous layer was back extracted with DCM (30 mL), and the combined organic solutions were dried with MgSO_4 and evaporated to yield a crude yellow oil that was free of starting material by TLC. Product was purified by column chromatography (ISCO, 12 g SiO_2 , 0 - 100% B (70:30:2 of DCM:MeOH: NH_4OH) in DCM after equilibrating in 5% B) to give the pure product as a off white waxy solid (120.7 mg, 63%). $R_f = 0.20$ (90:10:1, DCM:MeOH: NH_4OH). IR (ν_{max} , cm^{-1}): 3354, 3245, 2928, 2856, 1581, 1458, 1376, 1331, 1077, 849, 814, 726. $[\alpha]_{\text{D}}^{24} = +1.5^\circ$ ($c = 3.67$ in CHCl_3). ^1H NMR (400 MHz, CDCl_3) δ 3.83 (m, 1 H), 3.45 (m, 1 H), 3.10 (bs, 4 H), 2.74 (m, 1 H), 2.11 (m, 4 H), 1.61 (d, $J = 14.09$ Hz, 1 H), 1.54 - 1.20 (m, 17 H), 1.08 (d, $J = 6.26$ Hz, 3 H), 0.87 (t, $J = 6.65$ Hz, 3 H). ^{13}C NMR (125 MHz, CDCl_3) δ 80.5, 80.2, 76.6, 72.0, 51.8, 40.2, 38.1, 31.5, 29.3 (2 C), 29.1, 28.7, 25.2, 22.7, 20.7, 18.9 (2 C), 14.2. HRMS (ESI) $m/z = 298.27420$ (Theo. for $\text{C}_{18}\text{H}_{32}\text{F}_3\text{NO}_2 + \text{H}$: 298.27406). Anal. calcd. for $\text{C}_{18}\text{H}_{35}\text{NO}_2 + 0.85 \cdot \text{H}_2\text{O}$: C, 69.12; H, 11.83; N, 4.48. Found: C 69.10; H 11.30; N, 4.25%.



(2S,3S,5S)-2-Amino-18,18,18-trifluorooctadec-11-yne-3,5-diol (4): (*S*)-1-((4*S*,6*S*)-2,2-Dimethyl-6-(13,13,13-trifluorotridec-6-ynyl)-1,3-dioxan-4-yl)ethanamine (104.3 mg, 0.266 mmol) was dissolved in MeOH (3 mL), to which tosic acid monohydrate (184 mg, 1.07 mmol) was added. The reaction was stirred at RT for 8 hours, at which time LCMS showed 90% conversion to the product. The solvent was evaporated down to 1 mL, then the mixture was diluted with DCM (20 mL) and washed with sat'd NaHCO₃ (2 mL). The organic solution was then dried with MgSO₄, and evaporated to yield a crude yellow oil which showed only product by LCMS. The product was purified by column chromatography (ISCO, 4 g SiO₂, 0 - 50% B (70:30:2 of DCM:MeOH:NH₄OH) in DCM after equilibrating in 5% B) to give the product as an off white crystalline solid (62.3 mg, 67%). $R_f = 0.25$ (70:30:2, DCM:MeOH:NH₄OH). MP: 63 – 64 °C. IR (ν_{\max} , cm⁻¹): 3407, 3338, 3269, 2925, 2844, 2803, 2717, 1577, 1458, 1434, 1327, 1295, 1252, 1190, 1128, 1054, 1034, 990, 927, 837, 809, 723, 655. $[\alpha]_D^{24} = +1.4^\circ$ ($c = 1.49$ in CHCl₃). ¹H NMR (400 MHz, CDCl₃) δ 3.85 (m, 1 H), 3.45 (m, 1 H), 2.95 (bs, 4 H), 2.74 (m, 1 H), 2.15 (m, 4 H), 2.06 (m, 2 H), 1.66 - 1.28 (m, 16 H), 1.10 (d, $J = 6.65$ Hz, 3 H). ¹³C NMR (125 MHz, CDCl₃) δ 127.4 (q, $J = 267$ Hz, 1 C), 80.8, 79.8, 76.7, 72.0, 51.8, 40.4, 38.1, 33.8 (q, $J = 28.2$ Hz), 29.2, 29.1, 28.8, 28.0, 25.2, 21.6 (q, $J = 3.0$ Hz, 1 C), 20.9, 18.9, 18.7. ¹⁹F NMR (400 MHz, CDCl₃) δ -66.35 (t, $J = 10.3$ Hz, 3 F). HRMS (ESI) $m/z = 352.24589$ (Theo. for C₁₈H₃₂F₃NO₂+H: 352.24579). Anal. calcd. for C₁₈H₃₂F₃NO₂: C, 61.51; H, 9.18; N, 3.99; F, 16.22. Found: C 61.76; H 9.14; N, 3.80; F, 16.01.

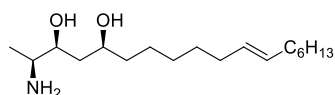


(2*S*,3*S*,5*S*,*Z*)-2-Amino-octadec-11-ene-3,5-diol (7): (2*S*,3*S*,5*S*)-2-amino-octadec-11-yne-3,5-diol (40.6 mg, 136 μ mol) was dissolved in MeOH (7 ml), to which quinoline (56 μ L, 0.47 mmol) and Lindlar's catalyst (30 mg) were added. The solution was degassed by bubbling argon through for 5 minutes with vigorous stirring. Next the flask was evacuated with house vacuum and filled with hydrogen gas (1 atm.) three times. After stirring vigorously for 12 minutes LCMS showed complete consumption of starting material. The heterogeneous mixture was filtered through a pad of Celite, which was washed with MeOH (50 mL). The solvent was evaporated to give a crude yellow that was purified by column chromatography (ISCO, 4 g SiO₂, 0 - 100% B (70:30:2 of DCM:MeOH:NH₄OH) in DCM after equilibrating in 5% B) to give the final product as an off white waxy solid (31.3 mg, 92 %). $R_f = 0.23$ (70:30:2, DCM:MeOH:NH₄OH). IR (ν_{\max} , cm⁻¹): 3350, 3277, 2924, 2854, 1572, 1460, 1376, 1078, 849, 724. $[\alpha]_D^{24} = +2.0^\circ$ ($c = 1.98$ in CHCl₃). ¹H NMR (400 MHz, CDCl₃) δ 5.34 (m, 2 H), 3.85 (m, 1 H), 3.46 (m, 1 H), 2.92 (bs, 4 H), 2.75 (m, 1 H), 2.02 (m, 4 H), 1.63 (d, $J = 14.3$ Hz, 1 H), 1.54 - 1.21 (m, 17 H), 1.11 (d, $J = 6.3$ Hz, 3 H), 0.88 (t, $J = 5.3$ Hz, 3 H). ¹³C NMR (125 MHz, CDCl₃) δ 130.2, 129.9, 76.6, 72.1, 51.8, 40.4, 38.2, 32.0, 29.9 (2 C), 29.6, 29.2, 27.4 (2 C), 25.6, 22.9, 20.9, 14.3. HRMS (ESI) $m/z = 300.28959$ (Theo. for C₁₈H₃₇NO₂+H: 300.29025). Anal. Calcd. for C₁₈H₃₇NO₂ + 0.40·H₂O: C, 70.49; H, 12.42; N, 4.57. Found: C 70.60; H 12.00, N 4.33.



(2*S*,3*S*,5*S*,*Z*)-2-Amino-18,18,18-trifluorooctadec-11-ene-3,5-diol (8): (2*S*,3*S*,5*S*)-2-amino-18,18,18-trifluorooctadec-11-yne-3,5-diol (62.3 mg, 0.177 mmol) was dissolved in MeOH (6 ml), to which quinoline (10 μ L, 84 μ mol) and Lindlar's catalyst (150 mg) were added. The solution was degassed by bubbling argon through for 5 minutes with vigorous stirring. Next the flask was evacuated with house vacuum and filled with hydrogen gas (1 atm.) twice. After

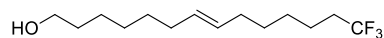
stirring vigorously for 15 minutes LCMS showed no remaining alkyne. The reaction was filtered over Celite, which was washed with plenty of MeOH (50 mL) and the filtrate was evaporated to give a yellow oil. The product was purified by column chromatography (ISCO, 4 g SiO₂, 0 - 100% B (70:30:2 of DCM:MeOH:NH₄OH) in DCM after equilibrating in 5% B) to give the product as a waxy off white solid (58 mg, 93%). $R_f = 0.25$ (70:30:2, DCM:MeOH:NH₄OH). IR (ν_{\max} , cm⁻¹): 3355, 3281, 2999, 2927, 2856, 1571, 1461, 1434, 1387, 1253, 1188, 1134, 1035, 847, 725, 653. $[\alpha]_D^{24} = +3.5^\circ$ ($c = 1.62$ in CHCl₃). ¹H NMR (400 MHz, CDCl₃) δ 5.34 (m, 2 H), 3.85 (m, 1 H), 3.45 (m, 1 H), 2.96 (bs, 4 H), 2.74 (m, 1 H), 2.07 (m, 2 H), 2.02 (m, 4 H), 1.62 (d, $J = 14.3$ Hz, 1 H), 1.58 - 1.22 (m, 15 H), 1.10 (d, $J = 6.7$ Hz, 3 H). ¹³C NMR (125 MHz, CDCl₃) δ 130.5, 129.5, 127.4 (q, $J = 267$ Hz, 1 C), 76.7, 72.1, 51.8, 40.4, 38.2, 33.8 (q, $J = 28.2$ Hz), 29.9, 29.6, 29.4, 28.4, 27.4, 27.0, 25.6, 22.0 (q, $J = 3.0$ Hz, 1 C), 20.9. ¹⁹F NMR (400 MHz, CDCl₃) δ -66.36 (t, $J = 11.0$ Hz, 3 F). HRMS (ESI) $m/z = 354.26146$ (Theo. for C₁₈H₃₂F₃NO₂+H: 354.26144). Anal. calcd. for C₁₈H₃₄F₃NO₂: C, 61.16; H, 9.70; N, 3.96; F, 16.12. Found: C 60.63; H 9.42; N, 3.83; F, 15.76.



(2S,3S,5S,E)-2-Aminooctadec-11-ene-3,5-diol (5): An argon purged round bottom flask (10 mL) containing (S)-1-((4S,6S)-2,2-dimethyl-6-(tridec-6-ynyl)-1,3-dioxan-4-yl)ethanamine (111 mg, 0.329 mmol) dissolved in THF (1 mL) was cooled to -55 °C and liquid ammonia (3 mL, 139 mmol) was added. Sodium metal (~100 mg, 4.4 mmol) was washed with hexanes, then added to the reaction mixture. The solution immediately turned blue and was stirred for 2 hours, at which point LCMS showed complete conversion to product. The reaction was quenched by drop wise addition of aq. NH₄OH (30 %) until the reaction ceased bubbling. The organics were brought up in Et₂O (20 mL), and washed with water (5 mL), sat'd NaHCO₃ (5 mL), and brine (10 mL). The

organic layer was dried over MgSO₄ and evaporated to give the crude yellow oil that was carried on to the next step without purification. R_f = 0.15 (90:10:1, DCM:MeOH:NH₄OH).

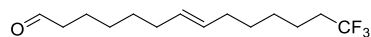
(S)-1-((4S,6S)-2,2-dimethyl-6-((E)-tridec-6-enyl)-1,3-dioxan-4-yl)ethanamine (100 mg, 0.295 mmol) was placed in a small vial (4 mL) containing a stir bar at room temperature, to which water (3 mL) and trifluoroacetic acid (1 mL, 13 mmol) were added. The mixture was stirred for 30 minutes, at which time LCMS showed complete conversion to product. The solution was transferred to an Erlenmeyer flask where it was neutralized with sat'd NaHCO₃ (10 mL). The aqueous phase was then extracted with DCM (3 x 20 mL), which was then dried with MgSO₄ and evaporated to give the crude yellow oil. The product was subject to purification by column chromatography (ISCO, 4 g SiO₂, 0 - 100 % B (70:30:2 of DCM/MeOH/HN₄OH) in DCM after equilibrating the column in 10 % B) to give the product as an off white solid (42.3 mg, 48% over 2 steps). R_f = 0.20 (70:30:2 of DCM/MeOH/HN₄OH). MP: 38 – 40 °C. IR (ν_{max}, cm⁻¹): 3350, 3281, 2923, 2853, 1572, 1459, 1376, 1078, 966, 849, 725. [α]_D²⁴ = +2.2 ° (c = 2.25 in CHCl₃). ¹H NMR (400 MHz, CDCl₃) δ 5.37 (m, 2 H), 3.84 (m, 1 H), 3.45 (m, 1 H), 2.99 (bs, 4 H), 2.74 (m, 1 H), 1.96 (m, 4 H), 1.32 (m, 1 H), 1.5-1.2 (m, 17 H), 1.09 (d, *J* = 6.3 Hz, 3 H), 0.87 (t, *J* = 5.3 Hz, 3 H). ¹³C NMR (125 MHz, CDCl₃) δ 130.6, 130.4, 76.7, 72.1, 51.8, 40.3, 38.2, 32.8, 32.7, 31.9, 29.8 (2 C), 29.4, 29.0, 25.5, 22.8, 20.8, 14.3. HRMS (ESI) *m/z* = 300.28959 (Theo. for C₁₈H₃₇NO₂+H: 300.29025). Anal. calcd. for C₁₈H₃₇NO₂ + 0.10·H₂O: C, 71.76; H, 12.44; N, 4.65. Found: C 71.63; H 12.24, N 4.41.



(E)-14,14,14-Trifluorotetradec-7-en-1-ol (38): Literature reported procedure.⁵⁷ 14,14,14-trifluorotetradec-7-en-1-ol (1.06 g, 4.01 mmol) in a dry, argon purged 50 mL round bottom flask, was brought up in DCM (14 mL) and recently purchased triethoxysilane (888 μL, 4.81 mmol)

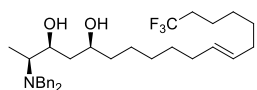
was added. The mixture was cooled to 0° C and [Cp*Ru(MeCN)₃]PF₆ (42 mg, 80 μmol) was added. The vial was immediately allowed to warm to RT, where it was stirred for 60 minutes. The reaction was then worked up by diluting the mixture with Et₂O (50 mL) whence the ruthenium catalyst formed a brown precipitate, which was filtered over a plug of Florisil (5 mL) in a 25 mL syringe, which was washed with plenty of ether (150 mL). The solvent was evaporated and the crude material was subject to high vac. for 30 minutes to remove any excess triethoxysilane, leaving the crude product as a clear yellow oil.

Next the crude vinyl-silane was brought up in THF (34 mL), to which recently purified copper(I) iodide (1.15 g, 6.02 mmol) was added. To the cloudy solution was added TBAF (1.0 M in THF, 12.0 ml, 12.0 mmol), which turned the solution clear and orange. The reaction was let stir under argon and heated to 35 °C overnight. The reaction mixture was passed through a plug of silica gel and washed with Et₂O (150 mL). The eluent was evaporated, and purified by column chromatography (ISCO, 120 g SiO₂, 0 - 40 % EtOAc in Hex) to give the product as a slightly yellow oil (402 mg, 37%). R_f = 0.45 (2:1, hexanes:EtOAc). IR (neat, cm⁻¹): 3331, 2927, 2856, 1462, 1440, 1388, 1253, 1135, 1037, 967 (**trans alkene**), 654. ¹H NMR (400 MHz, CDCl₃) δ 5.39 (m, 2 H), 3.65 (t, *J* = 6.7 Hz, 2 H), 2.14 - 1.95 (m, 6 H), 1.56 (m, 4 H), 1.36 (m, 11 H). ¹³C NMR (100 MHz, CDCl₃) δ 130.9, 130.0, 127.4 (q, *J* = 267 Hz, 1 C), 63.1, 33.9 (q, *J* = 28.2 Hz, 1 C), 32.9, 32.7, 32.4, 29.7, 29.3, 29.1, 28.3, 25.8, 21.9 (q, *J* = 3.1 Hz, 1 C). ¹⁹F NMR (400 MHz, CDCl₃) δ -66.69 (t, *J* = 11.8 Hz, 3 F). HRMS (ESI) *m/z* 267.19292 (Theo. for C₁₄H₂₃FO+H: 267.19303). Anal. calcd: C 63.13; H 9.46; F 21.40. Found: C 63.43; H 9.41; F 21.13.



(E)-14,14,14-Trifluorotetradec-7-en-1-ol (39): (E)-14,14,14-trifluorotetradec-7-en-1-ol (770 mg, 2.89 mmol) was dissolved in dry DCM (70 mL), to which Dess-Martin periodinane (1.53 g,

3.61 mmol) was added. The reaction was stirred at room temperature under argon for 2 hours. TLC showed complete conversion to product. The homogenous reaction mixture was diluted with Et₂O (200 mL), and to the resulting suspension of was added to aq. NaOH (1.0 M, 7 mL) to hydrolyze the periodinane to the water soluble 2-iodosobenzoate. The mixture was stirred for 10 minutes, then the organic layer was washed with aq. NaOH (1.0 M, 7 mL), water (10 mL), and brine (10 mL). The organic layer was then dried over MgSO₄ and evaporated to give the crude product that was free of byproducts by NMR, and used directly in next reaction immediately (720 mg, 94%). *R_f* = 0.70 (3:1, hexanes:EtOAc). IR (neat, cm⁻¹): 2930, 2852, 2709, 2361, **1726**, 1385, 1253, 1135, 1037, **968** (trans-alkene), 731, 653. ¹H NMR (400 MHz, CDCl₃) δ 9.76 (t, *J* = 1.8 Hz, 1 H), 5.38 (m, 2 H), 2.42 (dt, *J* = 7.3, 1.8 Hz, 2 H), 2.14 - 1.95 (m, 6 H), 1.63 (m, 2 H), 1.55 (m, 2 H), 1.36 (m, 8 H). ¹³C NMR (125 MHz, CDCl₃) δ 203.0, 130.6, 130.3, 127.4 (q, *J* = 276.2 Hz), 44.0, 33.9 (q, *J* = 28.2 Hz), 32.5, 32.4, 29.4, 29.3, 28.8, 28.3, 22.1, 21.9 (q, *J* = 3.1 Hz). ¹⁹F NMR (400 MHz, CDCl₃; referenced to TFA) δ -66.68 (t, *J* = 11.1 Hz, 3 F). HRMS (ESI) *m/z* 265.17725 (Theo. for C₁₄H₂₃FO+H: 265.17738).

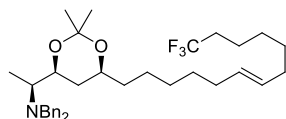


(2S,3S,5S,E)-2-(Dibenzylamino)-18,18,18-trifluorooctadec-11-ene-3,5-diol (40): To a stirred solution of (-)-DIP-Cl (50-65 wt% in hexanes, 2.80 ml, 3.90 mmol) in a flame dried flask (100 mL) with THF (20.0 mL), N,N-dimethylethylamine (1.26 ml, 11.7 mmol) was added drop wise at room temperature. The clear reaction mixture was cooled to -30 °C, and a solution of recently prepared (S)-3-(dibenzylamino)butan-2-one (935 mg, 3.50 mmol) in THF (10.0 mL) was added drop wise over a 2 minute period. The resulting cloudy white mixture was stirred for 1.5 hours more at -30 °C turning yellow, then was cooled to -78 °C. A solution of freshly prepared (E)-14,14,14-trifluorotetradec-7-enal (770 mg, 2.91 mmol) in THF (10.0 ml) was added drop wise

over the next 5 minutes. The reaction vessel was kept at $-78\text{ }^{\circ}\text{C}$ for 2.5 hours, then allowed to warm to $-20\text{ }^{\circ}\text{C}$ overnight. LCMS ($m/z = 532$) and TLC showed nearly complete conversion to product. The reaction mixture was quenched by the addition of a phosphate buffer (10.0 mL, pH = 7) over 3 minutes at $-20\text{ }^{\circ}\text{C}$, and stirring was continued over the next hour while the reaction was allowed to warm to room temperature. The mixture was then cooled to $-20\text{ }^{\circ}\text{C}$, and hydrogen peroxide (30% aq., 0.811 mL, 7.87 mmol) was added drop wise to the stirring mixture. After stirring for an additional hour and warming back to RT, the reaction mixture was diluted into Et_2O (100 mL), washed with brine (100 mL), dried over MgSO_4 , filtered, and concentrated under vacuum (theoretical yield = 1.5 g, crude mass = 3.3 g). This clear colorless oil was immediately taken to the next step without further purification or analysis. $R_f = 0.55$ (3:1, hexanes:EtOAc).

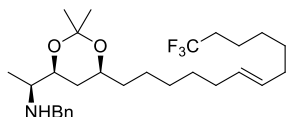
To a stirred solution of crude (2S,5S,E)-2-(dibenzylamino)-18,18,18-trifluoro-5-hydroxyoctadec-11-en-3-one in MeOH (35 mL) at $-20\text{ }^{\circ}\text{C}$ was added powdered sodium borohydride (190 mg, 8.26 mmol) in portions of 30 mg each until no more bubbles were formed and LCMS showed no remaining ketone. The resulting mixture was quenched by the drop wise addition of acetic acid (15 drops) until bubbling ceases. The solvent was carefully removed from the crude mixture, which was brought up in Et_2O (150 mL), to which aq. HCl (1 N, 3 mL) was added, which was neutralized with a sat'd NaHCO_3 wash (150 mL). The organic layer was then separated and washed with water (100 mL), then brine (150 mL), dried over MgSO_4 , and finally concentrated to give a clear colorless oil. Pinene byproduct was removed from the crude mixture by sublimation overnight at $50\text{ }^{\circ}\text{C}$ and full vacuum. The following day, the crude product was purified with some difficulty by column chromatography (ISCO, 80 g SiO_2 , 0 - 20 % EtOAc in hexanes each with 1.5 % Et_3N) to give the product as a clear colorless oil (1.05 g, 68% over 2 steps). $R_f = 0.40$ (3:1, hexanes:EtOAc). $[\alpha]_D^{24} = +26.3\text{ }^{\circ}$ ($c = 3.14$ in CHCl_3). IR (ν_{max} , cm^{-1}):

3510, 3399, 3027, 2927, 2844, 1454, 1377, 1253, 1136, 1032, 968, 844, 747, 733, 699, 654. ^1H NMR (400 MHz, CDCl_3) δ 7.34 - 7.24 (m, 10 H), 5.36 (m, 2 H), 4.76 (bs, 1 H), 4.05 (bs, 1 H), 3.85 (m, 1 H), 3.80 (d, $J = 13.3$ Hz, 2 H), 3.64 (dt, $J = 10.4, 2.4$ Hz, 1 H), 3.29 (d, $J = 13.3$ Hz, 2 H), 2.55 (m, 1 H), 2.10 - 1.90 (m, 6 H), 1.60 - 1.22 (m, 15 H), 1.14 (m, 1 H), 1.00 (d, $J = 6.7$ Hz, 3 H). ^{13}C NMR (100 MHz, CDCl_3) δ 138.8 (2 C), 131.0, 129.9, 129.2 (4 C), 128.7 (4 C), 127.5 (2 C), 127.5 (q, $J = 267$ Hz, 1 C), 72.2, 72.1, 59.0, 53.3, 40.3, 37.8, 33.9 (q, $J = 28.2$ Hz, 1 C), 32.7, 32.4, 29.7, 29.4, 29.3, 28.3, 25.5, 21.9 (q, $J = 3.1$ Hz, 1 C), 8.2. ^{19}F NMR (400 MHz, CDCl_3) δ -66.60 (t, $J = 11.06$ Hz, 3 F). HRMS (ESI) $m/z = 534.35559$ (Theo. for $\text{C}_{32}\text{H}_{44}\text{F}_3\text{NO}_2 + \text{H}$: 534.35534). Anal. calcd. for $\text{C}_{32}\text{H}_{44}\text{F}_3\text{NO}_2$: C, 72.01; H, 8.69; N, 2.62; F 10.68. Found: C, 72.29; H, 8.74; N, 2.67; F 10.79.



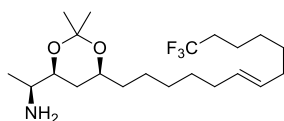
(S)-N,N-Dibenzyl-1-((4S,6S)-2,2-dimethyl-6-((E)-13,13,13-trifluorotridec-6-en-1-yl)-1,3-dioxan-4-yl)ethanamine (41): (2S,3S,5S,E)-2-(dibenzylamino)-18,18,18-trifluorooctadec-11-ene-3,5-diol (1.01 g, 1.89 mmol) was dissolved in 2,2-dimethoxypropane (20.0 mL, 163 mmol), to which tosic acid monohydrate (81 mg, 0.47 mmol) was added. The reaction was heated to 40 °C. After 19 hours, TLC showed 90% conversion. The reaction was worked up by diluting with Et_2O (100 mL), washing with sat'd NaHCO_3 (30 mL), and the aqueous layer was back extracted with Et_2O (30 mL). The combined organic layers were dried with brine (50 mL), then over MgSO_4 and evaporated to dryness. To get rid of any remaining volatile dimethoxypropane, the mixture was brought back up in Et_2O (2 x 5 mL) and evaporated again. The crude product was purified by column chromatography on neutralized silica (ISCO, 80 g SiO_2 , 0 - 20% EtOAc in Hex, each with 1.5% Et_3N) to give the product as a clear colorless oil (1.01 g, 93%). $R_f = 0.75$

(5:1, hexanes:EtOAc). IR (ν_{\max} , cm^{-1}): 3027, 2983, 2929, 2848, 1491, 1450, 1377, 1254, 1200, 1175, 1135, 1031, 967, 872, 744, 730, 698, 645. $[\alpha]_{\text{D}}^{24} = -7.3^\circ$ ($c = 1.08$ in CHCl_3). ^1H NMR (400 MHz, CDCl_3) δ 7.40 (m, 4 H), 7.27 (m, 4 H), 7.12 (m, 2 H), 5.38 (m, 2 H), 3.92 (d, $J = 13.73$ Hz, 2 H), 3.86 (m, 1 H), 3.76 (m, 1 H), 3.51 (d, $J = 13.73$ Hz, 2 H), 2.69 (m, 1 H), 2.05 (m, 2 H), 1.98 (m, 4 H), 1.55 - 1.45 (m, 3 H), 1.43 (s, 6 H), 1.40 - 1.24 (m, 12 H), 1.19 (dt, $J = 12.82, 2.44$ Hz, 1 H), 1.02 (d, $J = 6.71$ Hz, 3 H). ^{13}C NMR (100 MHz, CDCl_3) δ 141.4 (2 C), 131.0, 130.0, 129.0 (4 C), 128.2 (4 C), 127.5 (q, $J = 267$ Hz, 1 C), 126.7 (2 C), 98.4, 72.6, 69.3, 56.3, 54.8 (2 C), 36.8, 34.7, 33.9 (q, $J = 28.2$ Hz, 1 C), 32.7, 32.5, 30.6, 29.8, 29.3 (2 C), 28.3, 25.1, 21.9 (q, $J = 3.1$ Hz, 1 C), 19.7, 11.4. ^{19}F NMR (400 MHz, CDCl_3) δ -66.59 (t, $J = 11.06$ Hz, 3 F). HRMS (ESI) $m/z = 574.38606$ (Theo. for $\text{C}_{32}\text{H}_{44}\text{F}_3\text{NO}_2 + \text{H}$: 574.38664). Anal. calcd. for $\text{C}_{32}\text{H}_{44}\text{F}_3\text{NO}_2$: C, 73.27; H, 8.78; N, 2.44; F 9.93. Found: C 73.01; H 8.76, N 2.44, F 9.93.



(S)-N-Benzyl-1-((4S,6S)-2,2-dimethyl-6-((E)-13,13,13-trifluorotridec-6-en-1-yl)-1,3-dioxan-4-yl)ethanamine (42): (S)-N,N-dibenzyl-1-((4S,6S)-2,2-dimethyl-6-((E)-13,13,13-trifluorotridec-6-enyl)-1,3-dioxan-4-yl)ethanamine (985 mg, 1.72 mmol) was brought in DCM (40 mL), to which was added N-Iodosuccinimide (1.16 g, 5.15 mmol). The reaction was stirred for 3 min, at which time the color was dark brown. The reaction was then quenched immediately by diluting with DCM (100 mL), then quenching with sat'd sodium thiosulfate (15 mL). The organic layer was separated and washed with sat'd NaHCO_3 (100 mL), water (100 mL), brine (100 mL), then dried over MgSO_4 before evaporating. The crude yellow oil was purified by column chromatography on neutralized silica (ISCO, 40 g SiO_2 , 0 - 80% B (90:10:1 of DCM:MeOH: NH_4OH) in DCM after equilibrating in 10% B) to give the product as a clear yellow

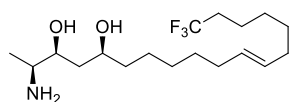
oil (730 mg, 88%). $R_f = 0.05$ (4:1, hexanes:EtOAc), 0.78 (89:10:1, DCM:MeOH:NH₄OH). ¹H NMR (400 MHz, CDCl₃) δ 7.33 (m, 4 H), 7.24 (m, 1 H), 5.39 (m, 2 H), 3.90 (d, $J = 13.7$ Hz, 1 H), 3.79 (m, 1 H), 3.69 (d, $J = 13.7$ Hz, 1 H), 3.68 (m, 1 H), 2.64 (m, 1 H), 2.28 (bs, 1 H), 2.06 (m, 2 H), 1.99 (m, 4 H), 1.60 - 1.48 (m, 4 H), 1.42 (s, 3 H), 1.39 (s, 3 H), 1.39 - 1.25 (m, 12 H), 1.03 (d, $J = 6.7$ Hz, 3 H). ¹³C NMR (100 MHz, CDCl₃) δ 140.9, 130.9, 130.0, 128.6 (2 C), 128.3 (2 C), 127.4 (q, $J = 267$ Hz, 1 C), 127.0, 98.7, 72.9, 69.0, 57.2, 51.2, 36.7, 33.9 (q, $J = 28.2$ Hz, 1 C), 33.5, 32.7, 32.4, 30.4, 29.7, 29.3 (2 C), 28.3, 25.0, 21.9 (q, $J = 3.1$ Hz, 1 C), 20.1, 15.3. ¹⁹F NMR (400 MHz, CDCl₃) δ -66.60 (t, $J = 11.1$ Hz, 3 F). HRMS (ESI) $m/z = 484.33984$ (Theo. for C₂₈H₄₄F₃NO₂+H: 484.33969).



(S)-1-((4S,6S)-2,2-Dimethyl-6-((E)-13,13,13-trifluorotridec-6-enyl)-1,3-dioxan-4-

yl)ethanamine (43): (*S*)-*N*-benzyl-1-((4*S*,6*S*)-2,2-dimethyl-6-((*E*)-13,13,13-trifluorotridec-6-enyl)-1,3-dioxan-4-yl)ethanamine (357 mg, 0.738 mmol) was dried under high vac and purged with argon in a 100 mL round bottom flask. To this was added DCM (20 ml), and finally Dess-Martin periodinane (470 mg, 1.107 mmol). The reaction was stirred under argon, and followed closely by LCMS. At 90 minutes, the reaction was quenched by diluting into Et₂O (125 mL) and adding aq. NaOH (1.0 M, 25 mL), then stirring vigorously for 10 minutes. The organic layer was separated, and washed with aq. NaOH (1.0 M, 25 mL), water (25 mL), and finally brine (50 mL), then dried over MgSO₄ and evaporated to give the crude product. This product was purified by chromatography on neutralized silica (ISCO, 40 g SiO₂, 0 - 100% B (70:30:2 of DCM:MeOH:NH₄OH) in DCM) to give a clear yellow oil (265 mg, 91%). $R_f = 0.45$ (70:30:2 of DCM:MeOH:NH₄OH). IR (ν_{\max} , cm⁻¹): 3387, 2991, 2929, 2857, 1580, 1461, 1439, 1379, 1334,

1254, 1199, 1176, 1135, 1036, 968, 935, 871, 837, 729, 654, 630. $[\alpha]_D^{24} = +1.9^\circ$ ($c = 1.82$ in CHCl_3). $^1\text{H NMR}$ (400 MHz, CDCl_3) δ 5.36 (m, 2 H), 3.78 (m, 1 H), 3.45 (m, 1 H), 2.77 (m, 1 H), 2.03 (m, 2 H), 1.97 (m, 4 H), 1.59 - 1.45 (m, 5 H), 1.41 (s, 3 H), 1.38 (s, 3 H), 1.38 - 1.24 (m, 12 H), 1.02 (d, $J = 6.71$ Hz, 3 H). $^{13}\text{C NMR}$ (100 MHz, CDCl_3) δ 130.9, 130.0, 127.5 (q, $J = 267$ Hz, 1 C), 98.7, 74.8, 68.9, 51.4, 36.7, 33.9 (q, $J = 28.2$ Hz, 1 C), 33.6, 32.7, 32.4, 30.4, 29.7, 29.3 (2 C), 28.3, 25.0, 21.9 (q, $J = 3.1$ Hz, 1 C), 20.1, 18.6. $^{19}\text{F NMR}$ (400 MHz, CDCl_3) δ -66.61 (t, $J = 11.1$ Hz, 3 F). HRMS (ESI) $m/z = 394.29252$ (Theo. for $\text{C}_{21}\text{H}_{38}\text{F}_3\text{NO}_2 + \text{H}$: 394.29274). Anal. calcd. for $\text{C}_{21}\text{H}_{38}\text{F}_3\text{NO}_2$: C, 64.09; H, 9.73; N, 3.56; F, 14.48. Found: C 63.95; H 9.78; N 3.52; F, 14.33.



(2S,3S,5S,E)-2-Amino-18,18,18-trifluorooctadec-11-ene-3,5-diol (6): (*S*)-1-((4*S*,6*S*)-2,2-dimethyl-6-((*E*)-13,13,13-trifluorotridec-6-enyl)-1,3-dioxan-4-yl)ethanamine (500 mg, 1.27 mmol) was dissolved in MeOH (5 mL), and trifluoroacetic acid (2.0 mL, 26 mmol) was added. The mixture was warmed to 40 °C and stirred for 4 hours at which time LCMS showed >90% conversion. The solvent was removed under reduced pressure and MeOH (1 mL) was added followed by evaporation again (3 x) to remove most of the remaining TFA, then the same was done with DCM (2 x 1 mL) to give the TFA salt of the product as a thick crude yellow oil. The product was freebased by bringing up in DCM (5 mL) and washing with sat'd NaHCO_3 (5 mL), drying the organic layer with MgSO_4 , and evaporating. The free amine that was purified by column chromatography on neutralized silica (ISCO, 40 g SiO_2 , 0 - 100% B (70:30:2 of DMC:MeOH: NH_4OH) in DCM after equilibrating in 5% B) to give the final product as a white solid (422 mg, 94%). $R_f = 0.25$ (80:20:1.5, DMC:MeOH: NH_4OH). MP: 58 – 60 °C. $[\alpha]_D^{24} = +2.0^\circ$ ($c = 1.38$ in CHCl_3). IR (ν_{max} , cm^{-1}): 3342, 3277, 2924, 2854, 1581, 1460, 1388, 1332, 1253,

1132, 1037, 967, 848, 731, 655. ^1H NMR (400 MHz, CDCl_3) δ 5.37 (m, 2 H), 3.85 (m, 1 H), 3.47 (m, 1 H), 2.98 (bs, 4 H), 2.76 (m, 1 H), 2.10 - 1.92 (m, 6 H), 1.66 - 1.24 (m, 18 H), 1.10 (d, $J = 6.26$ Hz, 3 H). ^{13}C NMR (100 MHz, CDCl_3) δ 130.9, 129.9, 127.4 (q, $J = 267$ Hz, 1 C), 76.7, 72.0, 51.8, 40.1, 38.2, 33.8 (q, $J = 28.2$ Hz, 1 C), 32.7, 32.4, 29.7, 29.4, 29.2, 28.2, 25.5, 21.8 (q, $J = 3.1$ Hz, 1 C), 20.6. ^{19}F NMR (400 MHz, CDCl_3 , Referenced to TFA) δ -66.61 (t, $J = 11.06$ Hz, 3 F). HRMS (ESI) $m/z = 354.26109$ (Theo. for $\text{C}_{18}\text{H}_{34}\text{F}_3\text{NO}_2 + \text{H}$: 354.21644). Anal. calcd: C 61.16; H 9.70; N 3.96; F 16.12. Found: C 60.86; H 9.46; N 3.84; F 15.84.

1.6.2 Biological Protocols

Protocol for the pharmacokinetic study of trifluoromethyl-enigmol (**2**)

- **Purpose:** To estimate oral and i.v. PK parameters for CF_3 -enigmol in blood and 24 hour RBC and tissue concentrations after a single dose. To compare tissue concentrations of CF_3 -enigmol and **Enigmol** and both of their metabolites after a single oral dose. To compare endogenous sphingolipid profiles in tissues after oral dosing of the two compounds.
- **Personnel & Facility:** Randy Howard, Deborah Culver & Sarah Pruitt; EIDD, Emory University, Atlanta, GA. Experiment done in Emory DAR, Clinic B (South Clinics). Mark Baillie; Chemistry Department, Emory University. BCDMPK Group, EIDD, Emory University, Atwood Chemistry Center.
- **Materials:** **Enigmol**; CF_3 -enigmol (**2**); PEG 400 (PEG, EMD #PX1286B-2, lot #47360914); Ethanol (E, Decon Labs #2716, lot #A01190801L); Tween 80 (T80, Sigma #P8074, lot #018K00941); olive oil (OO, Sigma #O1514, lot #0001428703); sterile saline

(Hospira, NDC 0409-4888-10; lot #87-153-DK); sterile water (Hospira, NDC 0409-4887-20; lot #89-517-DK); 18G needles (BD); Li heparin microtainer tubes, 0.5 ml (BD 365971; lot #9328307); Eppendorf microcentrifuge tubes, 1.5 ml (Costar 3620; lot #277054-T22-799); Heparin Sodium, Porcine 10K U/ml (Abraxis Pharm Prods, 401807E, lot #600339); 50% Dextrose Solution (Hospira, NDC 0409-6648-02, lot #91-412-DK); 23G Luer stub adaptors (Intramedic, Fisher 14-826-19E). Also: blood centrifuge, vortex, ultrasonic bath, Gilson pipettes/tips, eppendorf test tube racks, blue pads, syringes (1, 3 & 5 ml), small forceps, small scissors, medium hemostat, wound clip removers, alcohol pads, beakers (100 & 250 ml) and clear glass vials for drug.

- **Animals:** 12 jugular pre-cannulated male SD Rats, 250-300 g (Harlan); 225-249 g ordered
- **Experimental Design/Methods/Groups:**
 1. Acclimatize the rats for ≥ 2 days after receipt. Weigh rats the day before dosing to calculate dosing volumes. Check cannula patency the morning of dosing. Leave food in cages during experiment.
 2. Vehicle, Drugs & Solutions:
 - Vehicles: Extra p.o. ethanol/olive oil (10/90) vehicle is not required. Make i.v. vehicle (PEG400/ethanol/Tween 80/Water; 40/10/3/47) components the day before use as follows: 1) Make 3 ml of PEG/E (80/20) organic by mixing 2.4 ml of PEG with 0.6 ml of E; and 2) Make 3 ml of 6% T80 aqueous diluent by mixing 0.18 ml of T80 in 2.82 ml sterile water. Make in 8 ml vials and store PEG/E at RT and

T80 in refrigerator. No vehicle for vehicle rats is needed in this experiment.

- **Drugs:** Make the dosing solutions in 16 ml (groups 1 & 2) or 8 ml (group 3) vials. Dosing solutions for Groups 1 & 2 are made the day before the experiment; Group 3 dosing solution is made the morning of the experiment. For Group 1, make 10X stock solution (20 mg/ml) by dissolving 15 mg ESPD-00500 in 0.75 ml ethanol. For Group 2, make stock solution by dissolving 15 mg ESPD-01183 in 0.75 ml ethanol. Then make 7.5 ml of 2 mg/ml dosing solution for each compound by diluting each stock 1:10 with 6.75 ml of olive oil while vortexing. For Group 3, make the dosing solution in the lab the morning of dosing. First make 2X stock (2 mg/ml) by dissolving 4 mg ESPD-01183 in 2 ml of PEG/E (80/20) in an 8 ml vial (vortex and sonicate). Then make 4 ml of 1 mg/ml dosing solution by adding 2 ml of 6% T80 drop wise while vortexing. Store oral dosing solutions at RT in the dark and i.v. solution at RT in the light.
- **Solutions:** One to two days before the experiment, make up the dextrose/heparin plug and saline/heparin plug solutions. Make 10 ml of 50% Dextrose/500 U/ml heparin plug solution by adding 0.5 ml of heparin stock (10K U/ml) to 9.5 ml of 50% Dextrose solution and mixing gently; store in refrigerator and dispense in a 1 ml syringe. Make 10 ml of saline/heparin (100 U/ml) plug solution by adding 0.1 ml of heparin stock (10K U/ml) to 9.9 ml of sterile saline; store in a

refrigerator and dispense in a 1 ml syringe. Bring at least 50 ml of regular sterile saline for blood volume replacement and dispense in a 5 ml syringe.

3. Dosing/Groups: Dose p.o. drugs @ 10 mg/kg, 2 mg/ml & 5 ml/kg (~1.5 ml/rat, see Table). Dose i.v. drug @ 2 mg/kg, 1 mg/ml & 2 ml/kg. Sample i.v. rats at 9 time points: 0.08, 0.25, 0.5, 1, 2, 4, 6, 8, & 24 hrs. Sample oral rats at 10 time points: 0.50, 1, 2, 4, 6, 8, 10, 12, 14 & 24 hrs. Group 3 (i.v. rats) will be done on Tuesday/Wednesday, 8/30-8/31. Groups 1 & 2 (oral rats) will be done on Thursday/Friday, 9/1-9/2. Begin dosing at 8 AM on each dosing day. Dose all 8 rats of Groups 1 & 2 at 3 minute intervals between 8:00 and 8:30 AM so they can be sampled within 30 minutes at each time point.

Group Variables

Group No.	No. of Animals	Test Article	Vehicle ¹	Dose Route	Dose Level (mg/kg)	Dose Volume (mL/kg)	Dose Conc. (mg/mL)
1	4	Enigmol	E/OO	p.o.	10	5	2
2	4	2	E/OO	p.o.	10	5	2
3	4	2	PEG/E/T/	i.v.	2	2	1
4	5	Untreated	N/A	N/A	N/A	N/A	N/A

¹Vehicles are: 1) ethanol/olive oil (10/90); 2) PEG 400/ethanol/Tween 80/Water (40/10/3/47)

4. Blood Draws: Blood Draws: Blood will be obtained from the jugular cannula (0.3 ml) at each time point listed above (see protocol MV-RPK-10-01 for details). Replace blood volume with 0.4 – 0.5 ml saline and refill cannula with 0.1 ml

dextrose/heparin lock solution for all time points. At the 24 hr time points, save both plasma and RBC pellet (for metabolite determination); then sack and take tissues (see below).

5. Blood Processing: Invert Li-Heparin tube with blood gently 2 or 3 times to mix well; then place in a rack in ice water until able to centrifuge (≤ 1 hour). As soon as practical, centrifuge blood at $\sim 2000 \times g$ for 10 min in a refrigerated centrifuge to obtain plasma. Then, using a 200 μL pipette, transfer each plasma sample to a labeled 1.5 ml Eppendorf tube in ice water; freeze as soon as convenient in freezer or on dry ice. At 24 hour time points, also mix and remove RBC pellets with a glass Pasteur pipette and transfer to Eppendorf tubes in ice water, then freeze. Store samples at $-80\text{ }^{\circ}\text{C}$ prior to analysis.
6. Organ Collection: At the 24 hour time points, sack rats with CO_2 , then remove and freeze on dry ice: brain, lungs, liver, kidney and prostate. Two additional control rats will be harvested on Wednesday, 8/31; three additional control rats will be harvested on Friday, 9/2. Save tissue in 15 or 50 ml culture tubes. Transport to BCDMPK lab and store in -80 freezer for analysis.

Chapter 2: Following in the steps of Otto Warburg. Design and Synthesis of Potential Pyruvate Kinase Inhibitors

ABSTRACT: Decreased dependence on oxidative phosphorylation for cellular energy production, a phenomenon referred to as the Warburg effect, is accompanied by a significant increase in the uptake of glucose and conversion to ATP through glycolysis alone. This phenomenon is observed in nearly all types of cancer, and may be the Achilles heel that medicinal chemists have been searching for in order to send rapidly proliferating tumors into programmed cell death. We synthesized a novel class of phosphoenolpyruvate (PEP) mimics as competitive inhibitors of pyruvate kinase (PK), an enzyme at the end of the glycolysis pathway. The synthesis of the densely functionalized difluorophosphonate tri-esters was achieved through a Krapcho decarboxylation and an Arbuzov reaction. The compounds induced cell death in MDA-MB231 (breast) and PC-3 (prostate) cancer cells at 100-300 μM . In addition, the tri-acid derivatives decreased the ability of PK to cleave PEP with an IC_{50} of 3.4 mM.

2.1 Introduction

2.1.1 Background and Significance

In 1956, Otto Warburg reported in *Science* his astute observation that cancer cells in culture use much less oxygen than their healthy counterparts, which is accompanied by a significant increase in lactic acid production.⁵⁸ By exact quantification of the oxygen used and lactic acid produced, he determined that cancer cells produce as much as half of their energy from “*anaerobic* fermentation” (now referred to as glycolysis), while normal cells typically “obtain about 100 times as much energy from respiration” (oxidative phosphorylation, or OXPHOR).⁵⁸ In healthy adult cells, OXPHOR is preferred when oxygen is present since it produces 38 units of energy (ATP) per molecule of glucose, while glycolysis alone yields 2 units. Warburg hypothesized that this reliance on fermentation was an adaptation to oxygen deprivation, and that any cell that underwent prolonged or repetitive assault with decreased oxygen levels would in turn become cancerous. This topic has since been heavily debated, and a consensus has not yet been reached on whether the dependence on glycolysis over OXPHOR, now termed the “Warburg effect”, is the cause or result of cancer.

Although a majority of the anti-cancer agents brought to the clinic in the twentieth century relied on targeting DNA, bioenergetics has been gaining steam as a promising therapeutic area.⁵⁹ When applying the concepts of the Warburg effect to induce cell death in cancer, there are two main approaches reported in the literature that select for cells that rely much more heavily on glycolysis. The first is referred to as the “Trojan horse”, where the increased level of glucose uptake is hijacked to deliver toxins selectively to cancer cells. The second approach utilizes lactic acid, the byproduct of glycolysis, against the cell by shutting down its export. If too much lactic acid is trapped inside the cell, the interior becomes acidic and

the cell dies by necrosis. The small molecule alpha-cyano-4-hydroxycinnamate (ACCA) has recently been shown to inhibit the lactic acid transport, leading to diminishing viability in neuroblastoma cells.⁶⁰

2-Fluorodeoxy-D-glucose Positron Emission Tomography (FDG-PET, Figure 12) is a tumor imaging agent that shows the utility of the Trojan horse delivery method, selectively introducing radio-labeled ¹⁸F-labeled glucose into tumors cells in order to gain a high concentration of the radiolabel in tumors. For therapeutic application, toxic agents are conjugated to glucose and piggy-back along for the ride. The drug Glufosphamide (Figure 12) works by this principle, tethering the DNA-alkylating agent iphosphoramide to glucose, which shuttles the toxin into cancer cells at a concentration over a hundred fold greater than is found in healthy cells.⁶¹ 3-Bromo pyruvate (**3-BrPA**, Figure 12) is a small molecule that likely relies on the selective uptake *via* lactic acid transporters, which are over-expressed in cancer cells.⁶² Initially it was reported that **3-BrPA** exerts the anti-cancer effect by inhibition of hexokinase, but this has recently come under some scrutiny.⁶³ Preliminary data showed complete tumor eradication in animal models with little host toxicity across a variety of tumor xenografts, a very impressive feat in cancer biology. Surprisingly, the publication of very promising data for **3-BrPA** in 2006 has not been followed by clinical trials. This may be related to some of the known pitfalls of this molecule, specifically a lack of stability in solution, required intra-arterial delivery, the requirement for very high concentrations (100 μM) to achieve efficacy, and minimal patent coverage for composition of matter.

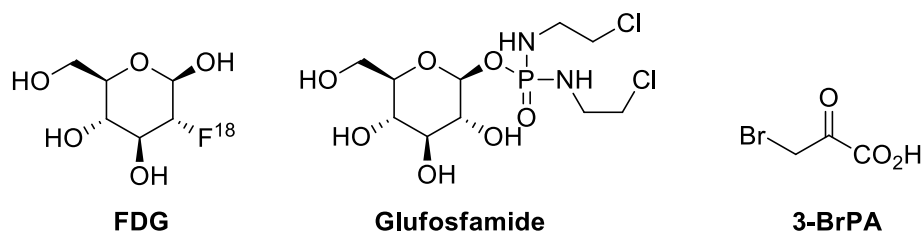
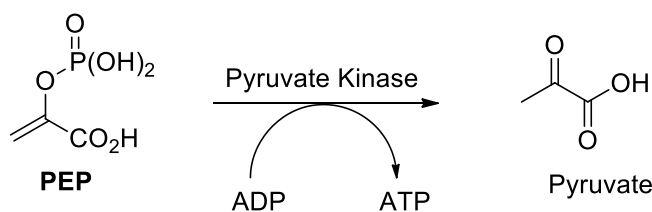


Figure 12: Structures of molecules that take advantage of the dependence of a cancer cell on glycolysis.

In addition to the commonly reported approaches mentioned above that kill cancer cells through our understanding of the Warburg effect, inhibition of the less well understood pyruvate kinase (PK) has not been heavily exploited. This enzyme is responsible for breaking down phosphoenolpyruvate (PEP) to yield pyruvate, generating one unit of ATP during the last step in glycolysis (Scheme 13). In the last few years, a hand full of groups have expressed interest, but inhibitors of PK are still in their infancy.⁶⁴ What makes PK a promising target for anti-proliferative agents is that there are two isoforms of the enzyme, M1 and M2. During embryonic development PK M2 is the predominant form, but through maturation the expression of the PK M2 isoform is decreased and replaced by PK M1. In cancer cells, PK M2 once again becomes dominant, exposing an opportunity for selective targeting. If the PK M2 isoform were preferentially inhibited in adult cancer it would follow that off target effects and hence toxicity would be diminished leading to a better drug safety profile.



Scheme 13: Conversion of phosphoenolpyruvate (PEP) to pyruvate, catalyzed by Pyruvate Kinase. This reaction results in the net gain of one unit of ATP by the consumption of ADP.

2.1.2 Design of Novel PK Inhibitors

I set out to develop a set of competitive PK Inhibitors (PKI's) that would be similar in shape and size to PEP with the goal of molecular recognition by PK. However, we wanted to replace the labile phosphate bond (oxygen-phosphorus) with a phosphonate (carbon-phosphorus) bond (Figure 14) to prevent cleavage by PK, thus inhibiting the enzyme from turning over and freezing the cellular machinery. Apoptosis would follow this major defect in the glycolytic pathway.

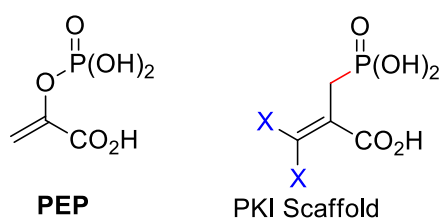


Figure 14: Comparison of phosphoenolpyruvate (**PEP**) with our proposed phosphonate PKI's. The red bond highlights the removal of the cleavable P-O bond, replaced by a P-C bond. Blue atoms show site of halogenations, which hold potential to tune PK isoform specificity.

To build in selectivity for cancer cells over healthy cells, we envisioned that alterations in size and electronegativity of the atoms on the terminus of the alkene may impart some selectivity for PK M2 over M1. To this end, our targets included X to be hydrogen, fluorine, and chlorine. Fluorines introduce more electronegativity while maintaining a relatively small size, while chlorines significantly increase the sterics bulk while also having an increased electronegativity present at this site.

Although the proposed analogs in Figure 14 will closely mimic **PEP**, the three acid moieties in the molecules will render the molecule highly charged at physiological pH. This high concentration of negative charge will keep the PKI's from passing through cell membranes where they would impart their activity. To overcome this property, I designed pro-drug variants of our compounds which have the acid moieties capped as esters, shown in Figure 15. The esters

functionality should allow for uptake into cells, where they will be cleaved to the tri-acid that mimics **PEP**. Inside the cell, enzymes called esterases are known cleave esters from compounds such as **1–3** to the corresponding free acids, releasing the “active” PKI.

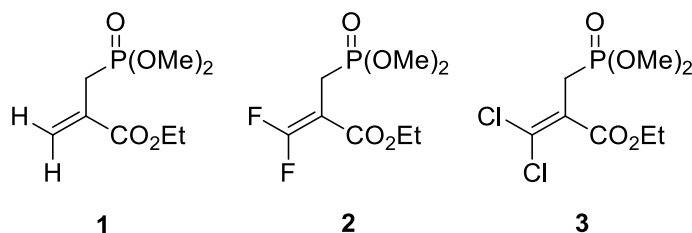


Figure 15: Specific examples of proposed pro-drug PKI's.

For comparison, I synthesized **PEP** pro-drugs previously reported in literature. Inside the cell, their mode of action is hypothesized to be recognition by PK, which will then cleave the phosphate bond to release a molecule of the 3-halopyruvate (monochloro-, monobromo-, or dibromo-pyruvate) in very close proximity to the site of energy production where they can be most effective. These compounds are synthesized *via* the Perkow rearrangement with dihalopyruvates and trimethylphosphite.⁶⁵ This series shown in Figure 16 are also ester pro-drugs, but still retain the phosphate linkage of **PEP**. In addition, the terminal alkene in the molecule is functionalized with either a single bromine or chlorine (**4–7**, in the E or Z geometry, separated by HPLC) or two bromines (**8**).

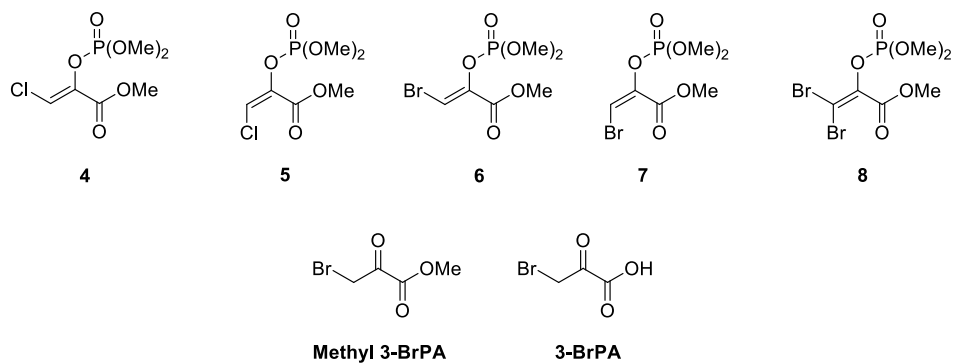
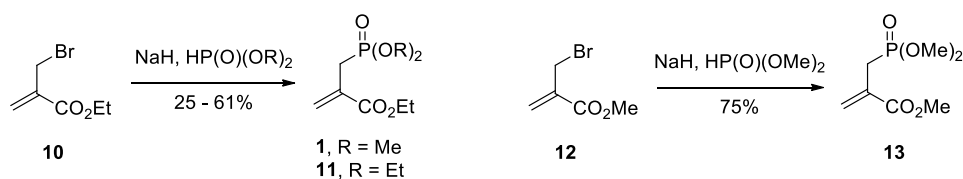


Figure 16: **PEP** analog pro-drugs **4–8** previously reported in literature,⁶⁵ synthesized for comparison in this study. **3-BrPA** and its ester derivative are commercially available.

2.2 Results

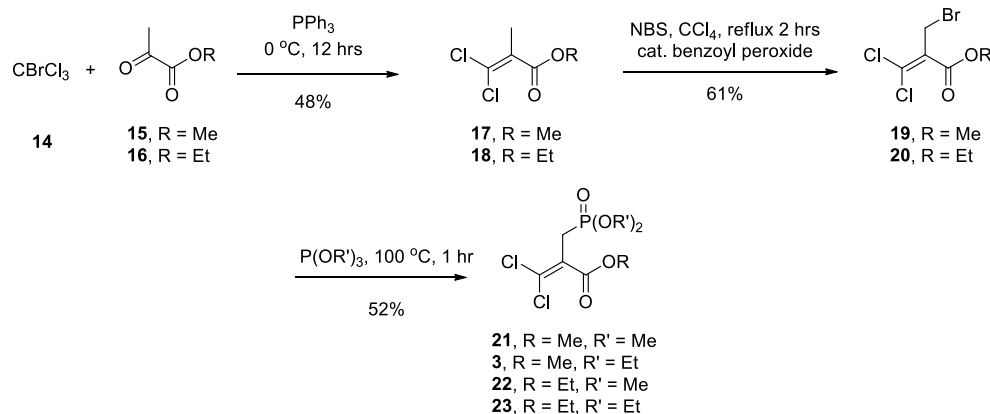
2.2.1 Synthesis of Novel PKI's

Synthesis of the dihydrophosphonate series was accomplished by a base mediated phosphonate bond forming reaction.⁶⁶ Specifically, the one step procedure used sodium hydride to deprotonate a dialkylphosphate, which in the presence of commercially available 2-(bromomethyl)acrylate esters **10** or **12** would create the desired phosphonate compounds **1**, **11**, and **13** (Scheme 19).



Scheme 19: One step synthesis of dihydrophosphonates **1**, **11**, and **13** via nucleophilic displacement of an alkyl-bromide.

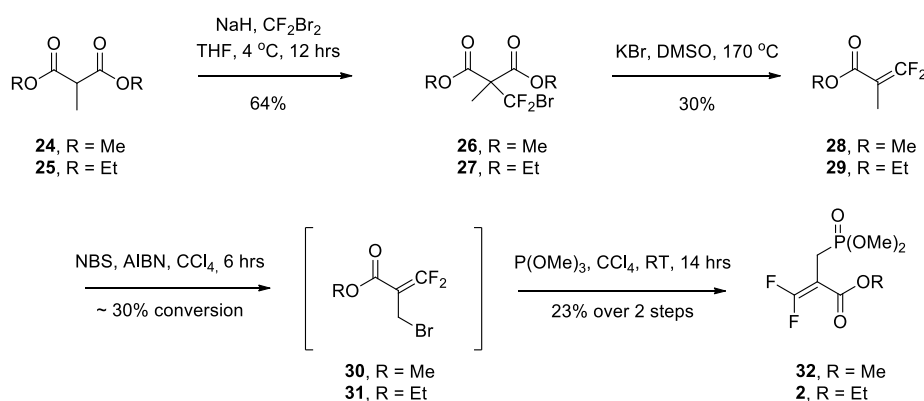
To generate the dichlorophosphonate analogs of **PEP**, the Wittig reaction was performed on an alkyl-pyruvate with trichlorobromomethane and triphenylphosphine to produce the terminal dichloroalkenes **17** and **18** (Scheme 20).⁶⁷ The allylic position on these intermediates was then brominated with *N*-bromosuccinamide (NBS) at reflux with a catalytic amount of the radical initiator benzoyl peroxide. After purification, intermediates **19** and **20** underwent an Arbuzov displacement in the presence of various trialkyl-phosphites to give the corresponding dichloro-phosphonates in moderate yields.



Scheme 20: Synthesis of target dichlorophosphonate analogs **3**, and **21-23**.

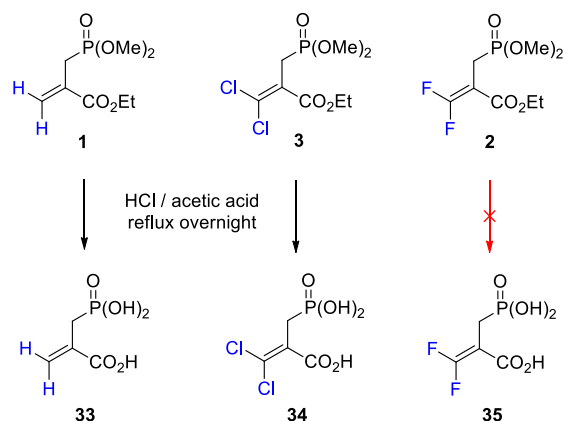
Although we will later mention some of the chemistry attempted prior to successfully attaining the difluorophosphonate products **32** and **2**, the final route that proved to be successful is shown in Scheme 21. This route began by alkylating dialkyl-methylmalonates **24** or **25** with sodium hydride and subsequent addition of condensed (-78 °C) dibromodifluoromethane.⁶⁸ Next the disubstituted malonates were subjected to the Krapcho decarboxylation with potassium bromide in DMSO at 170 °C, allowing the product to distill from the reaction mixture in a system that was vented only through a nitric acid bubble (to neutralize the evolving HBr).⁶⁹ It is important to note that this reaction can be quite violent. Within seconds of the completion of the initial decarboxylation, a secondary reaction occurs that releases large volumes of gas with urgency. If the distillation glassware is not quickly dismantled to allow pressure release and quenched with ice water, the excess pressure can lead to glassware explosion. However, if monitored carefully, the reaction can yield the desired decarboxylated product in reasonable yield. Although structurally similar to **19** and **20** in Scheme 20, the allylic position in **28/29** proved to be a greater challenge to brominate. After several attempts to purify bromo-intermediates **30** and **31**, I found I was able to attain much higher yields of the final product by subjecting the crude alkylbromide intermediates to the Arbuzov reaction with

trimethylphosphite. In spite of the difficulty in establishing conditions for this reaction, these reactions were easily monitored by ^1H NMR as the aprotic conditions allowed us to remove small aliquots of the reaction solution which were diluted into CDCl_3 in order to quantify the relative conversion of the methyl group in **28/29** to the bromomethyl product of **30/31** by ^1H NMR. The same principles were utilized during the Arbuzov reaction from **30/31** to **32/2** since this reaction was also run in CCl_4 . In this manner, the yield over the two steps was optimized up to 29% after purification by column chromatography and Kugelrohr distillation.



Scheme 21: Synthesis of the desired difluorophosphonate ester pro-drugs **32** and **2** with a Krapcho decarboxylation and Arbuzov displacement.

In order to investigate the *in vitro* efficacy of our PKI's we utilized an enzymatic assay that contained only PK. For this assay, we needed to test the tri-acids (active compounds) since there were no esterases in the cell-free assay to cleave our pro-drugs to their active form in this medium. The saponification of the tri-esters **1** and **3** was performed in a 1:1 mixture of concentrated HCl and glacial acetic acid at reflux overnight, yielding the desired tri-acids **33** and **34**. However, when difluorophosphante **2** was subject to the same conditions, complete decomposition of the starting material was observed.



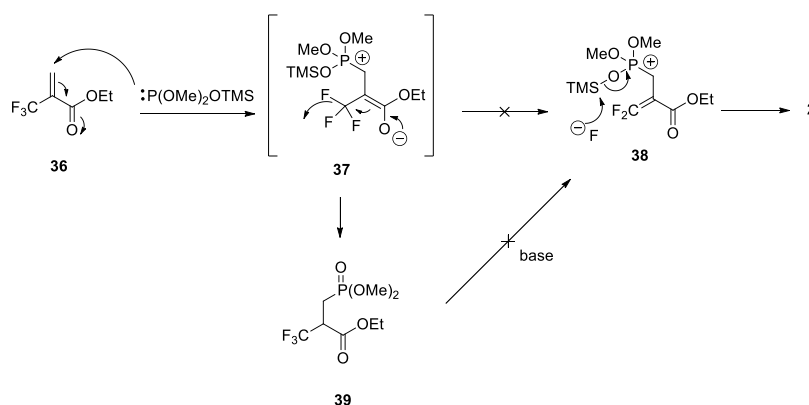
Scheme 22: Saponification of tri-esters was successful for **1** and **3** to yield **33** and **34** respectively. However, degradation was observed for the difluorophosphonate **2**.

Cleavage of the esters from **2** was attempted with 1 N HCl only to return unaltered starting material. Use of 6 N HCl showed initial promise by LCMS, but with slight heating mono-deprotection was briefly observed before the product decomposed. Additionally, we attempted saponification under a variety of basic conditions, a number of enzymes, and with halosilanes (such as TMS-I or TMS-Br) to no avail. Removal of the esters earlier in the synthesis on intermediate **29** was also unsuccessful, and transesterification of the ethyl ester of **2** or **29** for a benzyl ester also failed. In a final effort, we attempted the Finkelstein reaction, subjecting the dichlorophosphonate **PEP** analog **3** to halogen exchange in acetone with sodium fluoride to no effect. Compound **35** was never successfully attained.

2.2.2 Chemical Routes Attempted to Obtain the Difluorophosphonate PKI's

Although the final difluorophosphonate series was realized through the Krapcho decarboxylation in sequence with an Arbuzov reaction, all efforts were not reflected therein. Some of the interesting routes attempted are worth mentioning, and two extensive efforts will be described briefly in the following section.

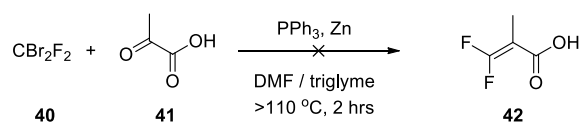
At the onset of this project, we envisioned an elegant yet simple conversion of ethyl α -trifluoromethylacrylate to the desired difluorophosphonate through a Michael addition to **36** followed by fluoride elimination from the enolate intermediate **37** to give the desired product **2**. Although envisioned to occur in one concise sequence as show in Scheme 23, this reaction turned out to produce the highly stable trifluoromethyl product **39**. Further manipulation of this trifluoromethyl compound under a variety of basic conditions did not yield the desired elimination product.



Scheme 23: Initially proposed synthetic route to **2** involving a Michael addition followed by fluoride elimination.

After successfully utilizing the Wittig reaction to obtain the chlorine derivatives shown in Scheme 20, we had hoped to apply this approach to the difluorophosphonate series. Our survey of the literature showed two reports of modified Wittig conditions between an ester derivative of pyruvate and dibromo-difluoro methane to yield the desired difluoro-alkene (Scheme 24).⁷⁰ Common to both reports was the use of a high boiling point solvent (DMF or triglyme, needed in order separate the volatile product from reaction mixture and solvent), along with the need for activated zinc to break up the highly stable bromo-phosphonium ylide intermediate. When applied in our lab, both of these methods failed to give the desired product. NMR analysis detected product formation, but this product was very difficult to isolate cleanly. In the end, this

route was abandoned due to very low product formation compounded by the high volatility of the difluoro terminal olefin **31** making isolation extremely difficult.



Scheme 24: Failed synthetic attempt to apply a modified Wittig procedure and to synthesize the desired terminal difluoro intermediate.

If the reaction in Scheme 24 were to be revisited, two changes to the protocol may help overcome these hurdles. Carrying the distilled mixture of solvent and **42** forward for radical bromination would only functionalize the allylic methyl group in the product. Hence, we could envision creating a separable mixture of product, unreacted starting material, and solvent. If an ester of **41** were to be utilized in this reaction, hydrogen bonding between the product and the solvent would be decreased potentially allowing us to circumvent some of the isolation issues we encountered.

2.3 Biological Evaluation

2.3.1 *In vitro* Cell-based Assays

In collaboration with the laboratories of Leyland and Petros at the Winship Cancer Institute, we determined the potency of novel compounds towards the inhibition of cancer cell growth in two cell based assays. This first study utilized MDA-MB231 breast cancer cells, reading cell kill with a MTT assay. The second cell line tested utilized PC-3 prostate cancer cells and quantifying results with a WST-1 assay. The compounds tested included **3-BrPA** as the gold standard, the **methyl 3-BrPA** to determine if the ester will give increased cellular permeation, one of each of the phosphonate series (compounds **1**, **2**, and **3**), and each of the phosphate prodrugs **4-8**. The results are summarized in Table 7.

Table 7: Summary of cancer cell growth inhibition assays results. IC₅₀'s were calculated for various synthetic PKI's in breast (MDA-MB231) and prostate (PC-3) cancer cells in culture.

Compound	Structure	MDA-MB231 IC ₅₀ (μ M)	PC-3 IC ₅₀ (μ M)
3-BrPA		100	300
Methyl-3-BrPA		333	-
1		130	500
2		>500	500
3		375	>500
4		23	70
5		20	50
6		20	25
7		10	30
8		40	>500

Interestingly, the phosphonate compounds did not show improved potency over **3-BrPA** and **methyl 3-BrPA** was far less potent in these cell lines. However, the literature compounds

that were much simpler halogenated phosphate pro-drug derivatives of **PEP** did prove to be an order of magnitude more potent for killing these cancer cells. This may be a result of higher uptake of the compounds into the cancer cells due to the pro-drug tempering potentially charged functional groups at physiological pH. Our collaborators in the laboratory of Leyland Jones are currently investigating these results further. However, these compounds have been reported in the literature and hence are not novel for this application.

2.3.2 *In vitro* Cell-free Assay

The lack of potency for the phosphonate compounds **1-3** in the above cell based assays could be attributed to 1) low cellular permeability, 2) lack of pro-drug cleavage to the tri-acid, or 3) the hypothesis was incorrect and the analogs are not competitive inhibitors of PK. The simplest assay to perform in order to determine the cause of the poor activity for the phosphonates is to evaluate *in vitro* activity against the solitary enzyme, PK (BioVision kit), with the tri-acids **33** and **34**. The kit was modified to determine the concentration of PKI required to inhibit the activity of PK. Specifically, the conversion of **PEP** to **pyruvate** and **ATP** was measured under a range of PKI concentrations from 100 nM to 10 μ M to determine the IC₅₀ for each compound in a dose response fashion. The colorometric output was monitored in a time dependant fashion by a UV-Vis plate reader and the results of this assay are shown in Figure 17.

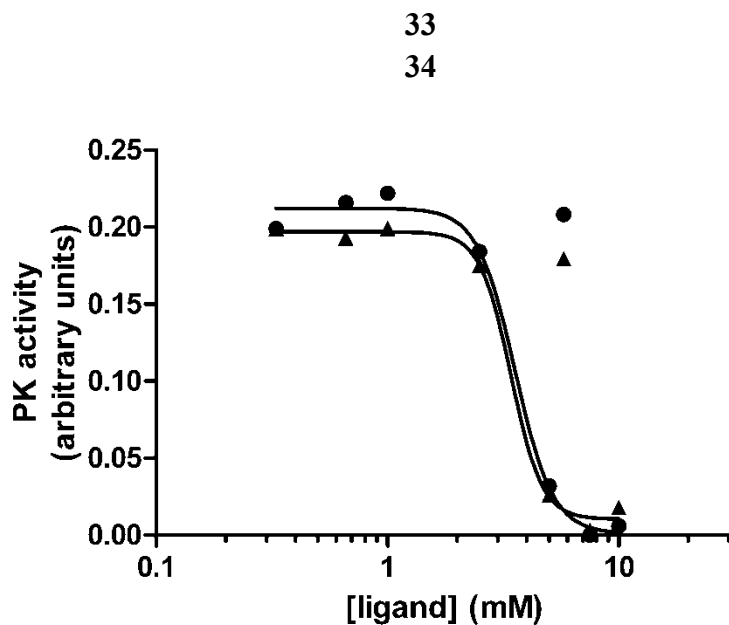


Figure 17: Pyruvate Kinase inhibition assay performed with the 2 tri-acid compounds **33** and **34**.

The two tri-acid compounds **33** and **34** did show complete inhibition of PK, but require extremely high concentrations to achieve this result. The concentration required to show reduction of the enzymes' output by 50% (EC_{50}) was 3.3 and 3.4 mM for compounds **33** and **34**, respectively.

2.4 Discussion

Initially my approach for leveraging the Warburg effect for the treatment of cancer cells was aimed at the competitive inhibition of Pyruvate Kinase. To this end, I developed non-cleavable derivatives of **PEP**, which were derivatized as ester pro-drugs to impart a more druggable degree of cellular permeability. In comparison to **3-BrPA**, the phosphonate compounds were less toxic to breast and prostate cancer cell lines. In combination with the data from the cell free Pyruvate Kinase assay showing that the EC_{50} 's of inhibition were >3 mM, we can draw the conclusion that this novel series of phosphonate compounds were unable to competitively inhibit the conversion of **PEP** to pyruvate and **ATP**. In addition, because the

inhibition of PK was an order of magnitude less potent than the cancer cell toxicity, the effect cannot be attributed to inhibition of PK and hence the mechanism of action is hereto unknown.

2.5 Conclusion

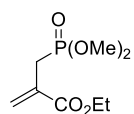
Towards the goal of creating a novel class of PK inhibitors, I synthesized six novel **PEP** mimics. Herein, we showed that they possess millimolar potency against the PK enzyme, and only slightly better activity against cancer cells in culture. This work shows that these phosphonate derivatives of **PEP** are not effective competitive inhibitors of PK.

2.6 Methods and Experimental Protocol

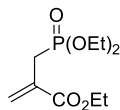
2.6.1 Experimental Protocol for Synthesis

General: ^1H , ^{19}F , and ^{13}C NMR spectra were recorded on Varian Inova 400 MHz spectrometer in deuterated chloroform (CDCl_3) with the solvent residual peak (CDCl_3 : ^1H = 7.27 ppm, ^{13}C = 77.2 ppm) as or (^{19}F , TFA = -75.8 ppm; ^{31}P , H_3PO_4 = 0 ppm) internal references unless otherwise specified. Data are reported in the following order: chemical shifts are given (δ); multiplicities are indicated as br (broadened), s (singlet), d (doublet), t (triplet), q (quartet), m (multiplet), app (apparent); coupling constants, J , are reported (Hz); integration is provided. Infrared absorption spectra were obtained on a Thermo Scientific Nicolet 370 FT-IR spectrophotometer via the Smart Orbit Diamond Attenuated Total Reflectance accessory. Peaks are reported (cm^{-1}). Elemental analyses were performed by Atlantic Microlab, Inc (Norcross, Ga.). High resolution mass spectrometry was performed by the Emory University Mass Spectrometry Center (Dr. Fred Strobel). Melting points (mp) were taken in open capillary tubes on a 200W MelTemp capillary melting points apparatus and are not corrected. Analytical thin-

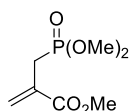
layer chromatography (TLC) was carried out on commercial Aldrich glass-supported silica gel plates with fluorescent indicator (F-254). Visualization was accomplished by UV light or stained with ninhydrin, potassium permanganate, or sulfuric acid (4% aqueous). Chromatography purification was performed with 60 Å silica gel (230-400 mesh) from Sorbent Technologies. Nominal mass spectra were obtained on either an Applied Biosystems AP150 or AP3000 by direct infusion.



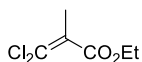
General Procedure for synthesis of the di-hydro alkene phosphonate series.⁷¹ Ethyl 2-((dimethoxyphosphoryl)methyl)acrylate (**1**): To a suspension of sodium hydride (157 mg, 6.2 mmol, 95%) in THF (50 mL) was added dimethoxy phosphite (570 μ L, 5.2 mmol) at 0 °C. After being stirred for 5 minutes, ethyl (bromomethyl)acrylate (715 μ l, 5.2 mmol) was added. The mixture was stirred at 0 °C for 2 hours and then at room temperature for 12 hours. The mixture was then poured into dilute HCl (0.1 N, 100 mL) and EtOAc (100 mL). The organic layer was washed with sat'd NaHCO₃ (50 mL), brine (50 mL), dried over MgSO₄, and concentrated. The crude residue was initially purified by column chromatography (ISCO, 12 g SiO₂, 40 - 100% EtOAc in Hex), then by Kugelrohr short-path distillation to yield the product as a clear colorless oil (284 mg, 25%). R_f = 0.27 (1:2, Hex:EtOAc). ¹H NMR (400 MHz, CDCl₃) δ 6.36 (d, J = 5.49 Hz, 1 H), 5.87 (dd, J = 5.49 Hz, 0.92 Hz, 1 H), 4.23 (q, J = 7.32 Hz, 2 H), 3.77 (s, 3 H), 3.74 (s, 3 H), 2.95 (dd, J = 22.0 Hz, 0.92 Hz, 2 H), 1.32 (t, J = 7.32 Hz, 3 H). ¹³C NMR (100 MHz, CDCl₃) δ 166.2 (d, J = 4.64 Hz), 131.3 (d, J = 10.7 Hz), 129.1 (d, J = 9.9 Hz), 61.5, 52.0 (d, J = 6.9 Hz, 2 C), 27.7 (d, J = 140 Hz), 14.3. ³¹P NMR (162 MHz, CDCl₃) δ 29.05 (t, J = 16.1 Hz). HRMS (ESI) m/z = 223.07296 (Theo. for C₈H₁₅O₅P+H: 223.07354).



Ethyl 2-((diethoxyphosphoryl)methyl)acrylate (**11**): Procedure deviated in that the reagent used was diethoxy phosphite. 797 mg, 61%. $R_f = 0.28$ (1:4, Hex:EtOAc). ^1H NMR (400 MHz, CDCl_3) δ 6.28 (d, $J = 5.72$ Hz, 1 H), 5.78 (d, $J = 4.40$ Hz, 1 H), 4.16 (q, $J = 7.31$ Hz, 2 H), 4.03 (app p, $J = 7.31$ Hz, 4 H), 2.88 (d, $J = 22.2$ Hz, 2 H), 1.23 (m, 9 H). ^{13}C NMR (100 MHz, CDCl_3) δ 166.1 (d, $J = 5.34$ Hz), 131.6 (d, $J = 10.69$ Hz), 128.6 (d, $J = 9.88$ Hz), 62.2, 62.1, 61.2, 28.5 (d, $J = 140$ Hz), 16.4, 16.3, 14.2. ^{31}P NMR (162 MHz, CDCl_3) δ 26.39 (t, $J = 13.4$ Hz). HRMS (ESI) $m/z = 251.10428$ (Theo. for $\text{C}_{10}\text{H}_{19}\text{O}_5\text{P}+\text{H}$: 251.10429).

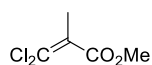


Ethyl 2-((dimethoxyphosphoryl)methyl)acrylate (**13**): Procedure deviated in that the starting material used was 3-methyl bromo methacrylate **12**. 4.38 g, 75%. $R_f = 0.33$ (95:5, DCM:MeOH). ^1H NMR (400 MHz, CDCl_3) δ 6.34 (dd, $J = 5.49, 0.81$ Hz, 1 H), 5.85 (dd, $J = 4.40, 0.81$ Hz, 1 H), 3.76 (s, 3 H), 3.72 (s, 3 H), 3.70 (s, 3 H), 2.93 (dd, $J = 22.2, 1.12$ Hz, 2 H). ^{13}C NMR (100 MHz, CDCl_3) δ 166.4 (d, $J = 5.23$ Hz), 130.9 (d, $J = 10.52$ Hz), 129.1 (d, $J = 7.48$ Hz), 52.8 (d, $J = 6.70$ Hz, 2 C), 52.3, 28.3, 26.9. ^{31}P NMR (162 MHz, CDCl_3) δ 28.84 (t, $J = 15.9$ Hz). HRMS (ESI) $m/z = 209.05732$ (Theo. for $\text{C}_7\text{H}_{13}\text{O}_5\text{P}+\text{H}$: 209.05789).

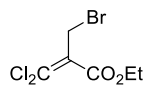


General procedure for Wittig to synthesize dichloro-alkenes.⁷² Ethyl 3,3-dichloro-2-methylacrylate (**18**): A mixture of triphenylphosphine (39 g, 150 mmol) and bromotrichloromethane (40 g, 200 mmol) was stirred in benzene (80 mL) under argon in an ice-cooled flask for 30 minutes. Ethyl pyruvate (8.2 mL, 75 mmol) was then added over 5 minutes. The reaction mixture was stirred at 4 °C overnight. The solvent was distilled out at atmospheric

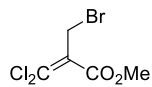
pressure, then unreacted bromotrichloromethane (b.p. = 40-50 °C / 15 mm Hg) was removed, followed closely by the desired product (b.p. = 50-75 °C / 15 mm Hg). The slightly contaminated product was purified with a silica plug, which was washed with hexanes, then the product was eluted with 5% EtOAc in Hex to give the final product as a clear colorless oil (6.77 mg, 48%). ¹H NMR (400 MHz, CDCl₃) δ 4.18 (q, *J* = 7.04 Hz, 2H), 2.00 (s, 3 H), 1.24 (t, *J* = 7.04 Hz, 3 H). ¹³C NMR (100 MHz, CDCl₃) δ 165.8, 128.5, 127.5, 61.8, 18.6, 14.2. Spectrum matches reported literature compound.⁷²



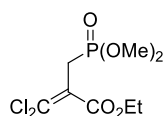
Methyl 3,3-dichloro-2-methylacrylate (**17**): (MTB-G-III-002; MB2-107) Procedure deviated in that the reactant used was methyl pyruvate. 7.84 g, 62 %. ¹H NMR (400 MHz, CDCl₃) δ 3.83 (s, 3H), 2.11 (s, 3 H). ¹³C NMR (100 MHz, CDCl₃) δ 166.2, 127.5, 119.3, 52.7, 18.6.



General procedure for radical bromination. Ethyl 2-(bromomethyl)-3,3-dichloroacrylate (**20**): Ethyl 3,3-dichloro-2-methylacrylate **18** (4.72 g, 26 mmol) was dissolved in CCl₄ (25 mL) in a dry flask, to which NBS (5.05 g, 28 mmol) and catalytic benzoyl peroxide (62 mg, 260 μmol) were added. The mixture was heated to reflux for 2 hours, at which time no starting material remained by NMR of reaction mixture. The reaction mixture was washed with water, dried over MgSO₄ evaporated to give the crude product, which was distilled under vacuum (95 – 120 °C at 0.5 mm Hg) to give the product as a colorless oil (4.13 g, 61%). ¹H NMR (400 MHz, CDCl₃) δ 4.43 (s, 2 H), 4.34 (q, *J* = 7.31 Hz, 2H), 1.36 (t, *J* = 7.31 Hz, 3 H). ¹³C NMR (100 MHz, CDCl₃) δ 163.2, 134.7, 129.3, 62.5, 28.4, 14.2. Spectrum matches reported literature compound.⁷²

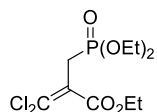


Methyl 2-(bromomethyl)-3,3-dichloroacrylate (**19**): Procedure deviated in that the starting material used was methyl 3,3-dichloro-2-methylacrylate **17**. 11.0 g, 86 %. ^1H NMR (400 MHz, CDCl_3) δ 4.43 (s, 2 H), 3.86 (s, 3 H). ^{13}C NMR (100 MHz, CDCl_3) δ 163.6, 135.4, 129.0, 53.1, 28.3.



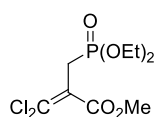
General procedure for Arbuzov displacement to generate di-chloro phosphonate series.

Ethyl 3,3-dichloro-2-((dimethoxyphosphoryl)methyl)acrylate (**3**); Ethyl 2-(bromomethyl)-3,3-dichloroacrylate **20** (2.06 g, 7.8 mmol) and trimethyl-phosphite (0.94 mL, 7.9 mmol) were brought up combined without solvent in a dry reaction vessel with a stir bar. The mixture was heated to 100 °C for 1 hour. The crude reaction mixture was initially purified by column chromatography (0 - 100% EtOAc in DCM), then further purified by Kugelrohr short-path distillation (187 °C at 2.0 mbar) to yield the product as a clear colorless oil (1.19 g, 52 %). R_f = 0.37 (EtOAc). B.P. = 115 °C (0.5 mm Hg). ^1H NMR (400 MHz, CDCl_3) δ 4.28 (q, J = 7.05 Hz, 2H), 3.74 (d, J = 10.9 Hz, 6 H), 3.20 (d, J = 21.9 Hz, 2H), 1.32 (t, J = 7.05 Hz, 3H). ^{13}C NMR (100 MHz, CDCl_3) δ 164.2, 130.6 (d, J = 14.5 Hz), 124.5 (d, J = 10.4 Hz), 62.3, 53.1 (d, J = 6.23 Hz), 30.3 (d, J = 14.1 Hz), 14.2. ^{31}P NMR (162 MHz, CDCl_3) δ 25.7 (m). HRMS (ESI) m/z = 290.99506 (Theo. for $\text{C}_8\text{H}_{13}\text{O}_5^{35}\text{Cl}_2\text{P}+\text{H}$: 290.99504). Anal. calcd. for $\text{C}_8\text{H}_{13}\text{O}_5\text{Cl}_2\text{P}$: C, 33.01; H, 4.50; O, 27.48; Cl, 24.36. Found: C 32.85; H 4.53; O, 27.77; Cl, 24.06.

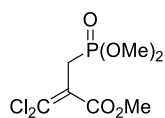


Ethyl 3,3-dichloro-2-((diethoxyphosphoryl)methyl)acrylate (**23**). Procedure deviated in that the reactant used was triethyl-phosphite, and distillation occurred at 195 °C and 1.0 mbar. 1.51 g,

60%. $R_f = 0.45$ (EtOAc). B.P. = 121 °C (0.5 mm Hg). ^1H NMR (400 MHz, CDCl_3) δ 4.28 (q, $J = 6.91$ Hz, 2 H), 4.09 (quintet, $J = 7.05$ Hz, 4 H), 3.18 (d, $J = 22.1$ Hz, 2 H), 1.29 (m, 9 H). ^{13}C NMR (100 MHz, CDCl_3) δ 164.2, 130.2 (d, $J = 14.5$ Hz), 124.9 (d, $J = 10.4$ Hz), 62.5 (d, $J = 6.22$ Hz, 2 C), 62.2, 31.1 (d, $J = 141$ Hz), 16.5 (d, $J = 6.22$ Hz, 2 C), 14.1. ^{31}P NMR (162 MHz, CDCl_3) δ 23.0 (m). HRMS (ESI) $m/z = 319.02637$ (Theo. for $\text{C}_{10}\text{H}_{18}\text{O}_5^{35}\text{Cl}_2\text{P}+\text{H}$: 319.02634). Anal. calcd. for $\text{C}_{10}\text{H}_{18}\text{O}_5^{35}\text{Cl}_2\text{P}$: C, 37.64; H, 5.37; O, 25.07; Cl, 22.22. Found: C 37.36; H 5.36; O, 25.32; Cl, 21.96. Spectrum matches reported literature compound.⁷²

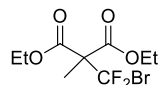


Methyl 3,3-dichloro-2-((diethoxyphosphoryl)methyl)acrylate (**3**). Procedure deviated in that the starting material used was methyl 2-(bromomethyl)-3,3-dichloroacrylate **19**, reactant was trimethyl-phosphite, and distillation occurred at 185 °C and 2.5 mbar. 3.42 g, 53%. $R_f = 0.40$ (EtOAc). B.P. = 116 °C (0.5 mm Hg). ^1H NMR (400 MHz, CDCl_3) δ 4.05 (app p, $J = 6.99$ Hz, 4 H), 3.78 (s, 3H), 3.15 (d, $J = 21.1$ Hz, 2 H), 1.26 (t, $J = 6.99$ Hz, 6 H). ^{13}C NMR (100 MHz, CDCl_3) δ 164.6, 130.5 (d, $J = 15.2$ Hz), 124.6 (d, $J = 10.5$ Hz), 62.5 (d, $J = 6.10$ Hz, 2 C), 52.8, 31.0 (d, $J = 144$ Hz), 16.5 (d, $J = 6.10$ Hz). ^{31}P NMR (162 MHz, CDCl_3) δ 22.88 (m). HRMS (ESI) $m/z = 605.01065$ (Theo. for $\text{C}_9\text{H}_{15}\text{O}_5^{35}\text{Cl}_2\text{P}+\text{H}$: 305.01069). Anal. calcd. for $\text{C}_9\text{H}_{15}\text{O}_5\text{Cl}_2\text{P}$: C, 35.43; H, 4.96; O, 26.22; Cl, 23.24. Found: C 35.25; H 4.97; O, 26.42; Cl, 23.04.



Methyl 3,3-dichloro-2-((dimethoxyphosphoryl)methyl)acrylate (**21**). Procedure deviated in that the starting material used was methyl 2-(bromomethyl)-3,3-dichloroacrylate **19**, and distillation occurred at 190 °C and 2.0 mbar. 2.60 g, 44%. $R_f = 0.33$ (EtOAc). B.P. = 117 °C (0.5 mm Hg).

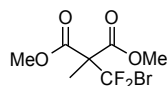
^1H NMR (400 MHz, CDCl_3) δ 3.78 (s, 3 H), 3.71 (s, 3 H), 3.69 (s, 3 H), 3.16 (d, $J = 21.9$ Hz, 2 H). ^{13}C NMR (100 MHz, CDCl_3) δ 164.5, 130.9 (d, $J = 16.6$ Hz), 124.2 (d, $J = 12.4$ Hz), 53.1 (d, $J = 6.22$ Hz), 52.9, 30.2 (d, $J = 141$ Hz). ^{31}P NMR (162 MHz, CDCl_3) δ 25.7 (m). HRMS (ESI) $m/z = 276.97936$ (Theo. for $\text{C}_7\text{H}_{11}\text{O}_5^{35}\text{Cl}_2\text{P}+\text{H}$: 276.97939). Anal. calcd. for $\text{C}_7\text{H}_{11}\text{O}_5\text{Cl}_2\text{P}$: C, 30.35; H, 4.00; O, 28.88; Cl, 25.59. Found: C 30.12; H 4.09; O, 29.14; Cl, 25.33.



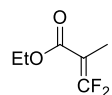
General procedure for formation of difluoro, bromo-methyl malonates:⁷³ diethyl 2-(bromodifluoromethyl)-2-methylmalonate (**27**): Sodium hydride (95% in oil, 0.60 g, 26 mmol) was placed in an anhydrous 50 mL crew-cap reaction vessel, temporarily capped with a septum under an argon atmosphere, and washed free of oil with hexanes. Dry THF (25 mL) was added followed by diethyl methyl malonate (4.3 mL, 25 mmol) via syringe pump at room temperature. Heat was generated and H_2 evolved as the sodium salts of the malonic esters anion formed. After addition, the reaction was stirred for 0.5 hours. Dibromodifluoromethane (2.4 mL minimum, 26 mmol) was condensed in a dry 5 mL dry round bottom flask cooled in acetone/dry ice, then poured into the reaction mixture quickly, capping the mixture immediately with the screw cap. An exothermic reaction was immediately obvious along with a change in appearance as the NaBr salt precipitated from the solution. The reaction was stirred overnight in a cold room at 4 °C. After 12 hours, the reaction was worked up by removing the THF *in vacuo*, taking up the residue in Et_2O (50 mL) and washing with water (3 x 20 mL). The organic layer was dried over MgSO_4 and concentrated *in vacuo* to yield the crude product, which was purified by vacuum distillation to give the product as a clear colorless oil (5.4 g, 64%) in 90% purity.

$R_f = 0.45$ (10:1 Hex:EtOAc). ^1H NMR (CDCl_3 , 400 MHz) δ 4.28 (q, $J = 6.99$ Hz, 4 H), 1.75 (s, 3 H), 1.30 (t, $J = 6.99$ Hz, 6 H). ^{13}C NMR (CDCl_3 , 100 MHz) δ 165.7 (2 C), 120.6 (t, $J = 314$ Hz),

65.6 (t, $J = 20.6$ Hz), 62.9, 18.8, 14.0 (2 C). ^{19}F NMR (CDCl_3 , 400 MHz) δ -47.30 p (s, 2 F). HRMS (ESI) $m/z = 303.00378$ (Theo. for $\text{C}_{14}\text{H}_{16}\text{N}_4\text{O}+\text{H}$: 303.00380).



Dimethyl 2-(bromodifluoromethyl)-2-methylmalonate (**26**): Procedure deviated in that the starting material was dimethyl methyl malonate, and the crude oil was purified by column chromatography (9:1 Hex:EtOAc). (34.0 g, 66%). $R_f = 0.28$ (10:1 Hex:EtOAc). ^1H NMR (CDCl_3 , 400 MHz) δ 3.83 (s, 6 H), 1.76 (s, 3 H). ^{13}C NMR (CDCl_3 , 100 MHz) δ 166.2 (2 C), 123.5 (t, $J = 319$ Hz), 65.1 (t, $J = 20.6$ Hz), 53.7 (2 C), 18.9. ^{19}F NMR (CDCl_3 , 400 MHz) δ -47.61 p (s, 2 F). HRMS (ESI) $m/z = 274.97269$ (Theo. for $\text{C}_{14}\text{H}_{16}\text{N}_4\text{O}+\text{H}$: 274.97305).

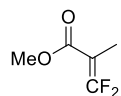


General procedure for Krapcho decarboxylation.⁷⁴ Ethyl 3,3-difluoro-2-methylacrylate (**29**):

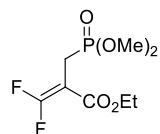
Caution: This reaction is explosive as there is a secondary reaction that builds enormous pressure seconds after the initial product ceases to distil over. Make very sure to grease joints so the reaction vessel can be quenched with ice water as soon as the initial distillate stops.

Diethyl 2-(bromodifluoromethyl)-2-methylmalonate **27** (7.00 g, 23.1 mmol) and flame dried potassium bromide (2.75 g, 23.1 mmol) were dissolved in dry DMSO (60 mL) in a flame dried 100 mL three neck flask. The flask was equipped with a thermometer, argon inlet, and flame dried short path distillation apparatus, which was vented to the atmosphere through a nitric acid bubbler to capture released bromine. The receiving flask was cooled to 0 °C. The inhomogeneous mixture was heated to 160 °C with vigorous stirring and maintained at this temperature until the distillate slows nearly to a stop and the reaction vessel begins to solidify. As soon as the solid was observed, the reaction vessel was disconnected from the distillation head, and placed in an

ice bath. The reaction was immediately quenched by adding ice to the reaction vessel, and when it reaches room temperature, decanting it into a beaker with ice. After storing the distillate overnight at -20 °C, the white precipitate is filtered off by passing through a glass frit. The clear colorless solution was then purified by distillation, first distilling off the dimethylsulfide impurity at 80-86 C (300 mbar), then the product distilled over at 100 °C (130 mbar) to yield a clear colorless free-flowing liquid (2.17 g, 30%). ¹H NMR (CDCl₃, 400 MHz) δ 4.21 (q, *J* = 7.05 Hz, 2 H), 1.78 (t, *J* = 3.51 Hz, 3 H), 1.28 (t, *J* = 7.05 Hz, 3 H). ¹³C NMR (CDCl₃, 100 MHz) δ 162.3 (dd, *J* = 13.73, 7.63 Hz), 159.6 (dd, *J* = 308, 295 Hz), 84.3 (dd, *J* = 24.4, 7.63 Hz), 61.2, 14.3, 9.76. ¹⁹F NMR (CDCl₃, 400 MHz) δ -80.07 (q, *J* = 3.20 Hz, 1F), -84.11 (q, *J* = 3.20 Hz, 1F).



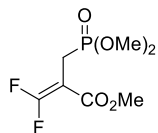
Methyl 3,3-difluoro-2-methylacrylate (**28**): Procedure deviated in that the starting material was dimethyl 2-(bromodifluoromethyl)-2-methylmalonate **26**. (3.51 g, 34%). ¹H NMR (CDCl₃, 400 MHz) δ 3.78 (s, 3 H), 1.80 (t, *J* = 3.49 Hz, 3 H). ¹³C NMR (CDCl₃, 100 MHz) δ 162.5 (dd, *J* = 13.73, 7.63 Hz), 159.6 (dd, *J* = 308, 295 Hz), 84.3 (dd, *J* = 24.4, 7.63 Hz), 52.3, 9.79 (m). ¹⁹F NMR (CDCl₃, 400 MHz) δ -79.87 (dq, *J* = 3.66, 1.83 Hz, 1F), -83.94 (dq, *J* = 3.66, 1.83 Hz, 1F). No HRMS as compound did not ionize.



General procedure for radical bromination, followed by Arbuzov displacement. Ethyl 2-((dimethoxyphosphoryl)methyl)-3,3-difluoroacrylate (**2**): In a flame dried three neck round bottom flask equipped with a reflux condenser and stir bar ethyl 3,3-difluoro-2-methylacrylate

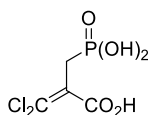
27 (2.17 g, 14.5 mmol) was dissolved in CCl₄ (35 mL), to which NBS (5.41 g, 30.4 mmol) and catalytic AIBN (238 mg, 1.44 mmol) were added. The reaction was brought up to reflux (80 °C). Small samples of the reaction solution could be analyzed directly by diluting into CDCl₃ and subjecting to NMR to determine consumption of starting material (¹H: t at 1.9 ppm converts to t at 4.2 ppm; ¹⁹F: appearance of two td at -64.19 and -67.69 ppm). After 6 hours, the heterogeneous mixture was filtered through a glass frit, and the solid was washed with CCl₄. The organic filtrate was washed with water (60 mL), which was back extracted with DCM (2 x 15 mL). The organic layers were combined, dried over MgSO₄, and evaporated at 80 mbar in a 35 °C water bath to avoid evaporation of the low molecular weight intermediate. After quick analysis by NMR (¹H and ¹⁹F) to verify the presence of some product (typically 30 %), the crude material was taken directly to the next step.

The crude ethyl 3,3-difluoro-2-methylacrylate (theoretically 851 mg, 3.72 mmol) was dissolved in CCl₄ (80 mL), to which trimethylphosphite (877 μL, 7.4 mmol) was added. The mixture was allowed to stir for 14 hours. The solvent and excess phosphate was removed by rotary evaporation followed by 30 minutes on high vacuum. The crude product was initially purified by column chromatography (ISCO, 120 g SiO₂, 0 - 50% EtOAc in DCM), then by Kugelrohr (short path) distillation (180 °C at 9.5 mm Hg to remove impurities, then 195 °C at 1 mm Hg for product) to yield the final product as a clear colorless oil (699 mg, 23 %). R_f = 0.36 (EtOAc). ¹H NMR (CDCl₃, 400 MHz) δ 4.25 (q, *J* = 7.01 Hz, 2 H), 3.73 (d, *J* = 10.8 Hz, 6 H), 2.81 (dt, *J* = 20.3, 2.22 Hz, 2 H), 1.29 (t, *J* = 7.23 Hz, 3 H). ¹³C NMR (CDCl₃, 100 MHz) δ 163.8 (m), 160.3 (app dt, *J* = 298, 10.2 Hz), 82.3 (m), 53.0 (d, *J* = 6.11 Hz, 2 C), 21.5 (d, *J* = 145 Hz) 14.2. ¹⁹F NMR (CDCl₃, 400 MHz) δ -63.98 (m, 1F), -67.68 (tt, *J* = 11.0, 2.71 Hz, 1F). ³¹P NMR (CDCl₃, 162 MHz) δ 27.91 (m). HRMS (ESI) *m/z* = 259.05386 (Theo. for C₁₄H₁₆N₄O+H: 259.05383).

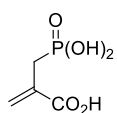


Methyl 2-((dimethoxyphosphoryl)methyl)-3,3-difluoroacrylate (**32**): Procedure deviated in that the starting material was methyl 3,3-difluoro-2-methylacrylate **28**. 420 mg, 29%.

$R_f = 0.25$ (EtOAc). $^1\text{H NMR}$ (CDCl_3 , 400 MHz) δ 4.25 (q, $J = 7.01$ Hz, 2 H), 3.78 (m, 9 H), 2.84 (dt, $J = 20.3, 2.22$ Hz, 2 H). $^{13}\text{C NMR}$ (CDCl_3 , 100 MHz) δ 163.8 (m), 160.3 (app dt, $J = 298, 10.2$ Hz), 82.3 (m), 53.0 (d, $J = 6.11$ Hz, 2 C), 21.5 (d, $J = 145$ Hz) 14.2. $^{19}\text{F NMR}$ (CDCl_3 , 400 MHz) δ -63.98 (m, 1F), -67.68 (m, 1F). $^{31}\text{P NMR}$ (CDCl_3 , 162 MHz) δ 28.34 (m). HRMS (ESI *neg.*) $m/z = 243.02766$ (Theo. for $\text{C}_7\text{H}_{11}\text{F}_2\text{O}_5\text{P-H}$: 243.02394).



General Procedure for saponification of tri-ester phosphonates. 3,3-Dichloro-2-(phosphonomethyl)acrylic acid (**34**): Saponification of methyl 3,3-dichloro-2-((diethoxyphosphoryl)methyl)acrylate **3** (1.16 g, 3.80 mmol) was achieved by refluxing in a 1:1 mixture of concentrated HCl and glacial acetic acid for 20 hours. After cooling, the solvents were aprotroped off with water, then the water was aprotroped off with benzene to give the crude product. The final product was crystallized from EtOAc to yield an off white solid (456 mg, 51 %). $^1\text{H NMR}$ (400 MHz, D_2O) δ 2.90 (d, $J = 21.3$ Hz, 2 H). $^{13}\text{C NMR}$ (100 MHz, D_2O) δ 170.8, 131.7 (d, $J = 15.2$ Hz), 127.7 (d, $J = 11.4$ Hz), 34.1 (d, $J = 134$ Hz). $^{31}\text{P NMR}$ (162 MHz, D_2O) δ 21.13 (d, $J = 15.9$ Hz). HRMS (ESI) $m/z = 216.92188$ (Theo. for $\text{C}_4\text{H}_5\text{O}_5^{35}\text{Cl}_2\text{P} - \text{H}_2\text{O}$: 216.92188). Spectrum matches reported literature compound.⁷²



2-(Phosphonomethyl)acrylic acid (**33**). Procedure deviated in that the starting material used was ethyl 2-((diethoxyphosphoryl)methyl)acrylate **1**. 572 mg, 72%. ^1H NMR (400 MHz, D_2O) δ 6.24 (dd, $J = 5.82, 0.60$ Hz, 1 H), 5.78 (dd, $J = 5.82$ Hz, 0.60 Hz, 1H), 2.81 (dd, $J = 21.8$ Hz, 1.1 Hz). ^{13}C NMR (100 MHz, D_2O) δ 168.3, 129.1 (d, $J = 15.2$ Hz), 125.9 (d, $J = 11.9$ Hz), 32.5 (d, $J = 33.0$ Hz). ^{31}P NMR (162 MHz, D_2O) δ 24.81 (t, $J = 14.7$ Hz). HRMS (ESI) $m/z = 148.99982$ (Theo. for $\text{C}_4\text{H}_7\text{O}_5\text{P} - \text{H}_2\text{O}$: 148.99978). Anal. calc'd. for $\text{C}_4\text{H}_7\text{O}_5\text{P}$: C, 28.93; H, 4.25; O, 48.17. Found: C, 28.87; H, 4.11; O, 47.94.

2.6.2 Biological Evaluation of anti-cancer agents

WST-1 ASSAY performed by Suzanne G. Mays on 10-6-10.

Drug preparation: Drugs were dissolved PBS and sterile-filtered. 2 mM stock solutions were used to treat cells.

WST-1 assay: 1.5×10^4 PC-3 cells were plated in each well of 96-well culture plates (in 100 μl media) and allowed to adhere overnight. Cells were then treated for 24 hours with 1 mM, 100 μM , 10 μM , 1 μM , or 0.1 μM of each compound (three wells for each treatment). To detect cell viability, 10 μl of the WST-1 reagent (Roche) was added to each well, and plates were incubated with the WST-1 reagent for 45 minutes at 37 $^\circ\text{C}$. Plates were read at 450 nm with a reference wavelength of 690 nm. Wells containing media but no cells were used as blanks. Signal from treated cells was normalized to that of untreated PC-3 cells.

Chapter 3: Design and Synthesis of Novel CXCR4 Modulators for Treatment of Macular Degeneration

ABSTRACT: Wet Age related Macular Degeneration (AMD) is a debilitating disease that leads to partial blindness resulting from angiogenesis behind the retina. Inefficient and difficult to administer therapeutics prompted us to develop a small molecule CXCR4 agonist for treatment of this disease. **WZ-41** is a partial CXCR4 agonist that has the potential to block angiogenesis and improve patient outcome. I designed a family of **WZ-41** analogs with the following characteristics: 1) could be administered topically to the eye, 2) capable of permeating through the cornea, and 3) retain interaction with CXCR4. Newly synthesized compounds were evaluated in a competitive binding assay against the CXCR4 binding peptide TN14003, where they were found to be efficacious in the low nanomolar range. However, when a subset of these molecules were subjected to a HUVEC vessel formation assay, all compounds including the parent compound **WZ-41** failed to reduce vessel formation at physiologically relevant concentrations, showing IC_{50} 's greater than 3 μ M.

3.1 Introduction

3.1.1 Background and Significance

AMD is characterized by the degradation of the macula, a spot on the middle of the retina (Figure 18) that is responsible for gathering information about the center of our field of vision. This disease is the number one cause of blindness in the U.S. among individuals over 50 years of age. The damage is caused either by the buildup of fatty tissue behind the retina, or an excess of new blood vessel growth behind the macula. The latter is referred to as “wet” macular degeneration, wherein the new vasculature can disrupt the vision in two ways. First, the vessels formed underneath the retina can put pressure on the macular nerves, reducing signal output. Second, the new vessels can grow through the macula, rupturing once they reach the surface, which creates scar tissue on top of the macula.

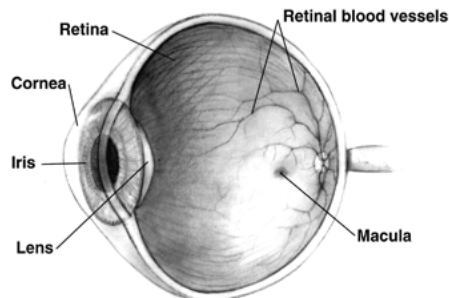


Figure 18: Cross section of the human eye.⁷⁵

Current therapeutic options exist for AMD, although they each have drawbacks. The most common FDA approved therapeutic treatments are 1) removing the outer layer of scar tissue on the macula by laser surgery, 2) cauterizing the leaky blood vessels with a laser, and 3) inhibiting angiogenesis with biochemical therapeutic agents.⁷⁶ Anti-angiogenic therapeutic drugs stop the growth of new blood vessels by targeting VEGF, a growth factor specifically involved in vasculature formation. MacugenTM is an aptamer (an RNA sequence) that has been optimized to

bind a specific target sequence within VEGF that blocks the activity of this vascular growth factor, while LucentisTM utilizes an antibody fragment to achieve the same goal. Both of these VEGF inhibitors are approximately 50 kDa, too large for diffusive deliver as an eye drop, and must be administered by an uncomfortable series of injections into the eye every few weeks. The injections are incredibly costly (\$800-2000 per treatment),⁷⁷ can last a number of years, and suffer from less than 40% improvement.⁷⁶

Site specific delivery of a therapeutic drug is an obstacle common to all diseases. Many times a drug binds to the desired target, resulting in the intended effect, but delivery to the site of the disease is problematic. The majority of clinically efficacious medications are most often administered orally, through injection, or topically. However, disease targets in the head become more difficult to reach because they must pass through the blood brain barrier.⁷⁸ To specifically target the eyes for the treatment of AMD, I set out to design a drug that was capable of permeating the cornea and could be delivered in an eye drop. Local, topical administration of a drug can minimize off target effects while maximizing the concentration at the site of disease.

When delivering a drug to the eye, two forms of drug delivery need to be examined more closely.⁷⁹ Topical dosing of a drug is difficult because the cornea is the only permeable part of the eye (Figure 18). The cornea only makes up a small fraction of the surface area of the eye and is a significant barrier for the entry of foreign objects.⁸⁰ Depending on the properties of the therapeutic agent, topical delivery to the cornea can be performed by several medias, including gels, ointments, suspensions, and solutions. Common pitfalls of direct application of drugs in any of these particular media are blurred vision, burning, difficulty formulating, and requirement of extremely high concentrations, respectively. Additionally, topically administered drugs by definition of being absorbed through diffusion require frequent administration as tearing washes

away much of each dose resulting in overall low bioavailability.⁸⁰ If the desired concentration of a drug within the eye is not achieved, the effectiveness of the drug will be decreased. On the other hand, injecting a therapeutic agent into the eye overcomes many of the hurdles of topical administration, especially that of delivering therapeutically relevant concentrations of the drug to the interior chamber of the eye. However, patient discomfort is a significant drawback, making it a less than desirable treatment method.

In order to successfully develop a topically administered drug, the composition of the cornea must first be understood. The cornea is made up of three tissue layers (Figure 19), creating a barrier that prohibits the vast majority of foreign objects from penetrating by alternating layers from hydrophobic to hydrophilic to hydrophobic again. The outermost is the epithelium, consisting of 4-5 layers of cells with a total thickness of 50-60 μm (Figure 19A).⁸¹ Next is the fibrous stroma, which makes up the majority of the thickness of the cornea. The last barrier to foreign objects is the endothelium, which is a monolayer of cells only 5 μm thick.

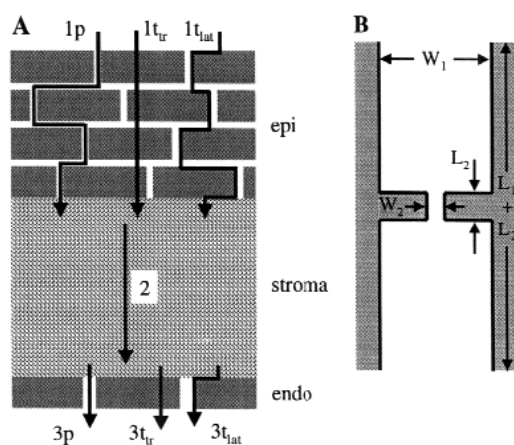


Figure 19: A schematic representation of the cornea, showing the possible pathways for molecules to diffuse through to the anterior chamber.⁸¹

To explain drug permeability through the epithelium layer of the cornea, Edwards *et al.* describe three pathways that a molecule can take.⁸¹ The first pathway is para-cellular permeation (Figure 19A, 1p), where hydrophilic compounds pass through the intercellular space by

squeezing through the tight junctions between cells. As these gaps are on the order of 1.5 nm, labeled W2 in Figure 19B. Molecular radius of the drug (termed r_s) is the most important attribute in determining diffusion rate. The second pathway is lateral transcellular diffusion (Figure 19A, lt_{lat}) which occurs for compounds that are more hydrophobic and can travel directly through the cell. An amphiphilic compound would likely pass through lipid bilayers as well as aqueous compartments by this route. Substantially hydrophobic compounds pass through the cell membrane in the epithelium by transverse diffusion ($1t_{tr}$), the third pathway. This pathway minimizes contact with the aqueous environment. As a measure of hydrophobicity, Edwards uses a modified K_{OW} (partition coefficient of a compound between octanol and water, also known as P in LogP) he refers to as Φ . The two are related by the equation $\Phi = K_{OW}^{0.87}$.

Diffusion across the stroma is surprisingly unaffected by Φ , and r_s has only a small effect. The pathways described for permeation through the epithelium are also relevant for the endothelium. However, since the epithelium is approximately 4 times thicker than the endothelium, diffusion through the former is the rate limiting process (Figure 20A). Analysis of Figure 20A and B lead us to conclude molecules with higher hydrophobicity, yet small radii are most likely to be successful in permeating through the cornea.

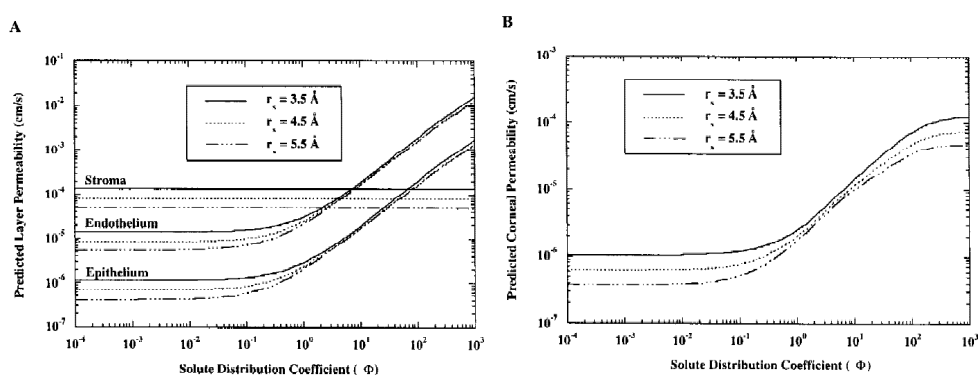


Figure 20: Predictive relationship between solute distribution coefficient Φ and permeability of the individual layers (A) and the whole cornea (B). Molecular radius is represented by line type.⁸¹ These trends for over 150 compounds were calculated based on models determined and tested in a composite porous medium.⁸¹

One major pitfall for this predictive model is that it only accounts for permeation of the corneal membrane in one direction. It does not consider flux, which is determined by the corneal permeability and the concentration difference across the cornea. Flux increases with permeability to a certain maximum then decrease once again.⁸¹ This must be kept in mind when designing molecules as well as choosing how best to evaluate these compounds in cell culture. While permeability predictions can be made based on these models, only physical testing of compounds can evaluate delivery successfully.⁸² The unknown influence of drug flux will likely play a role in the final drug design.

CXCR4 is a seven trans-membrane protein in the G protein-coupled receptor (GPCR) family. Discovered in 1994,⁸³ CXCR4 was first identified as a co-receptor mediating HIV entry into host cells for T-tropic strains.^{84,85} Interest in CXCR4 has been steadily gaining since its initial discovery. Over the ten years following its discovery, 1000 papers were published on the receptor, while in the last year >1600 articles have been published. CXCR4 is the exclusive binding site for CXCL12 (also known as SDF-1),⁸⁶ a chemo-attractant that plays a role in stem cell mobilization, trafficking, and homing.⁸⁷ CXCR4 knockout mice show malformation of the large vessels in the gut, resulting in embryonic lethality.⁸⁸ Disruption of the CXCR4/CXCL12 axis in adult nude mice severely impairs angiogenesis, shown by a decrease in the neovascularization after ischemia.⁸⁹ Breast, liver, colon, and pancreas tumor cells over express CXCR4, correlating to metastatic potential and poor patient prognosis.⁹⁰

Modulators of the CXCR4/CXCL12 interaction have been previously reported. **AMD3100** (Figure 21), the most well studied modulator, is a bicyclam possessing anti-HIV activity as a result of blocking viral entry *via* the CXCR4 coreceptor.⁹¹ In addition, **AMD3100** blocks the natural ligand CXCL12 from docking with an IC₅₀ of 3 nM.⁹² Initially **AMD3100**

entered clinical trials for the treatment of HIV but was withdrawn due to cardiotoxicity under prolonged exposure.⁹³ However, during these trials clinicians noticed leukocytosis, and after further development **AMD3100** received FDA approval for stem cell mobilization under the name PlerixaforTM.⁹⁴

A two-site binding model between CXCR4 and CXCL12 was proposed in 2001,⁹⁵ which has gained experimental support with the release of a CXCR4 crystal structure in 2010.⁹⁶ The first site is postulated to be a weak interaction at the surface of CXCR4. This would allow the chemokine to settle in the correct orientation for the second interaction, which is thought to be a tight interaction that occurs when the N-terminal domain loop of CXCL12 reaches into a pocket in CXCR4.

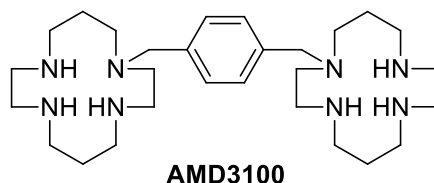


Figure 21: Structure of the bicyclam compound **AMD3100**, an inhibitor of CXCR4.

3.1.2 Developing a CXCR4 Modulator

In an effort to discover compounds with similarly potent inhibition of CXCL12 binding to CXCR4 but with no toxic side effects, Weiqiang Zhan in our lab synthesized a library of compounds that eliminated the cyclam moieties but retaining a similar distribution of heteroatoms from the central core of **AMD3100**. **WZ-40** and **WZ-41** (Figure 22) were the most promising showing EC_{50} values close to 1 nM in a competitive binding assay, displacing TN14003 from CXCR4 positive cells.⁹⁷ TN14003 is a rhodamine-labeled 14-mer peptide known to competitively inhibit binding of CXCL12 to CXCR4.⁹⁸ Although TN14003 is used to monitor interaction with CXCR4, the results of this assay are not directly translatable to blocking CXCL12 binding with CXCR4.⁹⁹ Additionally, these compounds were found to down-regulate

the cAMP pathway, a downstream signaling event of CXCR4/CXCL12 binding. In collaboration with Hyunsuk Shim at the Winship Cancer Institute (WCI), an *in vivo* study using nude mice with head and neck (686-LN) xenograft tumors was conducted with **WZ-40**. Untreated mice developed lung metastases after 30 days, while animals treated with a 40 mg/kg i.p. dose of **WZ-40**, three times weekly failed to develop any tumors.¹⁰⁰

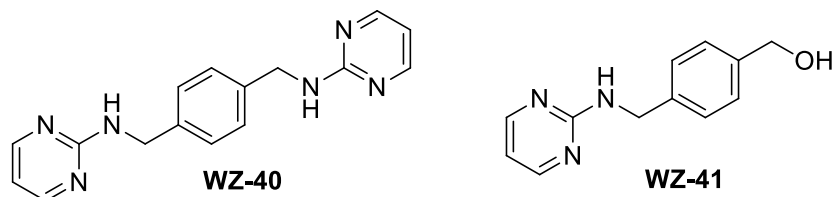


Figure 22: Lead CXCR4 antagonists developed in our laboratory by Weiqiang Zhan.

WZ-41 was used as inspiration to develop a series of compounds to treat AMD. From a synthetic perspective, **WZ-41** contains a hydroxyl group which can allow for additional modifications. Our main research aim was to derivatize **WZ-41** to optimize permeation of the cornea so that we could topically deliver this drug to halt the progression of AMD. Once inside the ocular chamber, we hypothesize that it should interfere with CXCR4/CXCL12 binding, decreasing angiogenesis and alleviating the symptoms of AMD. **WZ-41** has a Φ value of 9.60 and r_s of less than 5\AA .¹⁰¹ Based on the predictions made by Edwards and co-workers shown in Figure 20, our compound exhibits an ideal solution distribution coefficient and radius to be delivered successfully to the anterior chamber of the eye. In addition Serdar Kayakurt, a computational chemist in the EIDD, helped verify our synthetic targets with computational chemistry. Specifically, he developed a computational estimation for corneal permeability within the framework of a program called QuikProp (Maestro). As a training set of compounds, Kurtkaya drew from a library of 113 compounds reported by Prausnitz and Noonan which were tested *in vitro* for corneal permeability¹⁰² as well as computational work reported by Worth and Cronin.¹⁰³ We utilized this tool to pursue synthetic targets that were determined to fall within the

computational category of “highly permeable”, which have cLogP values ranging from 1 to 4, as well as two that fell outside this optimal range for comparison.¹⁰¹

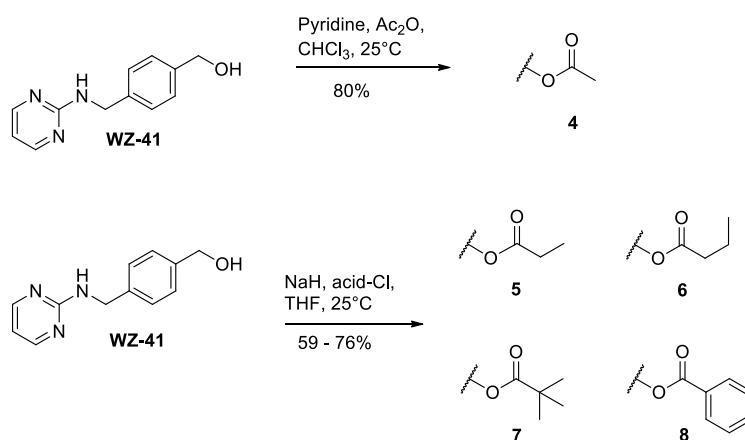
Covalent modifications may help increase the permeability of the compound, but may negatively impact the interaction with CXCR4. In addition to designing some modified variants of the lead compound that will require testing to determine interaction with CXCR4, we designed a number ester and amide pro-drugs. The pro-drugs will likely be substrates for esterases and amidases within the eye. Cleavage of these pro-drugs will release the benzylic alcohol **WZ-41** or the amine containing derivative.¹⁰⁴ Furthermore, we hypothesize the pro-drug moiety could be used to tune the corneal permeability, maximizing the concentration of compound that will reach the interior chamber of the eye. When the optimized pro-drugs reach the interior, they will be cleaved to yield the original parent compound **WZ-41** that is known to interact with CXCR4. In addition, the pro-drug will likely affect flux in a positive manner, driving the equilibrium forward towards the inside of the eye. As the pro-drug is cleaved to the parent compound it will be less capable of permeating back through the cornea.

In an attempt to take full advantage of the transverse delivery pathway described by Edwards, one subset of target compounds will contain amphiphilic functionality such as polyethylene glycol (PEG), allowing us to take advantage of the hydrophobic *and* hydrophilic environments in the cornea. These compounds may also enhance binding to CXCR4 as they can be envisioned to display a flexible heteroatom motif that could mimic the carbon/nitrogen theme in the cyclams of **AMD3100**.

3.2 Results

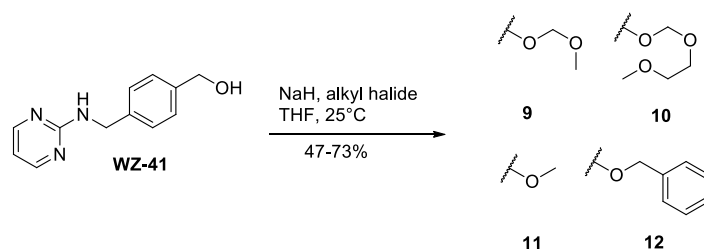
3.2.1 Synthesis of Novel WZ-41 Analogs

To produce a small library of compounds to probe ocular permeability, I began with **WZ-41** as a lead. This small molecule contains a benzylic alcohol, which supplies a handle for modifications. Ester analogs of **WZ-41** were made by deprotonation of the benzylic alcohol, followed by addition of acetic anhydride to make **4** in good yield, or commercially available acid chlorides to generate **5-8** in moderate yields (Scheme 25).¹⁰⁵



Scheme 25: Synthesis of ester analogs of **WZ-41**.

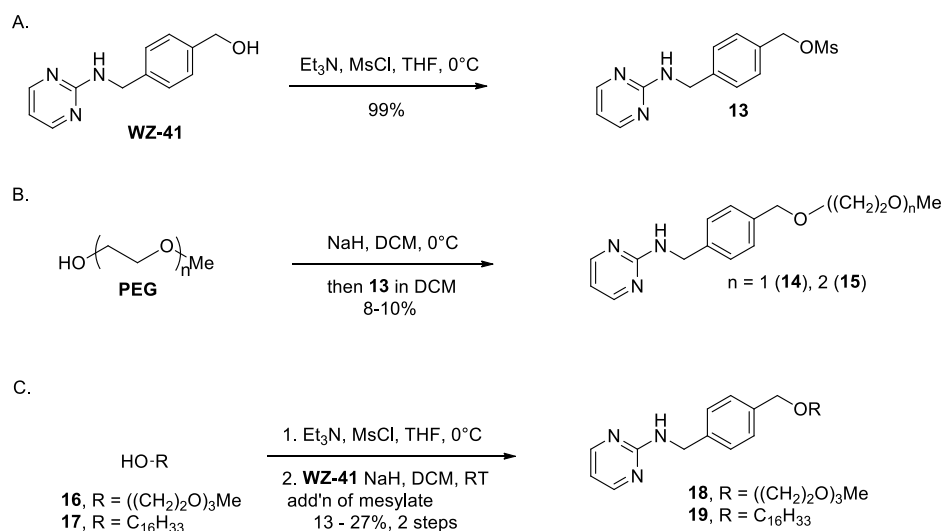
Acetal and ether linkages (Scheme 26) were synthesized via base mediated coupling with the corresponding alkyl halide. These afforded the methoxymethyl- (**9**),¹⁰⁶ 2-(methoxyethoxy)methyl- (**10**),¹⁰⁷ methoxy- (**11**), and benzyl- (**12**) conjugated analogs.



Scheme 26: Synthesis of ether linkages synthesized *via* the Williamson ether synthesis.

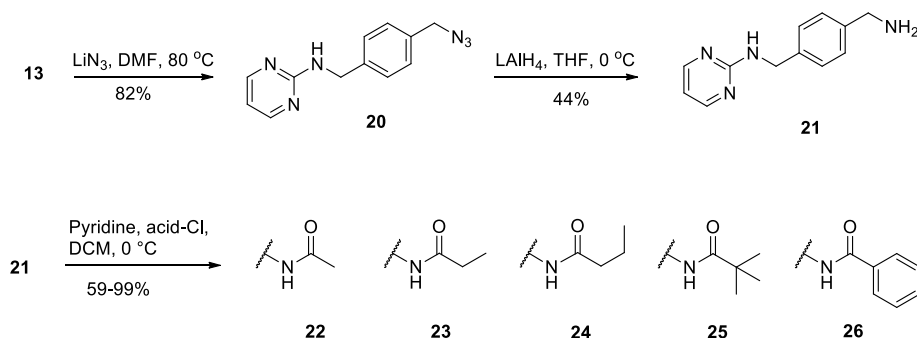
In order to access the amphiphillic PEG compounds, we utilized the Mitsunobu reaction with **WZ-41** as starting material. This route proved unsuccessful in obtaining the desired

products. However, addition of the alkoxy-anion of the PEG substrate to the mesylate of **WZ-41** (**13**) led to substitution for the mono- and di-PEG compounds **14** and **15** in low yields, but did not yield product for alcohols **16** and **17**. As summarized in Scheme 27C, the synthesis of the tri-PEG compound **18** and hexadecanol modified analog **19** were achieved by creating the mesylate of alcohols **16** and **17** and adding them to the alkoxy-anion of **WZ-41** to yield the desired products.



Scheme 27: Second generation compounds attained by Williamson ether synthesis.

Our next target was the benzylic amine derivative **21**. We initially sought to synthesize this target via the Gabriel synthesis. Phthalimide was used to displace the mesylate in compound **13**, but complex mixtures were obtained. Instead we found that nucleophilic displacement of the mesylate with lithium azide afforded **20** in good yield, and subsequent reduction with lithium aluminum hydride (LAH) gave clean conversion to the desired amine **21**. Treatment of the amine with acid chlorides in the presence of pyridine afforded a variety of amides in moderate to excellent yields (Scheme 28).



Scheme 28: Synthesis of amine and amide derivatives of **WZ-41** via formation of the azide intermediate **20**.

3.3 Biological Evaluation

3.3.1 *In vitro* Cell-based TN-14003 Binding Assay Results

To evaluate the ability of our newly synthesized analogs to interact with CXCR4, we utilized the cell based TN-14003 competitive binding assay (performed by members of the laboratory of Shim, Winship Cancer Institute). MB-231, a breast cancer cell line that over expresses CXCR4, was used. This particular competitive binding assay utilizes TN14003 (Figure 23A), a di-biotinylated 14-mer peptide that is known to competitively inhibit binding of CXCL12 to CXCR4.¹⁰⁸ If a new compound inhibits binding of TN14003 to the CXCR4 positive MB-231 cells, the compound is then presumed to interact with CXCR4 in a manner that would also block CXCL12 from binding.

Experimentally, MB-231 cells were incubated with a mixture of the new compound at 1, 10, 100 and 1000 nM, fixed, washed with PBS, then incubated with 0.05 g/mL solution of TN14003 (Figure 23B, step A). The cells were then washed three times with PBS (Figure 23B, step B or D), and TN14003 was quantified by incubation of the cells with a fluorescent streptavidin-rhodamine conjugate. This conjugate attaches to the biotin labels of TN14003 (Figure 23B, step C or E). In the case of no inhibition, maximal fluorescence is observed (Figure 23B, pathway E). However, upon introduction of an inhibitor that blocks binding, the magnitude

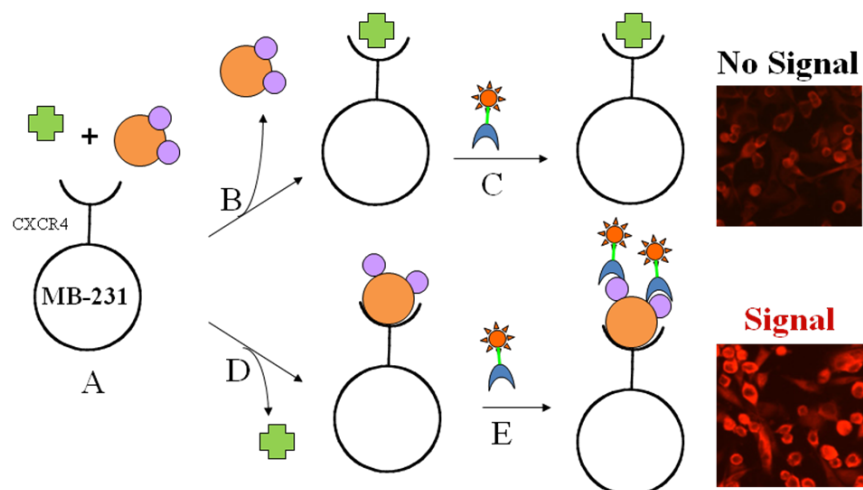
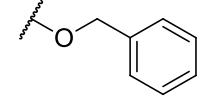
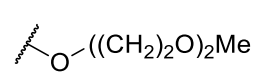
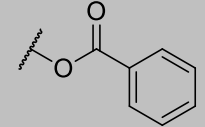
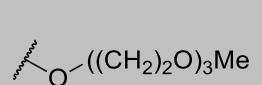
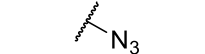
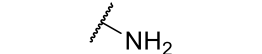
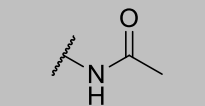
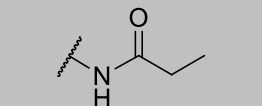
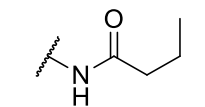
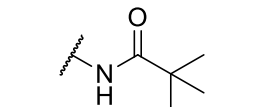
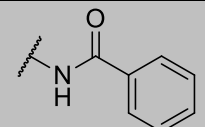


Figure 23: A) CXCL12 displacing peptide TN14003 used in the competitive binding assay. B) Bioassay used to measure interaction of novel compounds with CXCR4 on MB-231 breast cancer cells. Novel compound (green) competes with high affinity biotinylated-peptide TNF14003 (blue/purple). After washing away the unbound substrate, streptavidin-rhodamine conjugate complexes with biotinylated peptide. Inhibition of peptide binding by drug dampens fluorescent signal output.

All newly synthesized analogs were subject to the TN14003 binding assay described in Figure 23. The concentration at which the new compounds were able to decrease the fluorescent signal by ~50% is reported as the EC_{50} in Table 8. In addition, the predicted lipophilicities (cLogP) were calculated by Kurtkaya using QuikProp, a software suit in Maestro.

Table 8: Computational and biological testing values for **WZ-41** and analogues. cLogP values were calculated with QuikPro in Maestro.

Compound	R	cLogP	EC_{50}	Compound	R	cLogP	EC_{50}
WZ-41		1.93	1	11		2.72	1
4		2.79	1000	9		2.53	10
5		2.91	>1000	10		2.63	1
6		3.34	>1000	19		8.51	>1000
7		3.91	1000	14		2.98	10

12		4.51	>1000	15		3.19	10
8		4.08	100	18		3.20	>1000
20		1.63	>1000	21		1.45	>1000
22		1.82	>1000	23		2.24	>1000
24		2.52	>1000	25		2.93	>1000
26		3.80	>1000				

The inhibitory activity of **WZ-41** analogs spanned a wide range of values. Specifically, the methyl ether **11** and acetals **9** and **10** retained EC_{50} values at or below 10 nM. The amphiphilic PEG derivatives **14** and **15** also did not lose the ability to block the TN binding peptide. However, larger increases in hydrophobicity as exemplified by **12** and **19** showed no activity. As anticipated, compounds **4-8** were inactive in this TN-binding assay since these compounds were designed to be pro-drugs of **WZ-41**. The cleavable ester group on each of these molecules was installed to allow for tunable corneal permeability. Once inside the ocular chamber they would be enzymatically cleaved to release **WZ-41**. When substituting the benzylic alcohol in **WZ-41** for a benzylic amine (**21**) all activity was lost. Hence it is not surprising that the amide derivatives where the oxygen was substituted for a nitrogen (**22-26**) were inactive.

3.3.2 In vitro Vasculature Formation Assay Results

This data suggested that several of the compounds in this series interact with CXCR4 although their ability to block binding of CXCL12 and hence quell neovascularization was

unknown. To test the therapeutically desired effect, a small subset of the compounds (**WZ-40**, **WZ-41**, **9**, **10**, **11**, **15**, and **21**) were sent to Southern Research Institute (SRI) to undergo a tubule formation assay with human umbilical vascular endothelial cells (HUVEC). In this assay, the formation of new vessels was measured in triplicate (length and number of tubes) at concentrations of 0.001, 0.010, 0.100, 1.0, and 10 μM . The most active of these compounds was **WZ-41** with an IC_{50} of 3.9 μM , while others tested did not have an IC_{50} below the highest concentration of 10 μM as shown in Table 9.

Table 9: Tubule formation assay results from S.R.I.

Compound	WZ-40	WZ-41	9	10	11	15	21
IC_{50} (μM)	>10	3.9	>10	>10	>10	>10	>10

3.4 Conclusions

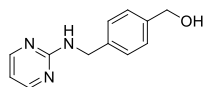
Starting with the benzylic alcohol **WZ-41** as the lead compound, I designed and synthesized a variety of derivatives to treat AMD. The first subset of the analogs were designed to be pro-drugs of **WZ-41** and hypothesized to increase permeation of the cornea followed by a release of the parent drug in the ocular chamber and hence were inactive in our CXCR4 assay. Replacement of the benzylic alcohol of **WZ-41** with an amine or amide eliminated the competitive inhibition against TN14003. The final subset entailed permanent modifications to the benzylic oxygen, maintaining similar potency in the TN binding assay as **WZ-41**. For these amphiphilic compounds, alternating carbon/oxygen chains of varying length probed the ability to interact with CXCR4 while at the same time modulating corneal permeability. Although some of the amphiphilic molecules **8-10** retained IC_{50} 's between 1-10 nM in the competitive binding assay with MB-231 cells and TN-14003 peptide, they failed to disrupt the growth of new

vasculature in cell culture when tested in a HUVEC assay conducted by Southern Research Institute.

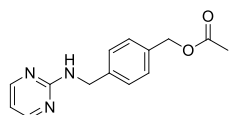
3.5 Methods and Experimental Protocol

3.5.1 Experimental Procedure for the Synthesis of Novel WZ-41 Analogs

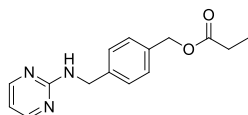
General: ^1H , ^{19}F , and ^{13}C NMR spectra were recorded on Varian Inova 400 MHz spectrometer in deuterated chloroform (CDCl_3) with the solvent residual peak (CDCl_3 : $^1\text{H} = 7.27$ ppm, $^{13}\text{C} = 77.2$ ppm) as internal references unless otherwise specified. Data are reported in the following order: chemical shifts are given (δ); multiplicities are indicated as br (broadened), s (singlet), d (doublet), t (triplet), q (quartet), m (multiplet), app (apparent); coupling constants, J , are reported (Hz); integration is provided. Infrared absorption spectra were obtained on a Thermo Scientific Nicolet 370 FT-IR spectrophotometer via the Smart Orbit Diamond Attenuated Total Reflectance accessory. Peaks are reported (cm^{-1}). Elemental analyses were performed by Atlantic Microlab, Inc (Norcross, Ga.). High resolution mass spectrometry was performed by the Emory University Mass Spectrometry Center (Dr. Fred Strobel). Melting points (mp) were taken in open capillary tubes on a 200W MelTemp capillary melting points apparatus and are not corrected. Analytical thin-layer chromatography (TLC) was carried out on commercial Aldrich glass-supported silica gel plates with fluorescent indicator (F-254). Visualization was accomplished by UV light or stained with ninhydrin, potassium permanganate, or sulfuric acid (4% aqueous). Chromatography purification was performed with 60 Å silica gel (230-400 mesh) from Sorbent Technologies. Nominal mass spectra were obtained on either an Applied Biosystems AP150 or AP3000 by direct infusion.



4-((Pyrimidin-2-ylamino)methyl)phenylmethanol (WZ-41): Compound supplied by iThemba Pharma (Pty) Ltd. Nominal MS $m/z = 216.5$. $^1\text{H NMR}$ (CDCl_3 , 400 MHz). 8.26 (d, $J = 4.80$ Hz, 2 H), 7.36 (m, 4 H), 6.56 (t, $J = 4.80$ Hz, 1 H), 5.44 (bs, 1 H), 4.69 (d, $J = 5.72$ Hz, 2 H), 4.62 (d, $J = 6.04$ Hz, 1 H), 1.96 (t, $J = 6.03$ Hz, 1 H).

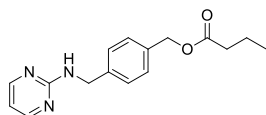


4-((Pyrimidin-2-ylamino)methyl)benzyl ethanoate (4): Pyridine (243 μL , 3.01 mmol) was allowed to equilibrate in CHCl_3 (5 mL) for 30 minutes before the addition of **WZ-41** (500 mg, 2.33 mmol). The mixture was cooled to -10 $^\circ\text{C}$ and stirred for 5 minutes, at which point acetic anhydride (307 mg, 3.0 mmol) was added. The reaction was kept at this temperature for 4 hours, then allowed to warm to RT overnight. The reaction was quenched with sat'd NH_4Cl , which was extracted with DCM. The product was purified by column chromatography (3:1 of EtOAc:hex as eluent) to obtain a white crystalline solid (478 mg, 80 %). $R_f = 0.10$ (1:1 hex:EtOAc). MP = 81-83 $^\circ\text{C}$. IR (cm^{-1}): 3236, 3072, 3007, 2938, 1726, 1590, 1575, 1531, 1454, 1358, 1234, 1029, 976, 805, 702, 639. $^1\text{H NMR}$ (CDCl_3 , 400 MHz) δ 8.29 (d, $J = 4.80$ Hz, 2 H), 7.33 (m, 4 H), 6.78 (t, $J = 4.80$ Hz, 1 H), 6.66 (bs, 1 H), 5.07 (s, 2 H), 4.65 (d, $J = 5.61$ Hz, 2 H), 2.08 (s, 3 H). $^{13}\text{C NMR}$ (CDCl_3 , 100 MHz) δ 171.0, 162.4, 158.1 (2 C), 139.5, 135.0, 128.7 (2 C), 127.8 (2 C), 110.9, 66.2, 45.2, 21.1. HRMS (ESI) $m/z = 258.12314$ (Theo. for $\text{C}_{14}\text{H}_{15}\text{N}_3\text{O}_2 + \text{H}$: 258.12425).



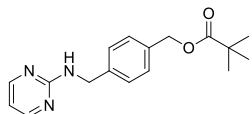
4-((Pyrimidin-2-ylamino)methyl)benzyl propanoate (5): Sodium hydride (95 wt%, 122 mg, 4.80 mmol) was allowed to equilibrate in THF (5 mL) for 30 minutes before the addition of **WZ-**

41 (500 mg, 2.33 mmol). After stirring at RT for 5 minutes, propionyl-chloride (236 mg, 2.56 mmol) was added. The reaction was followed by TLC, and found to be complete after 5 minutes. The reaction was quenched with sat'd NH₄Cl, extracted with DCM, which was dried with MgSO₄ and evaporated. The product was purified by column chromatography (3:2 of EtOAc:hex as eluent) to obtain a white solid (479 mg, 76%). R_f = 0.75 (2:3 hex:EtOAc. MP = 80-82 °C. IR (cm⁻¹): 3248, 3105, 2982, 1733, 1601, 1541, 1460, 1416, 1346, 1193, 799, 761, 711. ¹H NMR (CDCl₃, 400 MHz) δ 8.32 (d, *J* = 4.80 Hz, 2 H), 7.33 (m, 4 H), 6.61 (t, *J* = 4.80 Hz, 1 H), 6.30 (bs, 1 H), 5.09 (s, 2 H), 4.66 (d, *J* = 5.61 Hz, 2 H), 2.36 (d, *J* = 8.02 Hz, 2 H), 1.14 (t, *J* = 8.02 Hz, 3 H). ¹³C NMR (CDCl₃, 100 MHz) δ 174.3, 162.4, 158.1 (2 C), 139.4, 135.1, 128.6 (2 C), 127.9 (2 C), 110.6, 66.0, 45.2, 27.7, 9.2. HRMS (ESI) *m/z* = 272.13882 (Theo. for C₁₅H₁₇N₃O₂+H: 272.13990).

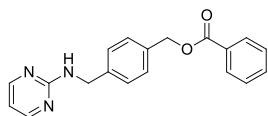


4-((pyrimidin-2-ylamino)methyl)benzyl butanoate (6): Sodium hydride (95 wt%, 122 mg, 4.80 mmol) was allowed to equilibrate in THF (5 mL) for 30 minutes before the addition of **WZ-41** (500 mg, 2.33 mmol). After stirring at RT for 5 minutes, butyryl-chloride (272 mg, 2.56 mmol) was added. The reaction was followed by TLC, and found to be complete after 15 minutes. The reaction was quenched with sat'd NH₄Cl, extracted with DCM, which was dried with MgSO₄ and evaporated. The product was purified by column chromatography (3:2 of EtOAc:hex as eluent) to obtain a white solid (501 mg, 76%). R_f = 0.20 (1:1 hex:EtOAc). MP = 62-64 °C. IR (cm⁻¹): 3256, 3097, 2958, 1726, 1599, 1537, 1454, 1415, 1361, 1169, 1110, 983, 765, 745. ¹H NMR (CDCl₃, 400 MHz) δ 8.32 (d, *J* = 4.80 Hz, 2 H), 7.33 (m, 4 H), 6.61 (t, *J* = 4.80 Hz, 1 H), 6.30 (bs, 1 H), 5.09 (s, 2 H), 4.66 (d, *J* = 5.62 Hz, 2 H), 2.33 (m, 2 H), 1.67 (m, 2

H), 0.95 (t, $J = 8.02$ Hz, 3 H). ^{13}C NMR (CDCl_3 , 100 MHz) δ 173.5, 162.1, 157.9 (2 C), 139.3, 135.1, 128.5 (2 C), 127.7 (2 C), 110.5, 65.8, 45.0, 36.2, 18.4, 13.7. HRMS (ESI) $m/z = 286.15445$ (Theo. for $\text{C}_{16}\text{H}_{19}\text{N}_3\text{O}_2+\text{H}$: 286.15555).

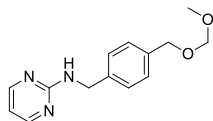


4-((Pyrimidin-2-ylamino)methyl)benzyl 2,2-dimethylpropanoate (7): Sodium hydride (95 wt%, 117 mg, 4.65 mmol) was allowed to equilibrate in THF (5 mL) for 30 minutes before the addition of **WZ-41** (500 mg, 2.33 mmol). After stirring at RT for 5 minutes, pivaloyl-chloride (308 mg, 2.56 mmol) was added. The reaction was followed by TLC, and found to be complete after 5 minutes. The reaction was quenched with sat'd NH_4Cl , extracted with DCM, which was dried with MgSO_4 and evaporated. The product was purified by column chromatography (3:2 of EtOAc:hex as eluent) to obtain a white solid (444 mg, 64%). $R_f = 0.90$ (2:3 hex:EtOAc. MP = 93-95 °C. IR (cm^{-1}): 3220, 2878, 2868, 1723, 1593, 1579, 1530, 1454, 1283, 1261, 1158, 816, 802. ^1H NMR (CDCl_3 , 400 MHz) δ 8.32 (d, $J = 4.80$ Hz, 2 H), 7.33 (m, 4 H), 6.60 (t, $J = 4.80$ Hz, 1 H), 6.40 (bs, 1 H), 5.07 (s, 2 H), 4.65 (d, $J = 5.62$ Hz, 2 H), 1.10 (s, 9 H). ^{13}C NMR (CDCl_3 , 100 MHz) δ 178.4, 162.4, 158.1 (2 C), 139.1, 135.6, 128.1 (2 C), 127.8 (2 C), 110.8, 65.9, 45.2, 38.9, 27.3 (3 C). HRMS (ESI) $m/z = 300.17010$ (Theo. for $\text{C}_{17}\text{H}_{21}\text{N}_3\text{O}_2+\text{H}$: 300.17120).



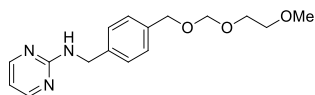
4-((Pyrimidin-2-ylamino)methyl)benzyl benzoate (8): Sodium hydride (95 wt%, 116 mg, 4.63 mmol) was allowed to equilibrate in THF (5 mL) for 30 minutes before the addition of **WZ-41** (500 mg, 2.33 mmol). After stirring at RT for 5 minutes, benzoyl-chloride (359 mg, 2.56 mmol)

was added. The reaction was followed by TLC, and found to be complete after 5 minutes. The reaction was quenched with sat'd NH_4Cl , extracted with DCM, which was dried with MgSO_4 and evaporated. The product was purified by column chromatography (5:3 of EtOAc:hex as eluent) to obtain a white solid (435 mg, 59%). $R_f = 0.15$ (1:1 hex:EtOAc). MP = 112-113 °C. IR (cm^{-1}): 3252, 3097, 2985, 1715, 1600, 1543, 1458, 1408, 1369, 1263, 1101, 1061, 941, 804, 712. ^1H NMR (CDCl_3 , 400 MHz) δ 8.32 (d, $J = 4.80$ Hz, 2 H), 8.08 (m, 2 H), 7.55 (m, 1 H), 7.41 (m, 6 H), 6.57 (t, $J = 4.80$ Hz, 1 H), 5.65 (bs, 1 H), 5.36 (s, 2 H), 4.67 (d, $J = 6.02$ Hz, 2 H). ^{13}C NMR (CDCl_3 , 100 MHz) δ 165.5, 162.4, 158.1 (2 C), 139.5, 135.1, 133.2, 129.8 (2 C), 128.6 (2 C), 128.5 (2 C), 127.9 (2 C), 110.8, 66.6, 45.2. HRMS (ESI) m/z 320.13976 (Theo. for $\text{C}_{19}\text{H}_{17}\text{N}_3\text{O}_2+\text{H}$: 320.13990).

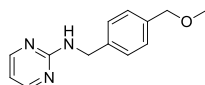


N-4-((Methoxymethoxy)methyl)benzylpyrimidin-2-amine (**9**): Sodium hydride (95 wt%, 122 mg, 4.66 mmol) was allowed to equilibrate in THF (5 mL) for 30 minutes before the addition of **WZ-41** (500 mg, 2.33 mmol). After stirring at RT for 5 minutes, methoxymethylchloride (229 μL , 3.02 mmol) was added. The reaction was followed by TLC, and found to be complete after 2 hours. The reaction was quenched with sat'd NH_4Cl , extracted with DCM, which was dried with MgSO_4 and evaporated. The product was purified by column chromatography (3:1 of EtOAc:hex as eluent) to obtain a white powder (391 mg, 65%). $R_f = 0.20$ (1:1 of EtOAc:hex). MP = 44-47 °C. IR (cm^{-1}): 3256, 3097, 3007, 2938, 1603, 1579, 1538, 1458, 1416, 1364, 1148, 1099, 1042, 918, 849, 797, 762, 720. ^1H NMR (CDCl_3 , 400 MHz) δ 8.29 (d, $J = 4.80$ Hz, 2 H), 7.31 (m, 4 H), 6.58 (t, $J = 4.80$ Hz, 1 H), 5.69 (bs, 1 H), 4.71 (s, 2 H), 4.65 (d, $J = 5.63$ Hz, 2 H), 4.58 (s, 2 H), 3.41 (s, 3 H). ^{13}C NMR (CDCl_3 , 100 MHz) δ 162.5,

158.2 (2 C), 138.8, 137.0, 128.4 (2 C), 127.8 (2 C), 110.9, 95.8, 69.0, 55.5, 45.3. HRMS (ESI) $m/z = 260.13885$ (Theo. for $C_{14}H_{18}N_3O_2+H$: 260.13990).

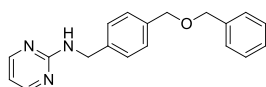


***N*-(4-(((2-Methoxyethoxy)methoxy)methyl)benzyl)pyrimidin-2-amine (10)**: Sodium hydride (95 wt%, 232 mg, 9.68 mmol) was allowed to equilibrate in THF (10 mL) for 30 minutes at 0 °C before the addition of **WZ-41** (1.04 g, 4.84 mmol). After stirring for 5 minutes, (methoxyethoxy)methoxymethyl-chloride (719 μ L, 6.29 mmol) was added. The reaction was followed by TLC, and found to be complete after 2 hours. The reaction was quenched with sat'd NH_4Cl , extracted with DCM, which was dried with $MgSO_4$ and evaporated. The product was purified by column chromatography (7:3 of DCM:EtOAc with 1% Et_3N as eluent), then recrystallized from hexanes to give a white crystalline solid (1.03 g, 70%). $R_f = 0.20$ (3:1 of EtOAc:hex). MP = 44-46 °C. IR (cm^{-1}): 3244, 3101, 2954, 2884, 1603, 1581, 1541, 1458, 1097, 1050, 1028, 1016, 841, 768. 1H NMR ($CDCl_3$, 400 MHz) δ 8.29 (bd, $J = 4.80$ Hz, 2 H), 7.31 (m, 4 H), 6.58 (t, $J = 4.80$ Hz, 1 H), 5.41 (bs, 1 H), 4.81 (s, 2 H), 4.64 (d, $J = 5.63$ Hz, 2 H), 4.61 (s, 2 H), 3.68 (m, 2 H), 3.58 (m, 2 H), 3.41 (s, 3 H). ^{13}C NMR ($CDCl_3$, 100 MHz) δ 162.5, 158.2 (2 C), 138.8, 137.0, 128.4 (2 C), 127.8 (2 C), 111.0, 94.9, 71.9, 69.2, 67.1, 55.2, 45.3. HRMS (ESI) $m/z = 304.16612$ (Theo. for $C_{16}H_{21}N_3O_3+H$: 304.16492).

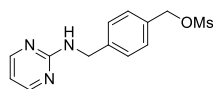


***N*-(4-(Methoxymethyl)benzyl)pyrimidin-2-amine (11)**: Sodium hydride (95 wt%, 122 mg, 5.08 mmol) was allowed to equilibrate in THF (5 mL) for 30 before the addition of **WZ-41** (500 mg, 2.33 mmol). After stirring at RT for 5 minutes, methyl iodide (156 μ L, 2.50 mmol) was added. The reaction was followed by TLC, and found to be complete after 1 hour. The reaction

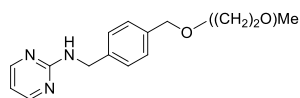
was quenched with sat'd NH_4Cl , extracted with DCM, which was dried with MgSO_4 and evaporated. The product was purified by column chromatography (3:1 of EtOAc:hex) to give a white powder (388 g, 73%). $R_f = 0.20$ (1:1 of EtOAc:hex). MP = 85-86 °C. IR (cm^{-1}): 3244, 3093, 2991, 2921, 2811, 1599, 1577, 1541, 1460, 1416, 1372, 1107, 979, 798, 766, 713, 638, 614. ^1H NMR (CDCl_3 , 400 MHz) δ 8.29 (d, $J = 4.80$ Hz, 2 H), 7.31 (m, 4 H), 6.59 (t, $J = 4.80$ Hz, 1 H), 5.81 (bs, 1 H), 4.64 (d, $J = 6.00$ Hz, 2 H), 4.42 (s, 2 H), 3.37 (s, 3 H). ^{13}C NMR (CDCl_3 , 100 MHz) δ 162.5, 158.2 (2 C), 138.7, 137.4, 128.2 (2 C), 127.8 (2 C), 111.0, 74.6, 58.2, 45.4. HRMS (ESI) $m/z = 230.12835$ (Theo. for $\text{C}_{13}\text{H}_{15}\text{N}_3\text{O}+\text{H}$: 230.12934).



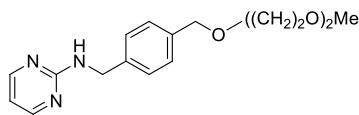
***N*-(4-(Benzyloxymethyl)benzyl)pyrimidin-2-amine (12)**: Sodium hydride (95 wt%, 122 mg, 4.66 mmol) was allowed to equilibrate in THF (5 mL) for 30 minutes before the addition of **WZ-41** (500 mg, 2.33 mmol). After stirring at RT for 5 minutes, benzylbromide (303 μL , 2.56 mmol) was added. The reaction was complete the following morning. The reaction was quenched with sat'd NH_4Cl , extracted with DCM, which was dried with MgSO_4 and evaporated. The product was purified by column chromatography (5:2 of EtOAc:hex as eluent) to obtain a white solid (336 mg, 47%). $R_f = 0.33$ (1:1 of EtOAc:hex). MP = 86-88 °C. IR (cm^{-1}): 3236, 3028, 2943, 1598, 1576, 1537, 1456, 1407, 1358, 1122, 1022, 799, 755, 728, 697. ^1H NMR (CDCl_3 , 400 MHz) δ 8.31 (d, $J = 3.60$ Hz, 2 H), 7.39-7.29 (m, 9 H), 6.59 (t, $J = 4.40$ Hz, 1 H), 5.85 (bs, 1 H), 4.67 (d, $J = 5.61$ Hz, 2 H), 4.56 (s, 2 H), 4.55 (s, 2 H). ^{13}C NMR (CDCl_3 , 100 MHz) δ 162.5, 158.2 (2 C), 138.7, 138.4, 137.4, 128.6 (2 C), 128.3 (2 C), 128.0 (2 C), 127.8, 127.7 (2 C), 110.9, 72.2, 72.0, 45.4. HRMS (ESI) $m/z = 306.15958$ (Theo. for $\text{C}_{19}\text{H}_{20}\text{N}_3\text{O}+\text{H}$: 306.16064).



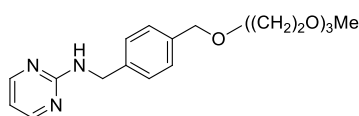
4-((Pyrimidin-2-ylamino)methyl)benzyl methanesulfonate (13): WZ-41 (5.06 g, 23.5 mmol) was dissolved in THF (50 mL) and cooled to 0 °C, and methylsulfanyl chloride (2.73 mL, 35.3 mmol) was added. To the mixture was added Et₃N (9.80 mL, 70.5 mmol) drop wise under continuous stirring. The reaction was stirred for 15 minutes at which time TLC showed complete conversion to the mesylate. The reaction was quenched with cold sat'd NaHCO₃, then extracted with DCM. The organic layer was dried over MgSO₄ and evaporated to give the crude product (7.24 g, 94%). This material was used crude in subsequent reactions. R_f = 0.38 (1:1 of EtOAc:hex). ¹H NMR (CDCl₃, 400 MHz) δ 8.28 (d, *J* = 4.80 Hz, 2 H), 7.31 (m, 4 H), 6.56 (t, *J* = 4.80 Hz, 1 H), 5.64 (bs, 1 H), 4.63 (d, *J* = 6.00 Hz, 2 H), 4.45 (s, 2 H), 2.98 (s, 3 H). ¹³C NMR (CDCl₃, 100 MHz) δ 162.5, 158.3 (2 C), 138.7, 137.4, 128.2 (2 C), 127.8 (2 C), 111.0, 70.7, 45.6, 38.2.



***N*-4-((2-Methoxyethoxy)methyl)benzylpyrimidin-2-amine (14):** 1-methoxy ethanol (184 μL, 2.33 mmol) was added to a stirring solution of sodium hydride (95% wt, 65 mg, 2.56 mmol) in DCM (20 mL) at 0 °C under argon. After stirring for 1 hour, the mesylate **13** (683 mg, 2.33 mmol) was added as a solution in DCM (18 mL). After 70 minutes, the reaction was quenched with the addition of sat'd NaHCO₃, followed by extraction with DCM. The organic layer was dried over MgSO₄, then evaporated to give the crude product as an oil. The product was purified by column chromatography (3:1 of EtOAc:hex as eluent) to obtain a clear oil that solidified into a wax after 5 days at RT (60 mg, 9.4%). R_f = 0.55 (3:1 of EtOAc:hex). IR (cm⁻¹): 3260, 2868, 1589, 1529, 1453, 1408, 1361, 1095, 1020, 801, 730, 640. ¹H NMR (CDCl₃, 400 MHz) δ 8.32 (d, *J* = 4.80 Hz, 2 H), 7.33 (m, 4 H), 6.61 (t, *J* = 4.80 Hz, 1 H), 6.30 (bs, 1 H), 5.46 (s, 1 H), 4.64 (d, *J* = 6.00 Hz, 2 H), 4.57 (s, 2 H), 3.60 (m, 4 H), 3.39 (s, 3 H).

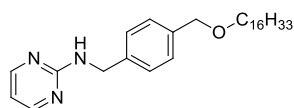


***N*-(4-((2-(2-Methoxyethoxy)ethoxy)methyl)benzyl)pyrimidin-2-amine** (15): 2-(2-methoxyethoxy)ethanol (274 μ L, 2.33 mmol) was added to a stirring solution of sodium hydride (95% wt, 141 mg, 5.59 mmol) in THF (10 mL) at 0 °C under argon. After stirring for 1 hour, the mesylate **13** (1.49 g, 5.08 mmol) was added as a solution in THF (10 mL). After 70 minutes, the reaction was quenched with the addition of sat'd NaHCO₃, followed by extraction with DCM. The organic layer was dried over MgSO₄, then evaporated to give the crude product as an oil. The product was purified by column chromatography (3:1 of EtOAc:hex as eluent) to obtain a clear oil that solidified into a wax after 5 days at RT (216 mg, 13%). R_f = 0.35 (3:1 of EtOAc:hex). IR (cm⁻¹): 3252, 2869, 1587, 1529, 1453, 140, 1360, 1096, 801, 729, 641. ¹H NMR (CDCl₃, 400 MHz) δ 8.32 (d, J = 4.80 Hz, 2 H), 7.33 (m, 4 H), 6.61 (t, J = 4.80 Hz, 1 H), 6.30 (s, 1 H), 5.46 (bs, 1 H), 4.64 (d, J = 6.00 Hz, 2 H), 4.57 (s, 2 H), 3.7 – 3.6 (m, 6 H), 3.57 (m, 2 H), 3.39 (s, 3 H). ¹³C NMR (CDCl₃, 100 MHz) δ 162.5, 158.3 (2 C), 138.7, 137.4, 128.3 (2 C), 127.8 (2 C), 110.9, 73.1, 72.1, 70.8, 70.7, 69.5, 59.3, 45.6. HRMS (ESI) m/z = 318.18110 (Theo. for C₁₉H₂₀N₃O+H: 318.18177).



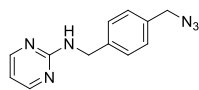
***N*-(4-(2,5,8,11-Tetraoxadodecyl)benzyl)pyrimidin-2-amine** (18): 2-(2-(2-methoxyethoxy)ethoxy)ethanol (365 μ L, 2.33 mmol) was dissolved in THF (6.3 mL), cooled to 0 °C, and methylsulfanyl chloride (198 μ L, 2.56 mmol) was added. To the mixture was stirred for 10 minutes, then Et₃N (972 μ L, 6.99 mmol) was added drop wise. The reaction was stirred for 30 minutes at which time TLC showed complete conversion to the mesylate. The reaction was

washed with water (5 mL), then the organic layer was diluted with DCM (15 mL) and washed with sat'd NaHCO₃, dried over MgSO₄ and evaporated to give the crude product which was used immediately without purification. **WZ-41** (502 mg, 2.33 mmol) was added to a stirring solution of sodium hydride (95 % wt, 76.5 mg, 3.03 mmol) in DMF (20 mL) at 0 °C under argon. The ice bath was removed and the reaction was allowed to warm to RT over 40 minutes, at which time the mesylate of 2-(2-(2-methoxyethoxy)ethoxy)ethanol (565 mg, 2.33 mmol) dissolved in DMF (9 mL) was added. The reaction went from clear and colorless to a dark red/orange over 90 minutes, at which time the reaction was quenched with slow addition of water (20 mL). The organics were extracted with EtOAc (50 mL), and the organic layer was washed with water (3 x 10 mL), brine (15 mL), then dried over MgSO₄. The solvent was then removed *in vacuo*, and the crude oil was purified by column chromatography (4:1 of hex:EtOAc as eluent) to obtain a waxy solid (67 mg, 8.0%). R_f = 0.20 (4:1 of hex:EtOAc). IR (cm⁻¹): 3253, 2876, 1588, 1529, 1453, 1408, 1360, 1095, 1020, 801, 639. ¹H NMR (CDCl₃, 400 MHz) δ 8.32 (m, 2 H), 7.33 (m, 4 H), 6.47 (m, 1 H), 6.15 (bs, 1 H), 4.59 (d, *J* = 5.87 Hz, 2 H), 4.53 (s, 2 H), 3.62 (m, 10 H), 3.52 (m, 2 H), 3.45 (s, 3 H). HRMS (ESI) *m/z* = 362.20715 (Theo. for C₂₈H₄₅N₃O+H: 362.20798).



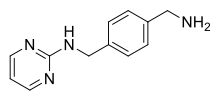
N-(4-((Hexadecyloxy)methyl)benzyl)pyrimidin-2-amine (19): Hexadecane-1-ol (565 mg, 2.33 mmol) was dissolved in THF (23 mL), cooled to 0 °C, and methylsulfonyl chloride (198 μL, 2.56 mmol) was added. To the mixture was stirred for 10 minutes, then Et₃N (980 μL, 7.05 mmol) was added drop wise. The reaction was stirred for 30 minutes at which time TLC showed complete conversion to the mesylate. The reaction was quenched with cold sat'd NaHCO₃, then extracted with DCM. The organic layer was dried over MgSO₄ and evaporated to give the crude

product which was used crude immediately. **WZ-41** (552 mg, 2.56 mmol) was added to a stirring solution of sodium hydride (60 % wt, 140 mg, 2.56 mmol) in DMF (30 mL) at 0 °C under argon. The ice bath was removed and the reaction was allowed to warm to RT over 30 minutes, at which time the mesylate of hexadecane-1-ol (747 mg, 2.33 mmol) dissolved in DMF (9 mL) was added. The reaction went from clear and colorless to a dark red/orange over 90 minutes, at which time the reaction was quenched with slow addition of water (20 mL). The organics were extracted with EtOAc (50 mL), and the organic layer was washed with water (3 x 10 mL), brine (15 mL), then dried over MgSO₄. The solvent was then removed in vacuo, and the crude oil was purified by column chromatography (4:1 of hex:EtOAc as eluent) to obtain a waxy solid (272 mg, 27%). R_f = 0.20 (4:1 of hex:EtOAc). MP = 73-74 °C. IR (cm⁻¹): 3252, 2915, 2849, 1609, 1580, 1543, 1463, 1416, 1364, 112, 798, 761, 718. ¹H NMR (CDCl₃, 400 MHz) δ 8.30 (m, 2 H), 7.30 (m, 4 H), 6.57 (m, 1 H), 5.43 (bs, 1 H), 4.64 (d, *J* = 5.87 Hz, 2 H), 4.49 (s, 2 H), 3.45 (t, *J* = 6.51 Hz, 2 H), 1.60 (m, 2 H), 1.26 (m, 26 H), 0.89 (t, *J* = 6.65 Hz, 3 H). ¹³C NMR (CDCl₃, 100 MHz) δ 162.4, 158.3 (2 C), 138.5, 138.0, 128.1 (2 C), 127.7 (2 C), 111.1, 72.8, 70.7, 45.4, 32.1, 29.9 (11 C), 29.6, 22.9, 14.4. HRMS (ESI) *m/z* = 440.36304 (Theo. for C₂₈H₄₅N₃O+H: 440.36409).

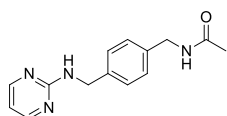


N-(4-(Azidomethyl)benzyl)pyrimidin-2-amine (20): Mesylate **13** (2.70 g, 9.20 mmol) was brought up in DMF (100 mL) to which lithium azide (451 mg, 9.20 mmol) was added and the mixture was heated to 80 °C for 4 hours with continuous stirring. At this time the solvent was removed under reduced pressure, and the crude product was purified by column chromatography (0 – 5% MeOH in DCM) to give the final product as a white solid (1.80 g, 81%). R_f = 0.25 (1:1 of EtOAc:hex). IR (cm⁻¹): 3248, 3007, 2917, 2099, 1586, 1574, 1528, 1451, 1418, 1359, 1260,

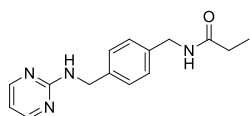
801, 785. ^1H NMR (CDCl_3 , 400 MHz) δ 8.21 (m, 2 H), 7.37 (m, 2 H), 7.27 (m, 2 H), 6.53 (t, J = 4.80 Hz, 1 H), 6.04 (bs, 1 H), 4.64 (d, J = 6.00 Hz, 2 H), 4.31 (s, 2 H). ^{13}C NMR (CDCl_3 , 100 MHz) δ 162.5, 158.3 (2 C), 139.6, 134.6, 128.7 (2 C), 128.1 (2 C), 111.3, 54.8, 45.3. HRMS (ESI) m/z = 241.11996 (Theo. for $\text{C}_{12}\text{H}_{12}\text{N}_6+\text{H}$: 241.12017).



***N*-(4-(Aminomethyl)benzyl)pyrimidin-2-amine (21)**: *N*-(4-(azidomethyl)benzyl)pyrimidin-2-amine **20** (1.67 g, 6.95 mmol) was dissolved in THF (75 mL) and cooled to 0 °C. Lithium aluminum hydride (2 M, 5.2 mL, 10.4 mmol) was added over 30 minutes. When bubbling ceases, the reaction was worked up by diluting with ether then quenching with slow addition of H_2O (0.75 mL). Next, 1M NaOH (0.75 mL) was added and the mixture was stirred for 5 minutes, followed by addition of more water (0.75 mL). The reaction was stirred for 30 minutes, at which time the heterogenous mixture is filtered and solids are washed with Et_2O . Organic layers were combined, dried over MgSO_4 and evaporated to give the crude product. Purification was accomplished by column chromatography (10 – 100% B (84:15:1 of DCM:MeOH: NH_4OH) in DCM) to give the final product as a white powder (659 mg, 44%). R_f = 0.38 (85:10:5 of DCM:MeOH: Et_3N). MP = 104-106 °C. IR (cm^{-1}): 3224, 3019, 2909, 2864, 2357, 1586, 1530, 1504, 1455, 1342, 1250, 800, 779, 640. ^1H NMR (CD_3OD , 400 MHz) δ 8.22 (d, J = 4.67 Hz, 2 H), 7.28 (m, 4 H), 6.57 (t, J = 4.67 Hz, 1 H), 6.04 (bs, 1 H), 4.88 (s, 3 H), 4.55 (s, 2 H), 3.74 (s, 2 H). ^{13}C NMR (CD_3OD , 100 MHz) δ 163.6, 159.5, 159.4, 142.4, 139.8, 128.6 (3 C), 111.6, 111.5, 46.5, 45.6. HRMS (ESI) m/z = 215.12970 (Theo. for $\text{C}_{12}\text{H}_{14}\text{N}_4+\text{H}$: 215.12967).

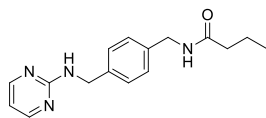


General procedure for acylation benzylic amine 21. *N*-(4-((Pyrimidin-2-ylamino)methyl)benzyl)acetamide (22): *N*-(4-(aminomethyl)benzyl)pyrimidin-2-amine **20** (80.0 mg, 373 μmol) was brought up in DCM (25 mL) and cooled to 0 °C. To the stirring mixture was added acetyl chloride (29.2 μL , 411 μmol) dissolved in DCM (20 mL) over 10 minutes via syringe pump. Upon completion of addition, the solution was stirred for 30 minutes, at which time pyridine (31.6 μL , 392 μmol) was added. TLC at 3 hours showed nearly complete conversion, so the reaction was quenched with sat'd NaHCO_3 . The organic layer was dried over MgSO_4 and evaporated to give the crude product. The product was purified by column chromatography (97:2:1 of DCM:MeOH: Et_3N as eluent) to obtain a white solid (48.8 mg, 51%). $R_f = 0.42$ (98:2 DCM:MeOH). MP = 187-189 °C. IR (cm^{-1}): 3269, 3105, 2958, 2356, 1629, 1597, 1540, 1516, 1457, 1413, 1365, 1283, 756, 737. ^1H NMR (CDCl_3 , 400 MHz) δ 8.30 (d, $J = 4.80$ Hz, 2 H), 7.32 (d, $J = 8.26$ Hz, 2 H), 7.25 (d, $J = 7.94$ Hz, 2 H), 6.58 (t, $J = 4.74$ Hz, 1 H), 5.61 (bs, 1 H), 5.43 (bs, 1 N), 4.64 (d, $J = 5.92$ Hz, 2 H), 4.43 (d, $J = 5.69$ Hz, 2 H), 2.03 (s, 3 H). ^{13}C NMR (CDCl_3 , 100 MHz) δ 173.2, 162.3, 158.3 (2 C), 138.6, 137.3, 128.3 (2 C), 127.9 (2 C), 111.1, 45.1, 43.5, 23.3. HRMS (ESI) $m/z = 257.14002$ (Theo. for $\text{C}_{14}\text{H}_{16}\text{N}_4\text{O}+\text{H}$: 257.13969).

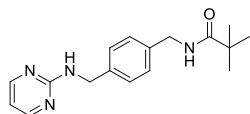


***N*-(4-((Pyrimidin-2-ylamino)methyl)benzyl)propionamide (23).** White solid (74.8 mg, 59%). $R_f = 0.47$ (98:2 DCM:MeOH). MP = 181-184 °C. IR (cm^{-1}): 3289, 2966, 2361, 1634, 1606, 1542, 1521, 1462, 1417, 1364, 1242, 1217, 1029, 799, 715. ^1H NMR (CDCl_3 , 400 MHz) δ 8.29 (d, $J = 6.40$ Hz, 2 H), 7.32 (d, $J = 8.26$ Hz, 2 H), 7.25 (d, $J = 7.94$ Hz, 2 H), 6.57 (t, $J = 4.74$ Hz, 1 H), 5.75 (bs, 1 H), 5.50 (bs, 1 N), 4.63 (d, $J = 5.92$ Hz, 2 H), 4.43 (d, $J = 5.69$ Hz, 2 H), 2.35 (q, $J = 7.58$ Hz, 2 H), 1.19 (t, $J = 7.58$ Hz, 3 H). ^{13}C NMR (CDCl_3 , 100 MHz) δ 173.9, 162.3,

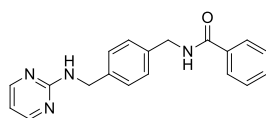
158.3 (2 C), 138.6, 137.5, 128.3 (2 C), 127.9 (2 C), 111.1, 45.1, 43.4, 29.9, 10.0. HRMS (ESI) $m/z = 271.15568$ (Theo. for $C_{14}H_{15}N_3O_2+H$: 271.15534).



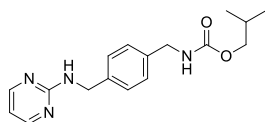
***N*-(4-((Pyrimidin-2-ylamino)methyl)benzyl)butyramide (24)**. White solid (17.7 mg, 59%). $R_f = 0.85$ (85:10:5 in DCM:MeOH:Et₃N). MP = 156-159 °C. IR (cm⁻¹): 3289, 3068, 2958, 2357, 1636, 1609, 1542, 1461, 1415, 1234, 1217, 708. ¹H NMR (CDCl₃, 400 MHz) δ 8.29 (d, $J = 4.76$ Hz, 2 H), 7.32 (d, $J = 8.26$ Hz, 2 H), 7.25 (d, $J = 7.94$ Hz, 2 H), 6.57 (t, $J = 4.74$ Hz, 1 H), 5.72 (bs, 1 H), 5.45 (bs, 1 N), 4.63 (d, $J = 6.04$ Hz, 2 H), 4.43 (d, $J = 5.71$ Hz, 2 H), 2.19 (t, $J = 7.58$ Hz, 3 H), 1.69 (m, 2 H), 1.19 (t, $J = 7.58$ Hz, 3 H). ¹³C NMR (CDCl₃, 100 MHz) δ 172.9, 163.1, 158.4 (2 C), 138.7, 137.7, 128.3 (2 C), 128.0 (2 C), 111.2, 45.3, 43.5, 38.9, 19.4, 14.0. HRMS (ESI) $m/z = 285.17134$ (Theo. for $C_{16}H_{20}N_4O+H$: 285.17099).



***N*-(4-((Pyrimidin-2-ylamino)methyl)benzyl)pivalamide (25)**. White solid (25.4 mg, 91%). $R_f = 0.89$ (85:10:5 in DCM:MeOH:Et₃N). MP = 164-166 °C. IR (cm⁻¹): 3248, 3072, 2974, 2349, 1631, 1599, 1535, 1453, 1348, 1213, 993, 704. ¹H NMR (CDCl₃, 400 MHz) δ 8.29 (m, 2 H), 7.32 (d, $J = 8.26$ Hz, 2 H), 7.22 (d, $J = 7.94$ Hz, 2 H), 6.54 (t, $J = 4.74$ Hz, 1 H), 5.92 (bs, 1 H), 5.76 (bs, 1 N), 4.62 (d, $J = 6.04$ Hz, 2 H), 1.22 (s, 9 H). ¹³C NMR (CDCl₃, 100 MHz) δ 178.2, 162.3, 158.3, 138.6, 137.8, 128.2 (2 C), 128.0 (2 C), 111.1, 45.3, 43.5, 38.7, 27.8 (3 C). HRMS (ESI) $m/z = 299.18700$ (Theo. for $C_{17}H_{12}N_4O+H$: 299.18664).



***N*-4-((Pyrimidin-2-ylamino)methyl)benzylbenzamide (26)**. White solid (34.5 mg, 99%). $R_f = 0.85$ (85:10:5 in DCM:MeOH:Et₃N). MP = 165-167 °C. IR (cm⁻¹): 3269, 3023, 2917, 2361, 1634, 1599, 1543, 1518, 1457, 1418, 1303, 798, 744, 695. ¹H NMR (CDCl₃, 400 MHz) δ 8.28 (d, $J = 4.76$ Hz, 2 H), 7.79 (m, 2 H), 7.53 – 7.40 (m, 3 H), 7.34 (m, 4 H), 6.56 (t, $J = 4.76$ Hz, 1 H), 6.44 (bs, 1 H), 5.55 (bs, 2 H), 4.64 (d, $J = 6.03$ Hz, 2 H). ¹³C NMR (CDCl₃, 100 MHz) δ 167.8, 162.3, 158.3 (2 C), 138.7, 137.4, 134.5, 131.8, 128.8 (2 C), 128.4 (2 C), 128.0 (2 C), 127.2 (2 C), 111.1, 45.1, 44.0. HRMS (ESI) $m/z = 319.15571$ (Theo. for C₁₉H₁₈N₄O₁+H: 319.15534).



Isobutyl 4-((pyrimidin-2-ylamino)methyl)benzylcarbamate (27). White solid (57.3 mg, 49 %). $R_f = 0.08$ (98:2 DCM:MeOH). MP = 125-127 °C. IR (cm⁻¹): 3297, 3040, 2946, 2357, 1678, 1605, 1538, 1457, 1362, 1256, 1054, 993, 780, 710, 660. ¹H NMR (CDCl₃, 400 MHz) δ 8.25 (d, $J = 4.75$ Hz, 2 H), 7.32 (d, $J = 8.26$ Hz, 2 H), 7.26 (d, $J = 7.94$ Hz, 2 H), 6.54 (t, $J = 4.75$ Hz, 1 H), 5.71 (bs, 1 H), 5.08 (s, 2 H), 4.62 (d, $J = 5.92$ Hz, 2 H), 4.35 (d, $J = 5.92$ Hz, 2 H), 3.87 (d, $J = 6.87$ Hz, 2 H), 2.08 (m 1 H), 0.92 (d, $J = 6.63$ Hz, 6 H). ¹³C NMR (CDCl₃, 100 MHz) δ 162.5, 158.2 (2 C), 157.0, 138.6, 137.9, 127.9 (4 C), 111.0, 71.4, 45.2, 44.9, 28.2, 19.2 (2 C). HRMS (ESI) $m/z = 315.18195$ (Theo. for C₁₇H₂₂N₄O+H: 315.18155).

3.5.2 Experimental Protocol for TN-14003 Binding Assay

Cell Culture/Reagents. Human breast carcinoma cell line, MDA-MB-231 were maintained in RPMI-1640 and DMEM/Ham's F-12 50:50 (Sigma, St. Louis, MO), respectively, supplemented with 10% FBS, 100 U/mL of penicillin sodium, and 100 μ g/mL of streptomycin sulfate (Pen/Strep), at 37°C in humidified air containing 5% carbon dioxide air atmosphere.

Initial screening of anti-CXCR4 small molecules based on a binding affinity assay. For compound screening based on a competition binding assay, 2 x 10⁴ MDA-MB-231 cells in a 200 µL of medium were seeded in 8-well slide chamber two days before the experiments. Various concentration of different compounds (1, 10, 100, and 1000 nM) were added to the separate wells, incubated for 10 minutes at room temperature, and then the cells were fixed in 4% of ice-cold paraformaldehyde. The cells were rehydrated in PBS and blocked to eliminate non-specific binding (Avidin and Biotin Blocking Solution, Zymed Laboratories, Inc., San Francisco, CA). The slides were subsequently incubated for 45 min at room temperature with 0.05 µg/mL of biotinylated **TN14003**, washed three times with PBS and incubated in streptavidin-rhodamine (1:150 dilution) (Jackson ImmunoResearch Laboratories, West Grove, PA) for 30 min at room temperature. Finally, the slides were washed with PBS, mounted in an antifade mounting solution (Molecular Probes, Eugene, OR), and the samples were analyzed on a Nikon Eclipse E800 microscope.

¹ American Cancer Society.

(<http://www.cancer.org/acs/groups/content/@epidemiologysurveillance/documents/document/acspc-029771.pdf>) accessed October 3, 2010.

² Goei, M.; Hickam, D.; Robinson, S.; Schechtel, M.; Davis, E.; King, V. "Treatments for Clinically Localized Prostate Cancer" *Compar. Effect. Rev. Summary Guides for Clin.* **2008**.

³ Pruett, S. T.; Bushnev, A.; Hagedorn, K.; Adiga, M.; Haynes, C. A.; Sullards, M. C.; Liotta, D. C.; Merrill, A. H. Jr. *J. Lipid Res.* **2008**, *49*, 1621-1639.

⁴ Thudichum, J. L. W. *A Treatise on the Chemical Constitution of Brain* (Bailliere, Tindall and Cox, London). **1884**.

⁵ Harder, T.; Simons, K. *Curr. Opin. Cell. Biol.* **1997**, *9*, 534-542.

⁶ Cuvillier, O.; Pirianov, G.; Kleuser, B.; Vanek, P. G.; Coso, O. A.; Gutkind, J. S.; Spiegel, S. *Nature* **1996**, 381, 800-803. Spiegel, S.; Milstien, S. *J. Biol. Chem.* **2002**, *277*, 25851-25854. Cullivier, O. *Biochim. Biophys. Acta* **2002**, *1585*, 153-162. Spiegel, S.; Milstien, S. *Nature Rev.* **2003**, *4*, 397-407. Ogretmen, B.; Hannun, Y. A. *Nature Rev. Cancer.* **2004**, *4*, 604-616.

⁷ A) Ogretmen, B.; Hannun, Y. A. *Nat. Rev. Cancer.* **2004**, *4*, 604. B) Bosquet, C. *Mol. Cancer Ther.* **2009**, *8* (4), 809. C) Spiegel, S. *Seminar at J. Lipid Res. Symposium* **2009**.

⁸ Guillermet-Guibert, J.; Davenne, L.; Pchejetski, D.; Saint-Laurent, N.; Brizuela, L.; Guilbeau-Frugier, C.; Delisle, M. B.; Cuvillier, O.; Susini, C.; Bousquet, C. *Mol. Cancer Ther.* **2009**, *8*, 2727-2733.

⁹ Cuvillier, O.; Pirianov, G.; Kleuser, B.; Vanek, P. G.; Coso, O. A.; Gutkind, J. S.; Spiegel, S. *Nature* **1996**, 381, 800-803.

¹⁰ Symolon, H.; Bushnev, A.; Peng, Q.; Ramaraju, H.; Mays, S. G.; Allegood, J. C.; Pruett, S. T.; Sullards, M. C.; Dillehay, D. L.; Liotta, D. C.; Merrill, Jr., A. H. *Mol. Cancer Ther.* **2011**, *10*, 648-657. Bergelin, N.; Blom, T.;

- Heikkia, J.; Alam, C.; Balthasar, S.; Slotten, J. P.; Hinkkanen, A.; Törnquist, K. *Endocrinology* **2009**, *150*, 2055-2063.
- ¹¹ Nigel, J.; Pyne, S. *Nat. Cancer Rev.* **2010**, *10*, 489-503.
- ¹² Allende, M. L.; Sasaki, T.; Hiromichi Kawai, H.; Olivera, A.; Mi, Y.; van Echten-Deckert, G.; Hajdu, R.; Rosenbach, M.; Keohane, C. A.; Mandala, S.; Spiegel, S.; Proia R. L. *J. Biol. Chem.* **2004**, *279*, 52487-52492.
- Nigel, J.; Pyne, S. *Nat. Cancer Rev.* **2010**, *10*, 489-503.
- ¹³ Bonhoure, E.; Pchejestski, D.; Aouali, N. Morjani, H.; Levade, T.; Kohama, T.; Cuvillier, O. *Leukemia* **2006**, *20*, 95-102.
- ¹⁴ Kennedy, A. J.; Mathews, T. P.; Kharel, Y.; Field, S. D.; Moyer, M. L.; East, J. E.; Houck, F. D.; Lynch, K. R.; Macdonald, T. L. *J. Med. Chem.* **2011**, *54*, 3524-3548.
- ¹⁵ Novartis media release 8-22-2010.
- ¹⁶ Lexicon Pharmaceuticals (<http://www.lexicon-genetics.com/pipeline/lx2931.html>). Accessed June 2011.
- ¹⁷ Actelion Media release 12-8-2009.
- ¹⁸ French, K. J.; Zhuang, Y.; Maines, L. W.; Gao, P.; Wang, W.; Beljanski, V.; Upson, J. J.; Green, C. L.; Keller, S. N.; Smith, C. D. *J. Pharm. Exp. Ther.* **2010**, *333*, 129-139.
- ¹⁹ A) Schroeder, J. J.; Crane, H. M.; Xia, J.; Liotta, D. C.; Merrill Jr., A. H. *J. Biol. Chem.* **1994**, *269*, 3475-3481. B) Sullards, M. C.; Wang, E.; Voss, K. A.; Riley, R. T.; Merrill Jr., A. H. *Environ. Health Perspect.* **2001**, *109*, 283-289.
- ²⁰ Merrill Jr., A. H.; Sullards, M. C.; Wang, E.; Voss, K. A.; Riley, R. T. *Environ. Health Perspect.* **2001**, *109*, 283-289.
- ²¹ Menaldino, D. S. Asymmetric Syntheses of Amino Alcohols as Bioactive Compounds. Chapter One: Syntheses of Sphingolipid Analogs as Inhibitors of the Protein Kinase C Enzyme System. Chapter Two: Syntheses of Fumonisin Analogs as Non-Metabolizable Protein Kinase C Inhibitors and as Proposed Ceramide Synthase Inhibitors. vol. PhD Thesis, Emory University, Atlanta, GA, **1992**.
- ²² Symolon, H.; Bushnev, A.; Peng, Q.; Ramaraju, H.; Mays, S. G.; Allegood, J. C.; Pruett, S. T.; Sullards, M. C.; Dillehay, D. L.; Liotta, D. C.; Merrill, Jr, A. H. *Mol. Cancer Ther.* **2011**, *10*, 648-657.
- ²³ Garnier-Amblard, E. C.; Mays, S. G.; Arrendale, R. F.; Baillie, M. T.; Bushnev, A. S.; Culver, D. G.; Evers, T. J.; Holt, J. J.; Howard, R. B.; Liebeskind, L. S.; Menaldino, D. S.; Natchus, M. G.; Petros, J. A.; Ramaraju, H.; Reddy, G. P.; Liotta, D. C. *ACS Med. Chem. Letters*, **2011**, *2*, 438 – 443.
- ²⁴ Wiseman, J. M.; McDonald, F. E.; Liotta, D. C. *Org. Lett.* **2005**, *7*, 3155-3157 (see also additions and correction Wiseman, J. M.; McDonald, F. E.; Liotta, D. C. *Org. Lett.* **2007**, *9*, 2959). Esteve J.; Lorente A.; Romea P.; Urpi F.; Rios-luci C.; Padron J. M. *Eur. J. Org. Chem.* **2011**, 960-967. Dias L.C.; Fattori J.; Perez C. C.; De Oliveira V. M.; Aguilar A. M. *Tetrahedron* **2008**, *64*, 5891-5903. Saikia, P. P.; Goswami, A.; Baishya, G.; Barua, N. C. *Tetrahedron Lett.* **2009**, *50*, 1328-1330.
- ²⁵ Siow, D.; Wattenberg, B. *Crit. Rev. Biochem. Mol. Biol.* **2011**, *5*, 365-375.
- ²⁶ Porcari, P.; Capuani, S.; D'Amore, E.; Lecce, M.; La Bella, A.; Fasano, F.; Campanella, R.; Migneco, L. M.; Pastore, F. S.; Maraviglia, B. *Phys. Med. Biol.* **2008**, *53*, 6979-6989.
- ²⁷ Pruett, S. Biological Mass Spectrometry of Sphingolipids in Drug Discovery and Development. Chapter Three: Investigation of Enigmol Mechanism of Action and Metabolism. Ph.D. Thesis, Emory University, Atlanta, GA, **2006**.
- ²⁸ Tokuyama, H.; Miyazaki, T.; Yokoshima, S.; Fukuyama, T. *Synlett* **2003**, *10*, 1512-1514.
- ²⁹ Mehta, V.; Sharma, A.; Van der Eycken, E. *Org. Lett.* **2008**, *10*, 1147-1150.
- ³⁰ Gouault, N.; Le Roch, M.; Cornee, C.; David, M.; Uriac, P. *J. Org. Chem.* **2009**, *74*, 5614-5617.
- ³¹ Gronowitz, S.; Roos, C. *Acta Chem. Scand.* **1975**, B29, 990-998. Gronowitz, S.; Malm, J.; Hoernfeldt, A. B. *Collect. Czech. Chem. Commun.* **1991**, *56*, 2340-51. Gronowitz, S.; Peters, D. *Heterocycles* **1990**, *30*, 645-658.
- ³² Gouault, N.; Le Roch, M.; Cornee, C.; David, M.; Uriac, P. *J. Org. Chem.* **2009**, *74*, 5614-5617.
- ³³ Liu, G.; Cogan, D. A.; Ellman, J. A. *J. Am. Chem. Soc.* **1997**, *119*, 9913-9914.
- ³⁴ Note: Although Ellman's reagent is stable as either of the enantiomers, the *t*Butylsulfinyl chloride racemizes quickly. Hence it is used to make a mixture of products, which in some cases like ours are separable by column chromatography.
- ³⁵ Yang, H.; Li, H.; Witteberg, R.; Egi, M.; Huang, W.; Liebeskind, L. *J. Am. Chem. Soc.* **2006**, *129*, 1132-1140.
- ³⁶ Bushnev, A. S.; Baillie, M. T.; Holt, J. J.; Menaldino, D. M.; Merrill, A. H.; Liotta, D. C. *Arkivoc* **2010** (viii), 263-277.
- ³⁷ Evans, D. A.; Rieger, D. L.; Bilodeau, M. T.; Urpi, F. *J. Am. Chem. Soc.* **1991**, *113*, 1047-1049.
- ³⁸ Yang, S. M.; Denmark, S. E. *J. Am. Chem. Soc.* **2002**, *124*(10), 2102-2103.

- ³⁹ Trost, B.; Ball, Z. T.; Jöge, T. *J. Am. Chem. Soc.* **2002**, *124*, 7922. Fürstner, A.; Radkowski, K. *Chem. Commun.* **2002**, 2182-2183.
- ⁴⁰ Thijs, L.; Zwaneburg, B. *Tetrahedron* **2004**, *60*, 5237-5252.
- ⁴¹ A) Frigerio, M.; Santagostino, M.; Sputore, S. *J. Org. Chem.* **1999**, *64*, 4537-4538. and B) Ireland, R. E.; Liu, L. *J. Org. Chem.* **1993**, *58*, 2899.
- ⁴² Grayson, E. J.; Davis, B. G. *Org. Lett.* **2005**, *12*, 2361-2364.
- ⁴³ Trost, B.; Ball, Z. T.; Jöge, T. *J. Am. Chem. Soc.* **2002**, *124*, 7922. Fürstner, A.; Radkowski, K. *Chem. Commun.* **2002**, 2182-2183.
- ⁴⁴ Unpublished data.
- ⁴⁵ Unpublished data.
- ⁴⁶ Bioavailability for **Enigmol** was calculated with the P.O. data from this study in concert with I.V. data from a previous study. Parameters were identical for the I.V. in this study (for compound **2**) and the previous study with **Enigmol**.
- ⁴⁷ A) Symolon, H.; Bushnev, A.; Peng, Q.; Ramaraju, H.; Mays, S. G.; Allegood, J. C.; Pruett, S. T.; Sullards, M. C.; Dillehay, D. L.; Liotta, D. C.; Merrill, Jr, A. H. *Mol. Cancer Ther.* **2011**, *10*, 648-657. B) Pruett, S. Biological Mass Spectrometry of Sphingolipids in Drug Discovery and Development. Chapter Three: Investigation of Enigmol Mechanism of Action and Metabolism. Ph.D. Thesis, Emory University, Atlanta, GA, **2006**.
- ⁴⁸ *Org. & Biomol. Chem.* **2007**, *5*, 1776. B) *J. Chem. Soc., Perkin Trans.* **2002**, *1*, 2243-2250.
- ⁴⁹ Yang, H.; Li, H.; Wittenberg, R.; Egi, M.; Huang, W.; Liebeskind, L. S. *J. Am. Chem. Soc.* **2007**, *129*, 1132-1140.
- ⁵⁰ Uriac, P, et al. *J. Org. Chem.* **2009**, *74*, 5614.
- ⁵¹ Yang, S. M.; Denmark, S. E. *J. Am. Chem. Soc.* **2002**, *124*(10), 2102-2103.
- ⁵² Thijs, L.; Zwaneburg, B. *Tetrahedron* **2004**, *60*, 5237-5252.
- ⁵³ A) *J. Am. Chem. Soc.* **1994**, *116*, 7616-7630. B) Takai, K.; Takagi, T.; Baba, T.; Kanamori, T. *J. Fluor. Chem.* **2007**, *128*, 120-126.
- ⁵⁴ A) Frigerio, M.; Santagostino, M.; Sputore, S. *J. Org. Chem.* **1999**, *64*, 4537-4538. and B) Ireland, R. E.; Liu, L. *J. Org. Chem.* **1993**, *58*, 2899.
- ⁵⁵ Grayson, E. J.; Davis, B. G. *Org. Lett.* **2005**, *12*, 2361-2364.
- ⁵⁶ Sueda, T.; Kajishima, D.; Goto, S., *J. Org. Chem.*, **2003**, *68*, 3307.
- ⁵⁷ Trost, B. et al. *J. Am. Chem. Soc.* **2002**, *124*, 7922.
- ⁵⁸ Warburg, O. *Science*, **1956**, *123*, 309-314.
- ⁵⁹ Pedersen, P. L. *J. Bioenerg. Biomembr.* **2007**, *39*, 1-12.
- ⁶⁰ Fang, J.; Quinones, Qu. J.; Holman, T. L.; Morowitz, M. J.; Wang, Q.; Zhao, H.; Sivo, F.; Maris, J. M.; Wahl, M. L. *Mol. Pharm.* **2006**, *70*, 2108-2115.
- ⁶¹ Ammons, S. W.; Wang, J.; Yang, Z. Tidmarsh, G. F.; Hoffman, R. M. *Neoplasia*. **2007**, *9*(8), 625-633.
- ⁶² Ko, Y. H.; Smith, B.L.; Wang, Y.; Pomper, M. G.; Rini, D. A.; Torbenson, M. S.; Hullihen, J.; Pedersen, P. L. *Biochem. Biophys. Res. Commun.* **2004**, *324*, 269-275.
- ⁶³ Periera da Silva, A. P.; El-Bacha, T.; Kway, N.; Santos, R. S.; Da Silva, W. S.; Almeida, F. C. L.; Da Poian, A. T.; Galina, A. *Biochem. J.* **2009**, *417*, 717-726.
- ⁶⁴ Boxer, M. B.; Jiang, J. K.; Vander Heiden, M. G.; Shen, M.; Skoumbourdis, A. P.; Southall, N.; Veith, H.; Leister, W.; Austin, C. P.; Park, H. W.; Inglese, J.; Cantley, L. C.; Auld, D. S.; Thomas, C. J. *J. Med. Chem.* **2010**, *53*, 1048-1055.
- ⁶⁵ a) Maryanoff, B. E.; Parvez, M.; Olofson, R. A. *J. Org. Chem.* **1990**, *55*, 760-764. b) Garci, L. F.; Erni, A. B. *Eur. J. Biochem.* **2002**, *269*, 3226-3236.
- ⁶⁶ K. Nakamura, K., Kimura, T., Kanno, H., *J. Antibiot.* **1995**, *48*, 1134-1137.
- ⁶⁷ Jenkins, C. L. D.; Harris, R. L. N.; McFadden, H. G. *Biochem. Int.* **1987**, *14*, 219-226.
- ⁶⁸ Everett, T. S.; Purrington, S. T.; Bumgardner, C. L. *J. Org. Chem.* **1984**, *49*, 3702-3706.
- ⁶⁹ Bumgardner, C. L.; Purgess, J. P.; Everett, T. S.; Purrington, S. T. *J. Fluor. Chem.* **1992**, *56*, 189-193.
- ⁷⁰ a) Botegghi, C.; Paganelli, S.; Sborgio, F.; Zarantonello, C. *Tet. Lett.* **1999**, *40*, 8435-8437, b) Bhadrury, P. S.; Palit, M.; Sharma, M.; Raza, S. K.; Jaiswal, D. K. *J. Fluor. Chem.* **2002**, *116*, 75-80.
- ⁷¹ K. Nakamura, K., Kimura, T., Kanno, H., *J. Antibiot.* **1995**, *48*, 1134-1137.
- ⁷² Jenkins, C. L. D.; Harris, R. L. N.; McFadden, H. G. *Biochem. Int.* **1987**, *14*, 219-226.
- ⁷³ Everett, T. S.; Purrington, S. T.; Bumgardner, C. L. *J. Org. Chem.* **1984**, *49*, 3702-3706.
- ⁷⁴ Bumgardner, C. L.; Burgess, J. P.; Everett, T. S.; Purrington, S. T. *J. Fluor. Chem.* **1992**, *56*, 189-193.
- ⁷⁵ NIH, N. E. I., Macular Hole. <http://www.nei.nih.gov/health/macularhole/index.asp>, (accessed April 19, 2006).

- ⁷⁶ AMD.org, Current Treatments. http://www.amd.org/site/PageServer?pagename=Current_Treatments (accessed April 19, 2006).
- ⁷⁷ Fierce Pharma news agency. <http://www.fiercepharma.com/story/medicare-code-favors-costly-lucentis-use/2009-10-02-0> (accessed September 26, 2011).
- ⁷⁸ a) Chu, P.H.; Tu, H. Methods for the treatment of macular degeneration with topiramate. U.S. Patent 6949518. June 14, 2005. <http://www.patentgenius.com/patent/6949518.html> (accessed September 13, 2011). b) Graff, G.; Hellberg, M. R.; Yanni, J. M. Treatment of ocular inflammatory and angiogenesis-related disorders of the posterior segment of the eye by using an amide from flurbiprofen or ketorolac. U.S. Patent 6646003. November 11, 2003. <http://www.patentgenius.com/patent/6646003.html> (accessed September 13, 2011). c) Kaur, I. P.; Aggarwal, D., *Trends in Glaucoma Research* **2005**, 67-93. d) Krieg, P. A. **Methods for modulating angiogenesis with apelin compositions**. U.S. Patent 7736646. June 15, 2010. <http://www.patentgenius.com/patent/7736646.html> (accessed September 13, 2011). e) Lai, C. S.; Vassilev, V. Therapeutic methods employing disulfide derivatives of dithiocarbamates and compositions useful therefore. U.S. Patent 6093743. July 25, 2000. <http://www.patentgenius.com/patent/6093743.html> (accessed September 13, 2011). f) Morris, D. L.; Pourgholami, M. H. Benzimidazole derivatives for VEGF inhibition, and their therapeutic use. World Patent 2006024092. March 9, 2006. g) Morris, J. P.; Nguyen, D.; Kappelman, J.; McCabe, M. M.; Potter, M. D.; Ziai, M. R.; Feldman, S.; Hartman, H. Composition of highly purified natural mixtures of type I interferon derived from leukocytes and methods. U.S. Patent 6433144. August 13, 2000. <http://www.patentgenius.com/patent/6433144.html> (accessed September 13, 2011). h) Petrus, E. J. Method and compositions for treatment of the aging eye. U.S. Patent 6573299. September 20, 1999. <http://www.patentgenius.com/patent/6573299.html> (accessed September 13, 2011). i) Van Den Bergh, H.; Lange, N. Conjugates of photosensitizers and oligonucleotides for selective photochemotherapy. U.S. Patent Application 2006105974.
- ⁷⁹ Lang, J. C. *Adv. Drug. Deliv. Rev.* **1995**, *16*, 39-43.
- ⁸⁰ Kaur, I. P.; Garg, A.; Singla, A. K.; Aggarwal, D. *Int. J. Pharm.* **2004**, *269*, 1-14.
- ⁸¹ Edwards, A.; Prausnitz, M. R. *Pharm. Res.* **2001**, *18*, 1497-1508.
- ⁸² A) Kaur, I. P.; Garg, A.; Singla, A. K.; Aggarwal, D. *Int. J. Pharm.* **2004**, *269*, 1-14. B) Kaur, I. P.; Aggarwal, D. *Trends in Glaucoma Res.* **2005**, 67-93. C) Aggarwal, D.; Garg, A.; Kaur, I. P. *J. Pharm. Pharmacol.* **2004**, *56*, 1509-1517. D) Kaur, I. P.; Kapil, M.; Smitha, R.; Aggarwal, D. *Curr. Drug. Deliv.* **2004**, *1*, 65-72.
- ⁸³ Loetscher, M.; Geiser, T.; O'Reilly, T.; Zwahlen, R.; Baggiolini, M.; Moser, B. *J. Biol. Chem.* **1994**, *269*, 232-237.
- ⁸⁴ Zaitseva, M.; Blauvelt, A.; Lee, S.; Lapham, C. K.; Kiaus-Kovrun, V.; Mostowski, H.; Manishewitz, J.; Golding, H. *Nature Med.* **1997**, *3*, 1369-1375.
- ⁸⁵ De Clercq, E. *Nat. Rev. Drug Disc.* **2003**, *2*, 581-587.
- ⁸⁶ Trent, J. O. W., Z. X.; Murray, J. L.; Shao, W.; Tamamura, H.; Fujii, N.; Peiper, S. C. *J. Biol. Chem.* **2003**, *278*, 47136-47144.
- ⁸⁷ Ratajczak, M. Z. R., R.; Wysoczynski, M.; Yan, J.; Ratajczak, J. *Exp. Hematol.* **2006**, *34*, 986-995.
- ⁸⁸ Ma, Q.; Jones, D.; Borghesani, P. R.; Segal, R. S.; Nagasawa, T.; Kishimoto, T.; Bronson, R. T.; Springer, T. A. *Proc. Nat. Acad. Sci.* **1998**, *95*, 9448-9453.
- ⁸⁹ Walter, D. H.; Haendeler, J.; Reinhold, J.; Rochwalsky, U.; Seeger, F.; Honold, J.; Hoffmann, J.; Urbich, C.; Lehmann, R.; Arenzana-Seisdesdos, F.; Aicher, A.; Heeschen, C.; Fichtlscherer, S.; Zeiher, A. M.; Dimmeler, S. *Circulation Res.* **2005**, *97*, 1142-1151.
- ⁹⁰ Scala, S. O. A.; Ascierto, P. A.; Cavalli, M.; Simon, E.; Giuliano, P.; Napolitano, M.; Franco, R.; Botti, G.; Castello, G. *Clin. Canc. Res.* **2005**, *11*, 1835-1841.
- ⁹¹ Donzella, G. A.; Schols, D.; Lin, S. W.; Este, J. A.; Nagashima, K. A.; Maddon, P. J.; Allaway, G. P.; Sakmar, T. P.; Henson, G.; DeClercq, E.; Moore, J. P. *Nature Med.* **1998**, *4*, 72-77.
- ⁹² Fricker, S. P.; Anastassov, V.; Cox, J.; Darkes, M. C.; Grujic, O.; Idzan, S. R.; Labrecque, J.; Lau, G.; Mosi, R. M.; Nelson, K. L.; Qin, L.; Santucci, Z.; Won, R. S. Y. *Biochem. Pharmacol.* **2006**, *72*, 588-596.
- ⁹³ A) Schwarz, M. K.; Wells, T. N. *Nat. Rev. Drug Discovery* **2002**, *1*, 347-358. B) De Clercq, E. *Nat. Rev. Drug Discov.* **2003**, *2*, 581-587.
- ⁹⁴ FDA approval of Plerixafor. <http://www.mednewsdirect.com/?p=622> (accessed September 14, 2011). DiPersio, J. F.; Micallef, I. N. M.; Stiff, P. J. et al. Poster presented at ASH Annual Meeting; *Blood* (ASH Annual Meeting Abstracts). 2008 112: Abstract 1136.
- ⁹⁵ Gupta, S. K.; Pillarisetti, K.; Thomas, R. A.; Aiyar, N. *Immun. Lett.* **2001**, *78*, 29-34.
- ⁹⁶ Wu, B.; Chien, E. Y. T.; Mol, C. D.; Fenalti, G.; Liu, W.; Katritch, V.; Abagyan, R.; Brooun, A.; Wells, P.; Bi, F. C.; Hamel, D. J.; Kuhn, P.; Handel, T. M.; Cherezov, V.; Stevens, R. C. *Science* **2010**, *330*, 1066-1071.

-
- ⁹⁷ Zhan, W.; Liang, Z.; Zhu, A.; Kurtkaya, S.; Shim, H.; Snyder, J. P.; Liotta, D. C. *J. Med. Chem.* **2007**, *50*, 5655-5664.
- ⁹⁸ A) Fujii, N.; Tamamura, H. *Curr. Opin. Invest. Drugs* **2001**, *2*, 1198-1202. B) Liang, Z.; Wu, T.; Lou, H.; Yu, X.; Taichman, R. S.; Lau, S. K.; Nie, S.; Umbreit, J.; Shim, H. *Cancer Res.* **2004**, *64*, 4302-4308.
- ⁹⁹ Unpublished data.
- ¹⁰⁰ A) Zhan, W.; Liang, Z.; Zhu, A.; Kurtkaya, S.; Shim, H.; Snyder, J. P.; Liotta, D. C. *J. Med. Chem.* **2007**, *50*, 5655-5664. B) Zhan, W. Design of Small Molecule CXCR4 Antagonists. Ph.D. Dissertation, Emory University. **2008**.
- ¹⁰¹ Novartis, Calculation of Molecular Properties and Drug-likeness: "molinspiration". <http://www.molinspiration.com/cgi-bin/properties>: (accessed April 10, 2006).
- ¹⁰² Prausnitz, M. R.; Noonan, J. S. *J. Pharm. Sci.* **1998**, *87*, 1479-1488.
- ¹⁰³ Worth, A. P.; Cronin, M. T. D. *ATLA* **2000**, *28*, 403-413.
- ¹⁰⁴ Sasaki, H.; Yamamura, K.; Mukai, T.; Nishida, K.; Nakamura, J.; Nakashima, M.; Ichikawa, M. *Crit. Rev. Ther. Drug Carrier Syst.* **1999**, *16*, 85-146.
- ¹⁰⁵ a) Stork, G.; Takahashi, T.; Kawamoto, I.; Suzuki, T. *J. Am. Chem. Soc.* **1978**, *100*, 8272-8273. b) Schlessinger, R. H.; Lopes, A. *J. Org. Chem.* **1981**, *46*, 5252-5253. c) Stork, G.; Takahashi, T. *J. Am. Chem. Soc.* **1977**, *99*, 1275-1276.
- ¹⁰⁶ Stork, G.; Takahashi, T. *J. Am. Chem. Soc.* **1977**, *99*, 1275-1276.
- ¹⁰⁷ Corey, E. J.; Gras, J. L.; Ulrich, P. *Tetrahedron Lett.* **1976**, *11*, 809-812.
- ¹⁰⁸ Liang, Z.; Wu, T.; Lou, H.; Yu, X.; Taichman, R. S.; Lau, S. K.; Nie, S.; Umbreit, J.; Shim, H. *Cancer Res.* **2004**, *64*, 4302-4308.
- ¹⁰⁹ Fricker, S. P.; Anastassov, V.; Cox, J.; Darkes, M. C.; Grujic, O.; Idzan, S. R.; Labrecque, J.; Lau, G.; Mosi, R. M.; Nelson, K. L.; Qin, L.; Santucci, Z.; Won, R. S. Y. *Biochem. Pharmacol.* **2006**, *72*, 588-596.